Ice-concrete bond analysis

Characterisation of ice adhesion strength in ice-structure interaction

B. A. Westerveld

Experimental research on influence of extrinsic parameters on ice-concrete bond strength and the role of ice adhesion in concrete abrasion

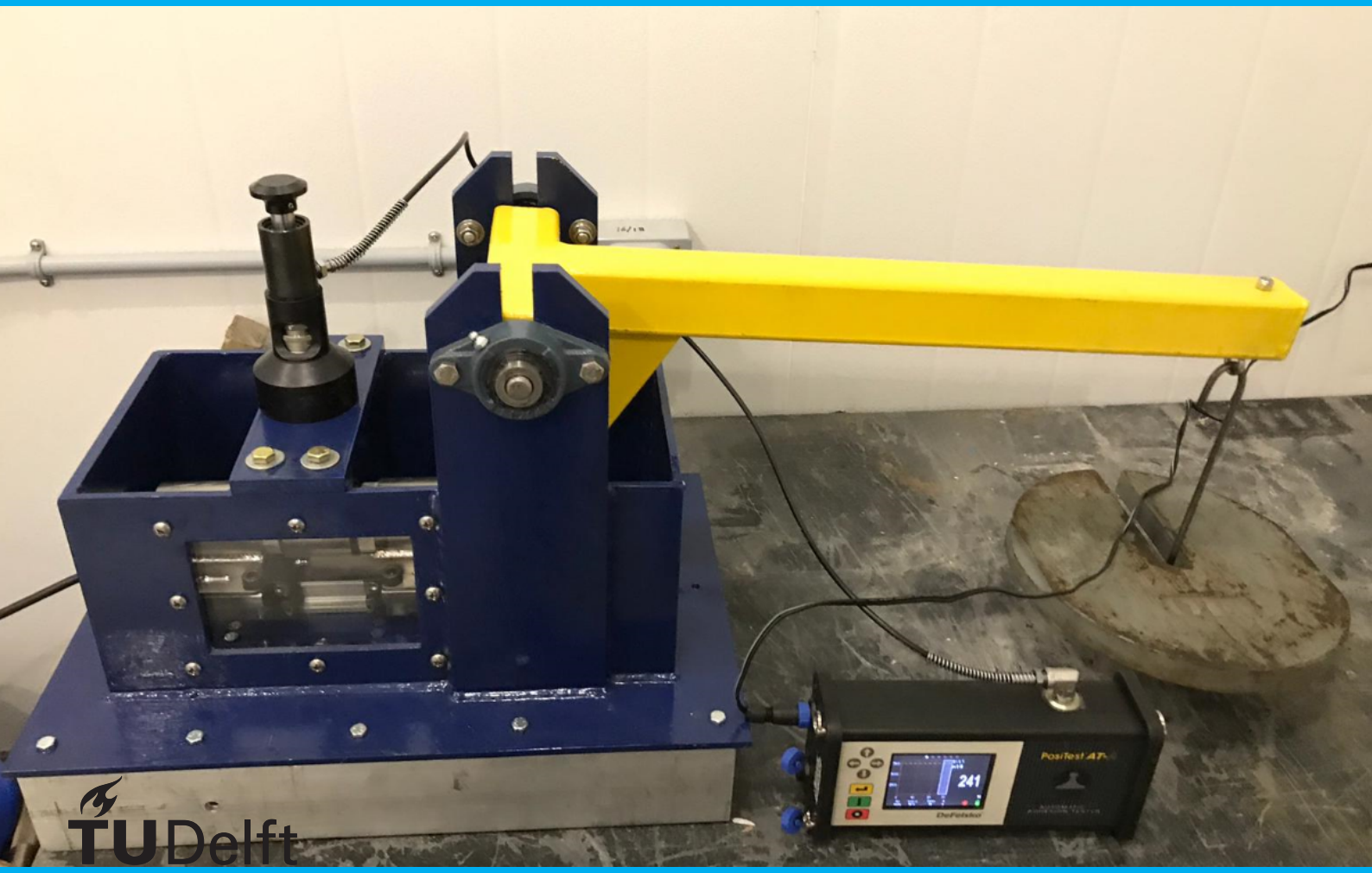

TU Delft

Ice-concrete bond analysis

Characterisation of ice adhesion strength in ice-structure interaction

by

B. A. Westerveld

to obtain the degree of Master of Science
at the Delft University of Technology.

Student number:	4179048	
Project duration:	February, 2019 –Oktober, 2019	
Thesis committee:	Prof. dr. A. Metrikine,	TU Delft, chairman
	Ir. J. S. Hoving,	TU Delft, supervisor
	Dr. S. E. Bruneau,	Memorial University of Newfoundland, supervisor

An electronic version of this thesis is available at `http://repository.tudelft.nl/`.

Abstract

In regions which experience arctic conditions, structures like offshore wind turbines, oil-platforms, light houses, piers and bridges suffer from abrasion by moving ice sheets. This results in challenging maintenance and repair works. At the ice-structure interface, several mechanisms exist which are responsible for the wear of concrete such as: freeze-thaw cycles, chemical effects of sea water, and mechanical loading of concrete. The main cause of concrete abrasion is however thought to be the flow of ice floes together with a layer of crushed ice, which is partly controlled by friction and adhesion between the two interfaces. Adhesion is thought to be the main component of the static friction and is, under certain circumstances, also directly responsible for concrete abrasion. It is yet not well known to what degree ice adhesion contributes to concrete abrasion, and how extrinsic parameters such as: pressure, hold time and submergence relate to the ice-concrete bond strength. This research aims to better understand the physical phenomena happening at the ice-concrete interface by shearing an adhesive ice-concrete bond to get a better understanding of the role of ice adhesion in concrete abrasion processes.

To achieve this goal, a double shear apparatus has been designed and ice-concrete shear tests have been performed in a thermal laboratory. The apparatus was designed to be relatively simple compared to conventional soil shearing machines. The design allowed for the ability of submergence, accurate and sustained application of normal load, improved implementation of standardisation procedures, and easy portability. The temperature during the test was remained relatively constant at around - 9° for dry the ice-concrete adhesion test, and around 0° C for submerged tests. The influence of hold time, varying from very short (6 seconds) to overnight, and pressure (51, 316 and 682 kPa) on the force required to break the ice-concrete bond has been investigated following a series of five test sequences. In sequence 1, the applied pressure was remained when shearing the ice. In test sequence 2, the shearing was initiated immediately after removing the applied pressure. In sequence 3, the time between removing the pressure and shearing has been varied. In sequence 4, different materials have been used to clamp in the ice and sequence in 5, both the concrete and the ice has been fully submerged before shearing. The force required to shear the ice has been measured using a load cell.

The results show a positive influence of holding time on the force required to perform the shearing, and although a higher normal load results in a higher shearing force, it is unclear what the result of a higher normal load is on the adhesive force. These result are found for both the remained and released pressure tests. The bond strength also appeared to increase when waiting after removing the applied load. Submergence showed to have a negative influence of the bond strength compared to the dry tests. When using a different surface as the concrete specimen, a pure paste surface showed to give the highest bond strength and a pure sandstone surface resulted in the lowest bond strength. The force required to break a bond between ice and a cut-concrete surface, as used in all other tests, was in between the pure paste and sandstone surfaces. All three types of failing mechanism have been observed. And the failing mechanism is dependent on hold time and pressure. Visual observations show an increase of ice stuck to the concrete surface for both higher normal loads and longer holding times.

It is concluded from the experiments in this research, that mechanical adhesion theory seems to be the main mechanism of ice-concrete bonding. The failure type of the ice-concrete bond is dependent on holding time and pressure. The bond strength is strongly dependent on holding time and it is unclear what the influence of pressure is on the bond strength. Ice adhesion has many mechanisms by which it can contribute to the abrasion of concrete.

Preface

Doing a research project abroad has ben a very interesting journey where I learned much more then I would've expected. I very much enjoyed my time studying at the Memorial University of Newfoundland in St Jonh's Canada. This whole experience wouldn't have been possible if it weren't for the following people which I would like to thank.

I would like to express my gratitudes to Prof. dr. Andrei Metrikine, Ir. Jeroen Hoving and Dr. Stephen Bruneau for being part of my graduation committee and for their helpful insights throughout my research. My sincere appreciations go out to Dr. Stephen Bruneau who has been a great daily supervisor during my time in Canada and I enjoyed his encouragement and innovative ideas on tackling many challenges. He has also been a great supervisor for the of office activities, I never thought I would be shooting golf balls from his own made cannon across a lake as part of my graduation project. I also would like to thank Ir. Jeroen Hoving for being my daily supervisor during the analysis part of this research in Delft.

I want to thank Titli Praminik for being a wonderful lab and office partner and also learned me how to make ice and helped me got acquainted in the lab. She even introduced me to the great contrast between warm and cold (-9 °C in the cold room and 24 °C in the office). I also would like to thank Dr. Amgad Hussein and Dr Assem Hassan at the Memorial University of Newfoundland for providing me with their help. Thanks to Mr. Mohamed Abdulhakim Zurgani for guiding me in making the concrete mix used in the experiments. I also enjoyed our regular visit to the Tim Horton's where we had many interesting discussions.

My research wouldn't have been as smooth as it went without the help of Craig Mitchell, Matt Curtis and Trevor Clark in the lab. Their hands-on mentality and experience enabled me to utilise the lab to the fullest. I want to thank William Bidgood for making the apparatus exactly as drawn in SolidWorks.

I would also like to thank Kvaerner Canada Limited and Research and Development Corporation of Newfoundland and Labrador (RDC) for their support which enabled me to perform this research.

And last but not least, I would like to thank my family and friends who supported me and gave me the motivation to complete this thesis.

B. A. Westerveld
Delft, October 3 2019

Contents

1

Introduction to ice-concrete adhesion and research

Offshore structures in regions which experience arctic conditions can suffer from severe abrasion by the movement of ice [17]. In the sea, structures like oil-platforms, bridges, lighthouses, piers and wind turbine foundations are exposed to sliding ice floes, which cause wear on the concrete of these structures. In lakes with freshwater ice, dams and bridge piers can experience similar conditions [14]. Although there are many mechanisms responsible for wear of the concrete, the flow of ice floes together with a layer of crushed ice, which is usually observed at the ice-structure interface, is thought to be one of the main causes of concrete abrasion [11]. This flow is partly controlled by the friction at the interface between ice and concrete. This friction can be divided in a static and a kinetic friction component. The adhesion of ice on concrete is thought to be the main component of the static friction and for slow velocities, also the kinetic friction. When ice and concrete interact, there will always partly be a zone where crushing, bending, splitting and other failure modes occur and a zone where the interaction is governed by sliding and friction, the shearing zone. These two interaction zones are illustrated in Figure 1.1.

Memorial University of Newfoundland in St John's Canada has initiated a 5-year sponsored program: a group research called the ICEWEAR project, run by Dr. Stephen Bruneau, Dr. Bruce Colbourne, Dr. Assem Hassan and Dr. Amgad Hussein. The goal is to improve the knowledge of surface wear and surface friction influences on the ice-induced wear of concrete structures in polar marine environments. The adhesion of ice to concrete is part of the scope of this project because it relates to the friction and the abrasion of the concrete.

1.1. Background and context of ice-concrete adhesion in ice-structure interaction

Adhesion of ice to structures plays two main different roles in ice-structure interaction, which are: in the abrasion of concrete by ice and in the structural loading of structures by ice.

1.1.1. The role of adhesion in abrasion of concrete by ice

In Figure 1.2, a moving ice sheet interacts with a structure, in this case the Confederation bridge between Prins Edward Island and New Brunswick, Canada. Visual observations of the bridge has shown significant wear of the concrete of the bridge. A more detailed picture showing the abrasion can be seen in Figure 2.2. In this case, ice slides along the concrete and experiences friction, which is partly related to the adhesion as illustrated in Figure 1.3.

Guzel Shamsutdinova and his colleagues [35] showed that abrasion is a function of the sliding distance of the ice along the concrete. This sliding is governed by friction because when the ice adheres to concrete, the ice can stop sliding. At the same time, it is possible that concrete particles will break off from the ice when the adhesive bond is broken. This has been observed in multiple tests in this research.

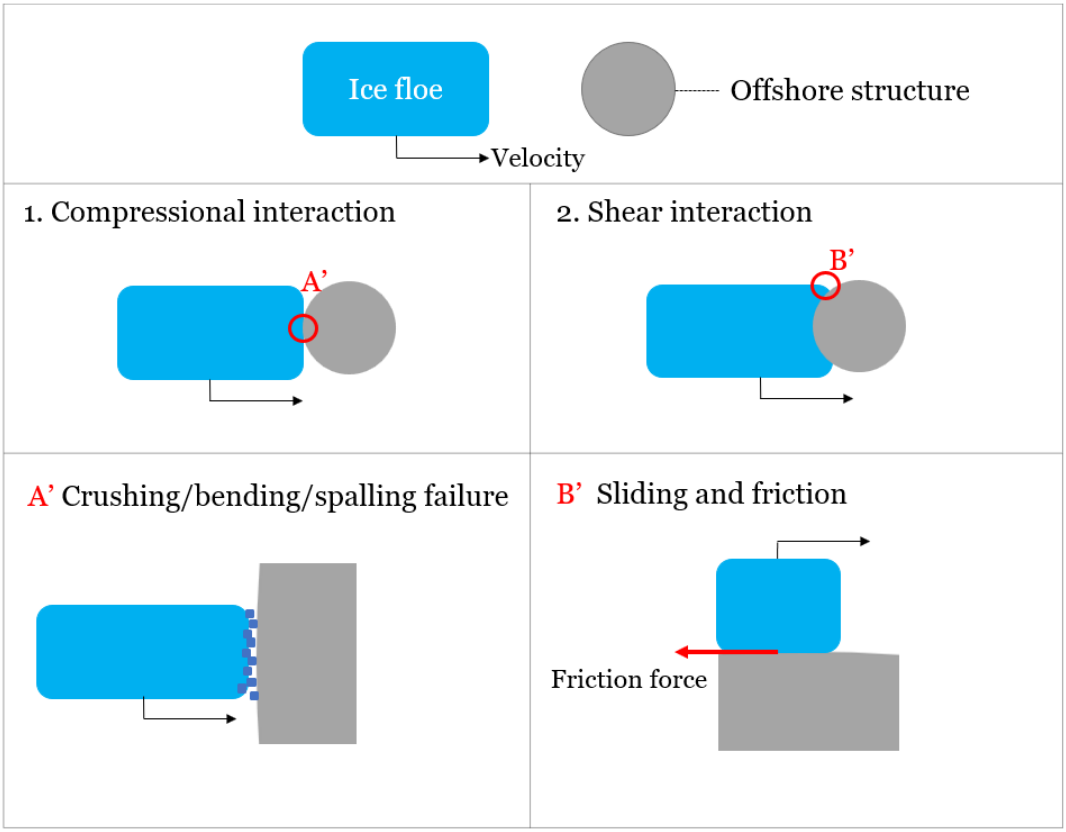

Figure 1.1: Two types of ice-concrete structure interaction

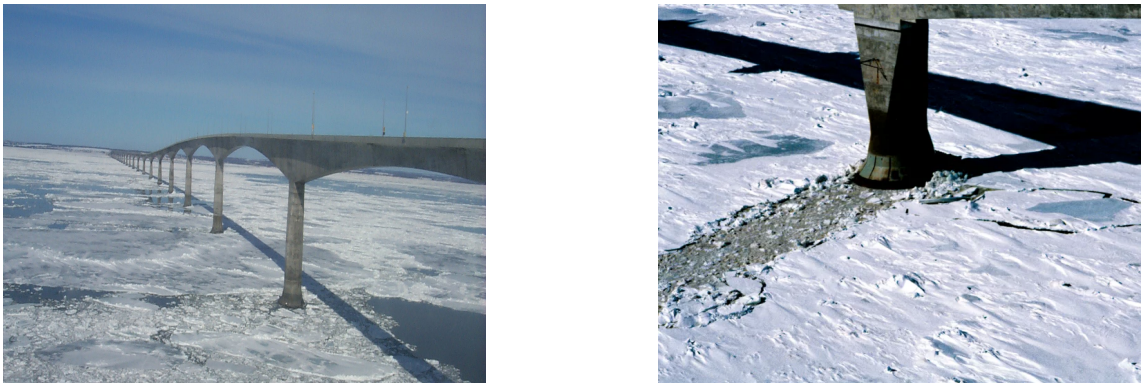

(a) xx (b)

Figure 1.2: Confederation bridge, Nova Scotia Canada (a). Moving ice sheet at one of the pillars (b).

1.1.2. The role of adhesion in ice loading

Adhesion of ice to structures can cause additional loads which should be accounted for in the design. Also, ice build-up on locks and dams causes problems. The freezing up of spillway gates could result in preventing from opening on short notice [9]. In studies looking into adhesion of ice on such structures, the focus is to prevent the ice to adhere to the structures as present ice removal techniques are costly and time consuming. The focus is to look into decreasing the adhesive strength of ice on concrete by several methods such as: electrical, chemical and mechanical techniques. Most research has been done in looking at hydrophobic coatings.

In offshore structures, the adhesion of ice to a concrete structure could cause horizontal and vertical forces on a structure when water levels are changing, as illustrated in Figure 1.5.

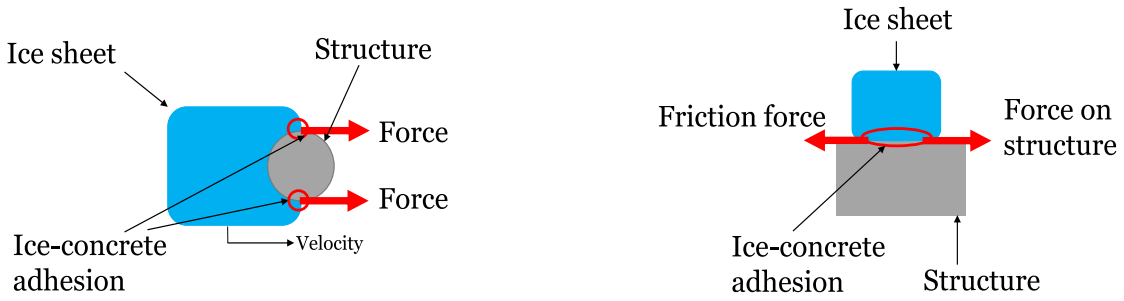

(a) (b)

Figure 1.3: illustration of ice-structure interaction indicating location where adhesion plays a role.

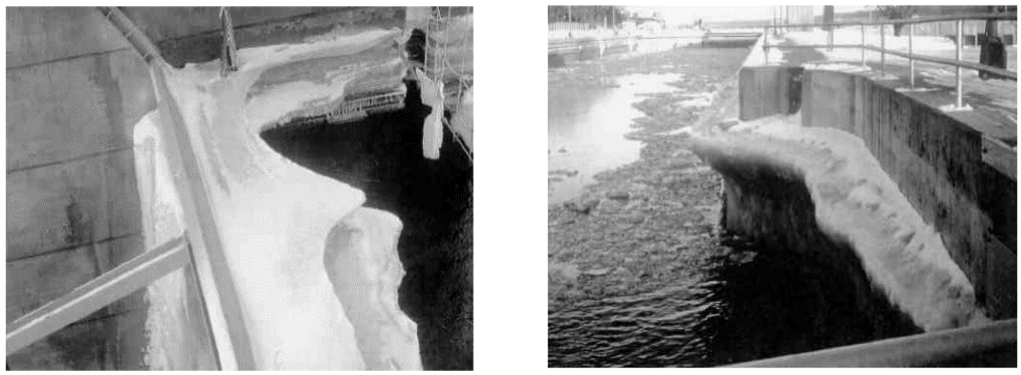

(a) (b)

Figure 1.4: Ice adhesion on lock (a) and on a dam (a)Confederation bridge, Nova Scotia Canada (a). Moving ice sheet at one of the pillars (b).

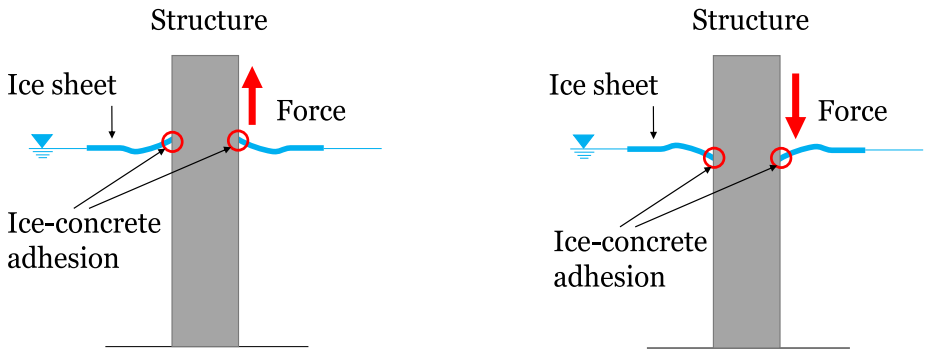

(a) (b)

Figure 1.5: Ice adhesion causing forces on structure when water level changes.

1.2. Scope and relevance of this thesis

Adhesion of ice to concrete is a complex phenomenon, mainly because of the many uncertainties which arise from the heterogeneity of both materials. Adhesion contributes to the abrasion of concrete and when the adhesive bond is broken, the effects of the ice on the structure suddenly change. It is therefore important to understand what determines when this bond breaks and what conditions determine the adhesive bond strength. This research will focus on investigating the factors influencing the adhesive bond strength between ice and concrete and what is happening at the interface between the two materials in order to asses how

adhesion can play a role in the abrasion processes of concrete by ice.

When ice and concrete experience shear interaction as illustrated in Figure 1.1, factors such as the ice floe velocity, geometry and mass will result in varying pressures at the ice-concrete interface and changing intervals between sliding and stopping. Also, the characteristics of the concrete surface, such as wetting, roughness, permeability and type of material have an influence on the adhesive bond strength. How exactly these factors influence the adhesive ice-concrete bond strength is not well understood and understanding this is relevant because it can help to better estimate the abrasion rates of concrete by ice. It can also add to a more accurately estimate of loads on structures induced by ice adhesion. The main focus on the ICEWEAR project is on the abrasion of concrete and this thesis will follow this scope.

1.3. Problem statement

The problem statement for this thesis can be described using the following sentences:

Concrete structures in marine environments with arctic conditions suffer from abrasion by ice. This results in challenging maintenance and repair works and in the worst case it can be a significant risk to the structural integrity. In order to optimize the design of these structures, one should consider the abrasion of concrete by ice, however:

The degree of abrasion rates by ice to concrete and the influence of adhesion processes are not well understood and knowledge must be improved in order to perform a more accurate assessment of the role played by adhesion.

1.4. Objective

To better understand the influence of adhesion on abrasion, first the processes of ice-concrete bonding and the influences of extrinsic parameters such as: pressure, holding time, wetting and more, on the ice-concrete bond strength should be better understood.

The goal of this graduation project is therefore to get a better understanding of the ice-concrete bond and the physical phenomena happening at the interface to get a better understanding what role adhesion plays in abrasion processes. This is done by following the approach outlined in section 1.5 and by trying to answer the following research questions:

"How are external factors and surface characteristics in ice-structure interaction influencing the adhesive ice-concrete bond strength and what role is played by adhesion in abrasion processes of concrete by ice?

In an effort to answer this question, the following sub-question will be answered:

1. *What are the processes for forming and breaking the adhesive ice-concrete bond?*
2. *Under what circumstances does ice-concrete adhesion contribute to the abrasion of concrete and when not?*
3. *What is the influence of extrinsic conditions such as bonding time, pressure, submergence, concrete surface on the adhesive bond strength between ice and concrete?*

1.5. Approach

First, a literature study has been done to identify the current state of knowledge on concrete abrasion by ice, friction between ice and concrete-ice adhesion to get a better understanding of the physical phenomena happening at the ice-concrete interface. Next, an apparatus has been designed to perform ice-concrete shearing experiments in order to simulate ice-structure interaction. The main principle of theses experiments are illustrated in Figure 1.6.

The device will be able to perform double shear pull-out tests for varying pressures and holding times to account for different incoming ice floe mass and velocities which result in different pressures. Then, experiments of which the procedure will be explained in chapter 4, will be done to obtain relations between the extrinsic parameters and force required to shear the materials and visual observations will provide supporting information. Next, a data analysis will be performed followed by a discussion of the results after which

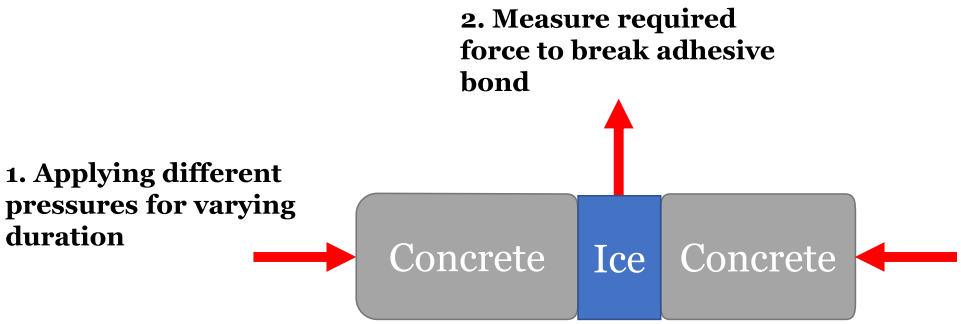

Figure 1.6: Basis of the approach taken in this thesis

conclusion have been drawn.

The analysis of the experimental results will help to answer the sub-questions. Answering question 1 will say something about the mechanism by which the adhesive ice-concrete bond breaks and could potentially investigate certain limits of the bond strength. Visual observations of the ice and concrete and analysing the pull curves after the experiments will form the basis of answering this question. The answer of question 2 helps with providing a link between adhesion and abrasion processes, and investigates the application on full-scale ice-structure interaction. Question 3 will be answered by looking at the output of the experiments. The output, after data processing, will be the force required to break the ice-concrete bond. The combination of the results will give an overview of the influence of the time, pressure, submergence and concrete surface on the strength of the ice-concrete bond. An empirical formula will be made to give a rough estimation of the force needed to break the ice-concrete bond for bonding in dry conditions.

1.6. Outline of this thesis

The structure of this thesis is as follows: First a literature study has been done to identify the current state of knowledge on concrete abrasion by ice, friction between ice and concrete and adhesion of ice on concrete, which can be found in Chapter 2. Chapter 3 outlines the design of the double shear apparatus and highlights the design considerations, the main features, and provides a validation of the measurements. The apparatus has been designed so it can simulate arctic offshore ice-structure interaction using standardised sized concrete and ice cylinders. Chapter 4 outlines the procedure which has been followed during the experiments. It shows the design of the experiments and provides information on the materials used. The Results of these experiments can be found in chapter 5. Chapter 6 consists of an analysis and discussion of the results which form the basis of the conclusions and recommendations found in chapter 7.

2

State-of-the-art ice-concrete interaction of structures in arctic regions

The interaction between ice and concrete is far from simple. The complexity arises due to both the ice's and concretes inhomogeneous characteristics. Factors such as surface micro- and macro structure, temperature, contaminants, ice type and concrete type all matter. In the experiments of this thesis, several of these factors will be remained constant to simplify the problem. To get more insight in the interaction between ice and concrete, a literature study has been done. This chapter first defines the different contact regions which are identified in ice-structure interaction. It then addresses abrasion of concrete due to ice loads, and gives an overview of the friction between ice and concrete, including the contribution of adhesion. Several mechanisms of ice-concrete adhesion are described afterwards and finally, a simple relationship between adhesion and abrasion will be illustrated.

2.1. Contact regions

When a moving ice sheet interacts with a structure, three different contact regions can be identified. A schematic overview can be seen in Figure 2.1, where the main contact zone, region 1, is the region where the highest normal loads are found. Region 2 experiences lower normal forces but higher shear forces. This is due to the forces from ice rubble being dragged along the surface of the concrete. Region 2 is also defined as the stick-slip area, where the ice shows unsteady sliding velocities. Region 3 is the steady sliding area which experiences the largest amount of accumulated debris, but the smallest forces. Jacobsen [17] has identified three regions in ice-structure contact. In region 1, the stresses by the large normal and shear forces exceed the resistance of concrete which results in damage. Here, region 2 is also identified as the stick-slip region, which sees a reduced abrasion compared to region 1. Several factors such as the velocity of ice, the angle of contact, and the type of concrete would determine the stick-slip cycles behaviour. Region 3 has lower stresses and experiences some abrasion. This research will focus on region 2, because the stick-slip behaviour is related to the adhesion between ice and concrete, where at low sliding velocities, the stick part is governed by adhesion.

2.2. Concrete abrasion due to ice loads

Concrete-ice abrasion can be defined as the surface degradation of concrete due to the interaction with drifting ice floes. Examples in the field show severe damage to the concrete after interaction with sliding ice. Different abrasion rates are measured at the same locations under varying pressures. A Finnish lighthouse in Helsinki measured an abrasion rate of about 300 mm over 30 years. Huovinen [15] found that the abrasion occurred mainly due the use of concrete which has a low resistance to frost, in combination with abrasion by ice.

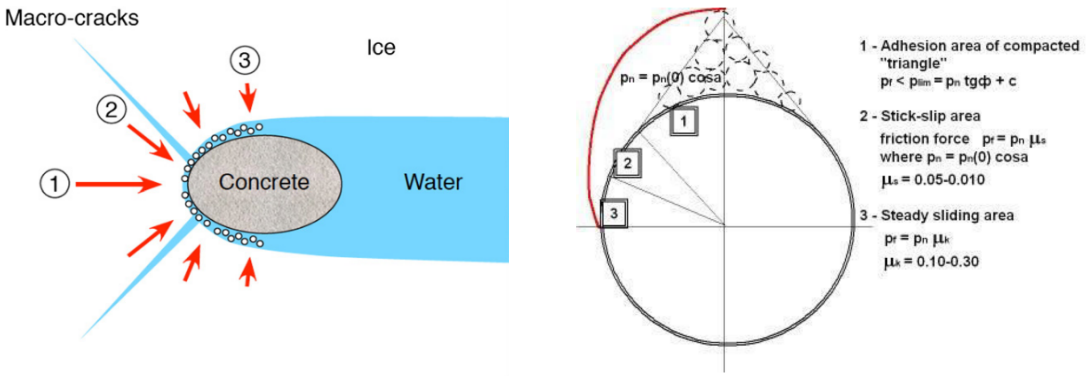

Figure 2.1: (a) Areas on surface of concrete GBS shaft with different abrasion effect. (b) The three regions as discussed by Jacobsen [16]

.

Figure 2.2: Abrasion by ice at concrete in Confederation Bridge at 0.3mm/year. [19]

In a more fundamental study, Huovinen [15] states there are many mechanisms which can cause abrasion of concrete by ice. The authors identified six different responsible mechanisms which are shown in Figure 2.3 and summed up below.

1. Cyclic mechanical loading: ice generates impact forces as it fails against a concrete structure, especially after the initial stage of general wear (described later in this section). The moving ice can give both a tensile and compressive force and is depended on the ice properties (size of the crystals, loading rate, temperature, ice type and aggregate size).

2. Freeze-thaw cycles: pressure build-ups due to repeating freezing and thawing of water in the concrete which causes micro-cracking and could eventually break the concrete. It appears that freeze-thaw damage resistance is increased for concrete with low permeability and air entrainment. Factors which affect the abrasion resistance of concrete are: air pores volume and space, water-cement ratio and the degree of saturation of the concrete.

3. Chemical effects of sea water: the mechanical properties of the cement may be changed due to interaction with chlorides in the sea water.

4. Carbonation of concrete. Due to interaction with the lime in concrete could change the pore structure of concrete.

5. Shrinkage of concrete: causes cracking which enables the penetration of moistures and salts.

6. Temperature gradients and changes: recurrent freezing of wetted concrete surfaces by waves exposes the concrete to high temperature gradients causes. The cement-stone bond will also deteriorate when temperature changes exceed dT =40°, which also increases the cracking of the cement.

Multiple experiments have been performed to study the effect of ice on concrete. Fiorio [11] focussed on the small-scale effects of friction-induced wear and found that the wear will cause concrete particles to enter

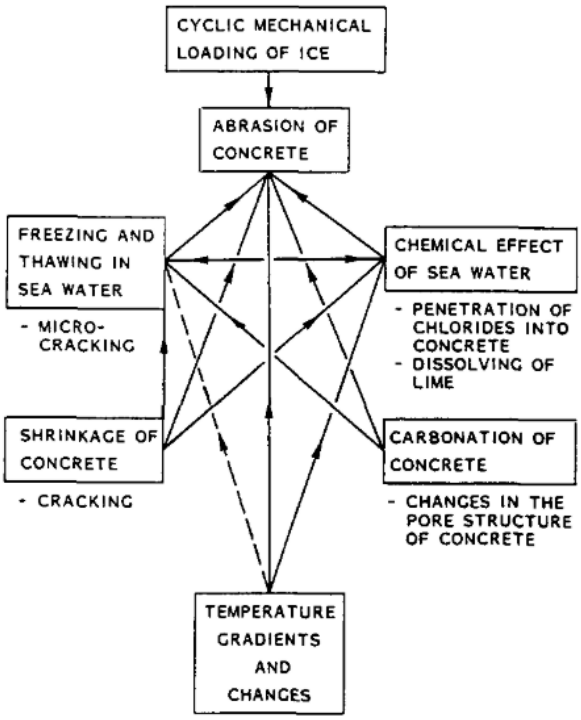

Figure 2.3: Abrasion by ice at concrete in Confederation Bridge at 0.3mm/year.

the interface, which influences the friction between concrete and ice. After erosion of the cement paste, a constant wear rate was measured and was dependent on the sliding speed and pressure, but not dependent on the average roughness. The author used the device shown in Figure 2.4 for his experiments

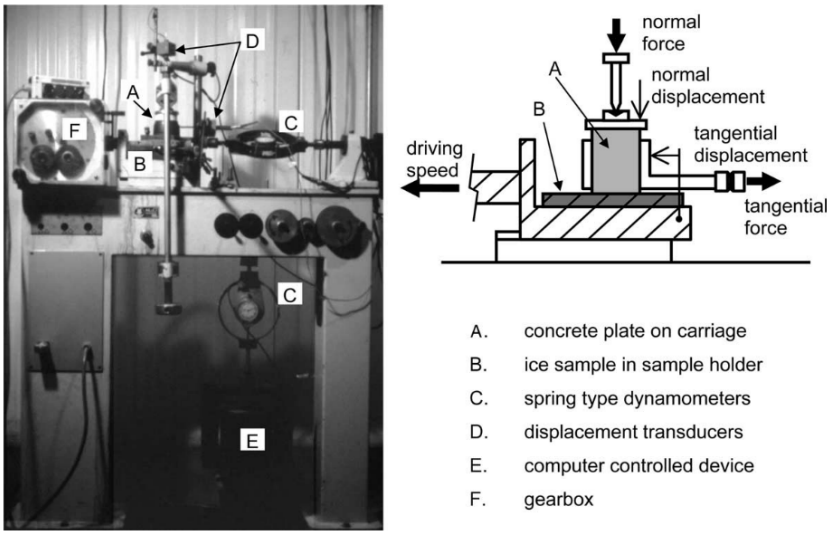

Figure 2.4: Friction apparatus as used by [11]

Shamsutdinova, Hendriks and Jacobsen [35] Performed a laboratory study of concrete-ice abrasion using two different concrete mixes, One stronger and a lighter weight mix. An abrasion machine was used in a cold room as showed in Figure 2.5. The machine slides at a velocity of 0.16m/s and an abrasion of 0.35mm was found after 3km of sliding, for the concrete samples with the lowest compressive strength.

The conclusion of this research was that for their given specific concrete composition, two mechanisms were responsible for the wear of the concrete which were the general wear and catastrophic wear. These two mechanisms occur in cycles.

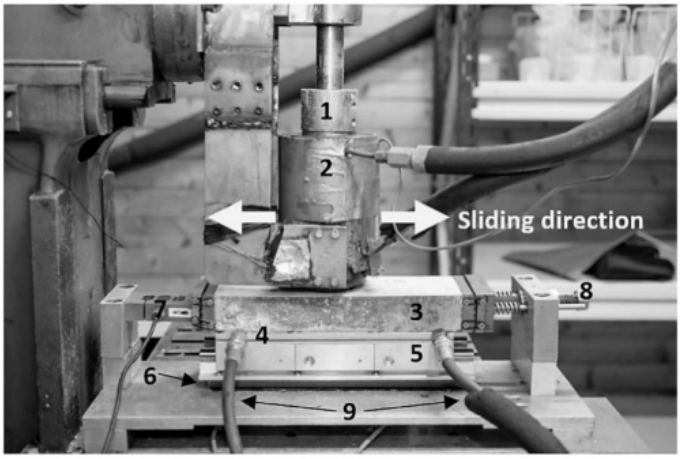

1 – Piston
2 – Ice sample inside the holder
3 – Concrete sample
4 – Aluminium heating plate
5 – Linear sliding system
6 – Vertical load cells (invisible, under the linear sliding system)
7 – Horizontal load cell
8 – Prestressing screw
9 – Inlet and outlet of heating liquid

Figure 2.5: Friction apparatus as used by Fiorio [11]

1. General wear

General wear is when ice and little wear particles flow along the concrete plate surface causes progressive erosion of the cement paste and small aggregate parts. The general wear has an initial stage and a permanent stage. The initial stage is characterized by a higher mean and maximum abrasion amount. In this stage, the upper layer of the cement paste is abraded which appears to abrade faster and is depended on the roughness. The permanent stage has lower abrasion rates and does not depend on the roughness. In the latter stage, the aggregate and sand particles are exposed which have a higher strength than the paste. When this occurs, the real contact area decreases and the stresses increase resulting in a tensile stress on the particle which is higher than the tensile strength of the material causing the material to wear down.

2. Catastrophic wear

This mechanism happens when general wear first weakens the cement paste-aggregate bond after which sudden ejection of aggregate particles occurs. This is illustrated in Figure 2.6 where in (a), general wear wears down the concrete's outer layer until the aggregate particles are exposed (b). The rate of the general wear slows down until the catastrophic wear causes the ejection of aggregate particles (c). Huovinen [15] also identified this phenomenon and used it to model the abrasion depth.

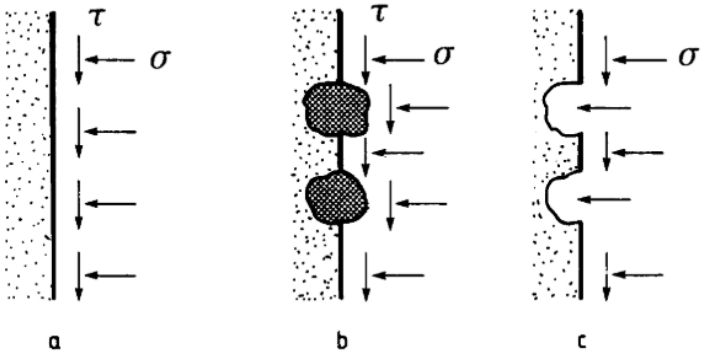

Figure 2.6: Illustration of general wear (a), catastrophic wear(b) and start of repetition of abrasion cycle with general wear (c)

Jacobsen [17] came to the same conclusion that concrete debris particles can act as sharp abrasive particles which enhance damages as the ice drags them along. Among this mechanism, two other mechanisms

may also contribute to abrasion damage. Tensile stresses created by asperities of ice sliding on concrete are sufficient to create micro cracks and water forced into surface defects can induce pressures which propagate these cracks. An illustration of these conditions is shown in Figure 2.7 They also Concluded that no freeze/thaw cycles were required for concrete abrasion.

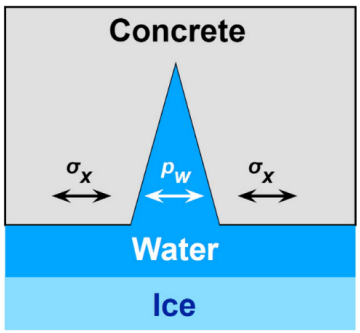

Figure 2.7: Ice pressure induced water penetration causing microcracks in concrete

After ice adheres to concrete, re-initiated movement of the ice sheet can also cause tensile forces creating these micro cracks.

2.3. Friction between ice and concrete

Much past research focused on the kinetic friction when ice slides over a certain material for different velocities. there has been much disagreement among results of different experimental studies. [13] Bowden and Hughes [4] came to the conclusion that water would act as a lubricant when the ice would be heated from the friction resulting in a lower friction factor. They found higher friction factors for when sliding velocity was relatively "low" and independent of normal load.

Barnes, Tabor and Walker [1] aimed to determine the creep behaviour of polycrystalline ice by studying ice friction. Here, the tip of a conical piece of ice was sliding over a test surface. The conditions were such that strong inter-facial adhesion appeared. Observed was a near proportionality between the friction and normal pressure and nominal area. Frictional heating resulted in the melting of the ice at the surface which causes the friction to reduce, having the water as a lubricator. The positive temperature difference when sliding was found to be estimated by:

$$\Delta T = \frac{\mu N g v}{4r} \frac{1}{k_i + k} \tag{2.1}$$

Where:

μ = friction coefficient
N = the normal force
g = acceleration of gravity
r = radius of circular contact area
v = velocity between surfaces
k_i =thermal conductivity of the ice
k = thermal conductivity of the interacting material

The Authors [1]also noted that "At very low sliding speeds recrystallization is produced in a thin zone of ice close to the interface, the basal planes being oriented preferentially in the plane of sliding". Enkvist [8] examined the friction of saline ice along the hull of a ship by pulling sleds across natural ice in the field and in the laboratory by pulling metal plates across ice. They found that friction was practically independent of velocities, for a velocity range of 0.25 to 1.75 m/s. A decreasing friction factor was observed for increasing normal loads (until a pressure of 16kPa in the field and approximately 1.3kPa in the lab). Also, the amount of roughness seemed to no impact the friction but the type of surface roughness did. Ryvlin [25] has had similar observations when towing steel sheets over both freshwater and sea ice. He observed an increasing kinetic friction coefficient for a decreasing pressure under 10kPa. For pressures over 10kPa, no dependency has been found. Evanse [10] theorized, based on the same idea as Bowden and Hughes [4], where the lubrication of

meltwater is present at the interface, and suggested that the friction coefficient between ice and a material is not determined by the dissipated energy when sliding the surfaces but rather by the heat flow at the contact surface.

Interestingly, Saeki [26] found no effect on the kinetic friction coefficient for different normal pressures. They investigated ice friction of various materials such as steel and concrete plates, by moving a cylindrical ice sample over test surfaces. The friction factor was however influenced by the type of material used. Calabrese [6] also found no influence of normal load on the ice friction coefficient.

Oksanen [23] Theorized that the dissipation of heat caused by friction between ice and a material is through the conduction into the bulk solids and by the latent heat of the meltwater at the interface. The theory states that the friction coefficient depends on the ambient temperature. Increasing normal loads caused a decrease in friction.

Also, more recently, friction between ice and concrete has been tested in laboratory using different methods. Most test set-ups have made their own apparatus and tests are focus ed on the kinetic friction coefficient for different pressures and sliding speeds. [12] performed cyclic friction tests using micro-concrete plates and laboratory grown columnar ice. The output of the experiments are presented in terms of friction coefficients. A schematic representation of the friction apparatus is shown in Figure 2.8. It is a modified direct shear box machine which is designed for solid mechanics studies but is now capable of performing inter-facial shear. It used a carriage which had a concrete plate attached so it could move horizontally. S2 columnar freshwater ice was used and shaped into cylinders which were held in place in the apparatus.

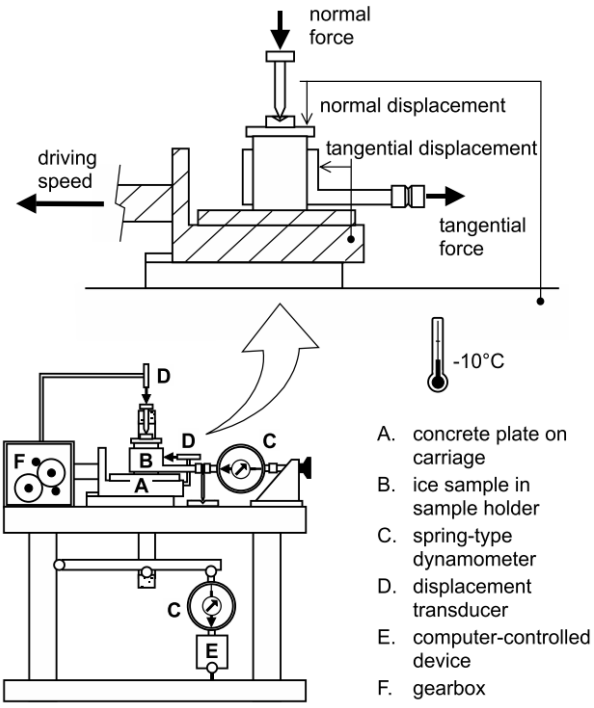

Figure 2.8: Friction apparatus used by Fiorio [12]

The effects of the normal stress on the final friction coefficient appeared to be positively related and had a stronger relation for higher sliding speeds. The results are showed in Figure 2.9.

Their analysis revealed two physical mechanisms responsible for friction for the conditions used, which are: (1) the visco-plasticity of ice, and (2) ice-concrete adhesion.

1. The visco-plasticity of ice could explain the influence of sliding velocity and average roughness of the surface of friction. The number of actual contacts between an ice surface and concrete plate is determined by the average roughness. Based on the assumption that, for a given sliding speed and normal load, the number of actual contacts will decrease as a function of average roughness, an increase of average roughness will result in an increase of the actual stress. This would then result in more penetration of the ice in the concrete asperities, resulting in an increase of the strain rate in ice near the

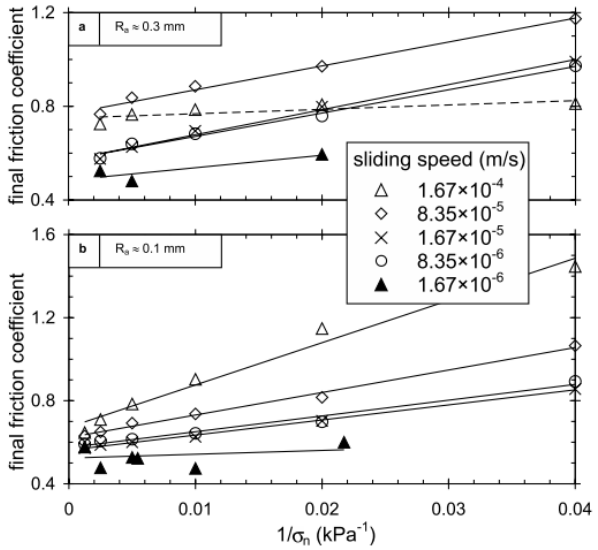

Figure 2.9: Effects of normal stress on the coefficient of friction [12]

asperities. Because of the viscoplasticity of the ice, the tangential stress and thus the friction, should be higher for a higher average roughness. The above described mechanism can visualised by Figure 2.10.

2. The ice-concrete adhesion seems to be the main component of friction at low normal stresses. In the latter case, the shear stress needed to break the adhesive bond is governing the friction. The influence of time is explained as that over time, the real contact area increases due to viscoplasticity of ice, which causes higher friction.

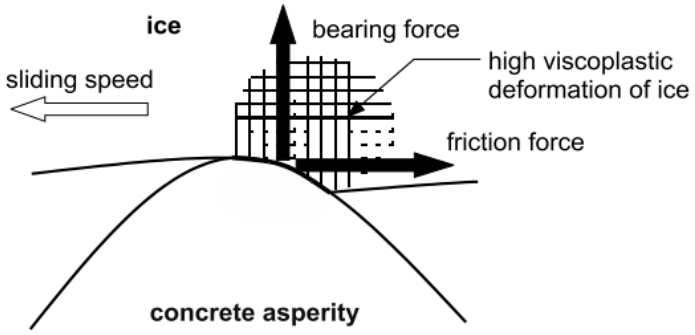

Figure 2.10: Horizontal component of normal stress causes friction

Both numerical simulations by Singh [36] and extrusion test by Sayed [30] [29] showed that the flow of a crushed ice layer is mainly governed by the friction between ice-structure friction. Several experiments showed that the amount of wear is related to the sliding distance.

2.4. Ice-concrete adhesion

Adhesion is defined as: "the state in which two dissimilar bodies are held together by intimate inter-facial contact such that mechanical force or work can be transferred across the interface" [7]. This section will describe the most known adhesion theories and look into ice-concrete adhesion.

2.4.1. Adhesion theory

The forces responsible for holding the two interfaces together may result from: Van der Waals forces, electrostatic attraction, or chemical bonding. Also, mechanical theory can be responsible for adhesion. Some

known adhesion theories are described below.

Mechanical adhesion theory
Penetration of the adhesive into pores, surface irregularities and cavities is the effect causing adhesion according to the mechanical theory. Mechanical interlocking gives a positive contribution to the adhesive bond strength. It is seen frequently that adhesives form a stronger bond between porous rough surfaces than smooth surfaces, although this is not always the case. Several factors may increase adhesion after abrading the surface of the substrate, possibly caused by mechanical interlocking or increase in real surface area.

Electrostatic adhesion theory
This theory suggests that electron transfer between adhesive and adherend is responsible for the adhesive force. Support for this theory comes from the fact that electrical discharge has been noticed when an adhesive is peeled from a substrate.

Diffusion theory
Adhesion developed through the inter-diffusion of molecules between the adhesive and the substrate is suggested by diffusion theory, which usually happens when both materials are polymers with molecules which are able to move. Diffusion theory is usually applicable for solvent cementing or heat welding thermoplastics situations. This theory does not seem to be very applicable to ice-concrete bonding.

Wetting theory for adhesion
Molecular contact between two materials and the surface forces that develop are the main sources of adhesive strength in the wetting theory. Wetting is the process of establishing continuous contact between the adhesive and substrate. The surface tension of the adhesive has to be lower than the critical surface tension of the substrate in order for wetting to occur. Figure 2.11 illustrates wetting of an adhesive over a surface.

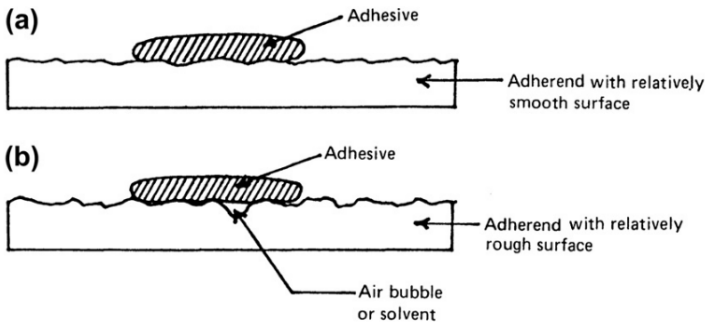

Figure 2.11: (a) complete wetting. (b) Incomplete wetting [7]

Chemical Bonding
Hydrogen bonds, covalent bonds, ionic bonds are all attributable for the formation of an adhesive bond to surface chemical forces. Covalent and ionic bonds provide much higher adhesion values than those by secondary forces such as hydrogen bonds and Van der Waals forces. Covalent bonds won't necessarily exist in ice-concrete interaction as it requires mutually reactive chemical groups.

According to Ebnesajjad [7], it is to difficult to fully ascribe one mechanism responsible for adhesion and that it is most probable that a combination of different mechanisms are responsible for the adhesive bond. In the case of this research, ice is seen as the adhesive and concrete as the substrate.

2.4.2. Other research on ice-concrete adhesion
The majority of the research on ice adhesion is focuses on marine-icing, which is a problem in arctic conditions combined with severe winds causing significant weight of ice to adhere to eg. ships and other floating structures. Many properties such as: chemical composition, surface morphology, stiffness and thermal expansion coefficient of substrate material are related to the adhesive strength of ice. Makkonen [21] also states that temperature is an important factor. They found that : Generally, the higher the water contact angle of

the material the lower the ice adhesion strength. The uneven and complex surface in concrete will cause many different contact angles to occur. ChenyuWang [38] performed a laboratory test using commercial instrumentation to test the ice adhesive strength of an ice cylinder on a polymer coating. Its advantage is that it doesn't need a custom build apparatus. Zou [39] has found that the adhesion strength are lower for samples with a more smooth surface when compared to rougher surfaces. It was found that the ice adhesion strength is correlated to the water contact angles of the samples only for surfaces with similar roughness: the ice adhesion strength decreases with the increase in water contact angle. Ice adhesion seems to be a complex phenomenon depended on many factors and many of the adhesion mechanisms are poorly understood. Jia [18] performed adhesion strength tests of freshwater frozen ice to concrete material at five different temperatures (-2 °C, -4°C, -6°C, -8°C and -10 °C) and a varying displacement rate of between around 10-4 - 10 mm/s. The device used was a compression testing machine for ice, powered by an electro-hydraulic system to apply the load. The device can be seen in Figure 2.12

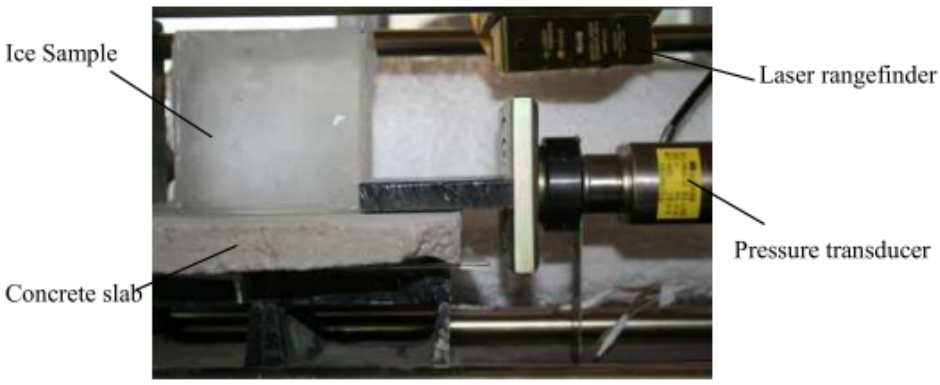

Figure 2.12: Ice adhesion strength test device [18]

The author collected local ice samples on November 26, 2009 at 46°36'N, 125°16'E and cut the large blocks into small 10 cm$X$10 cm$X$10 cm blocks. the ice was then put into iced-water and then quickly frozen to the concrete surface. The machine then exerts force on the ice block with a constant displacement rate in different temperatures. The results can be seen in Figure 2.13.

Concluded here was that:

1. The frozen adhesion strength is increasing with an increasing displacement rate at the tested rate.
2. A decreasing temperature will see an increasing peak frozen adhesion strength.
3. The concrete slab with a rougher surface sees higher adhesive bond strength than that to a smooth concrete surface.

Schulson [34] performed systematic slide-hold-slide experiments on both freshwater ice and first year sea ice at a temperature of -10 °C. A schematic representation of the double shear device used can be found in Schulson's work [33]. The Author used low sliding velocities, ranging from 10^{-6} to 10^{-4} ms^{-1} under a pressure of 60 KPa for holding times ranging from 1 to 10^4 s. They found that for an increasing hold time, the force to re-initiate sliding would increase for an increasing holding time following a threshold period. It appeared to have a large effect on the coefficient of static friction for both the freshwater ice and first year sea ice. The effect is called static strengthening and the influence of the holding time is illustrated in Figures 2.14a and 2.14b.

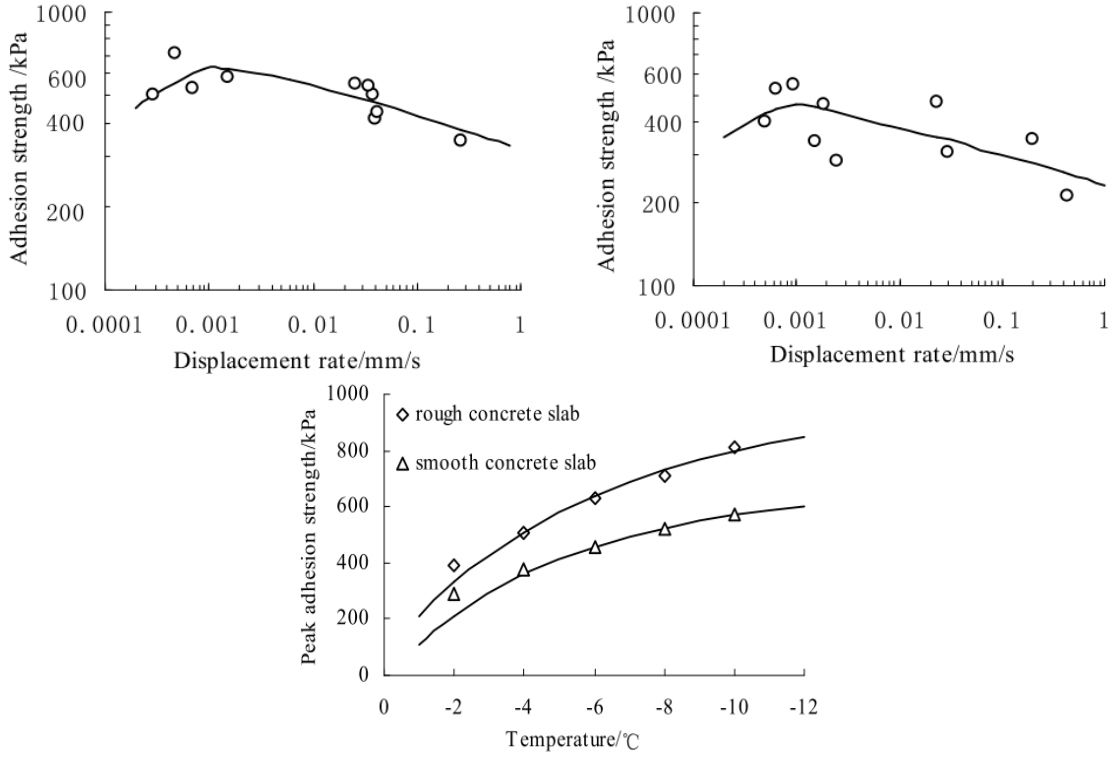

Figure 2.13: Adhesion strength versus displacement rate of the (a) rough concrete slab and (b) smooth concrete slab at 6 °C. (c) Adhesion versus temperature. [18]

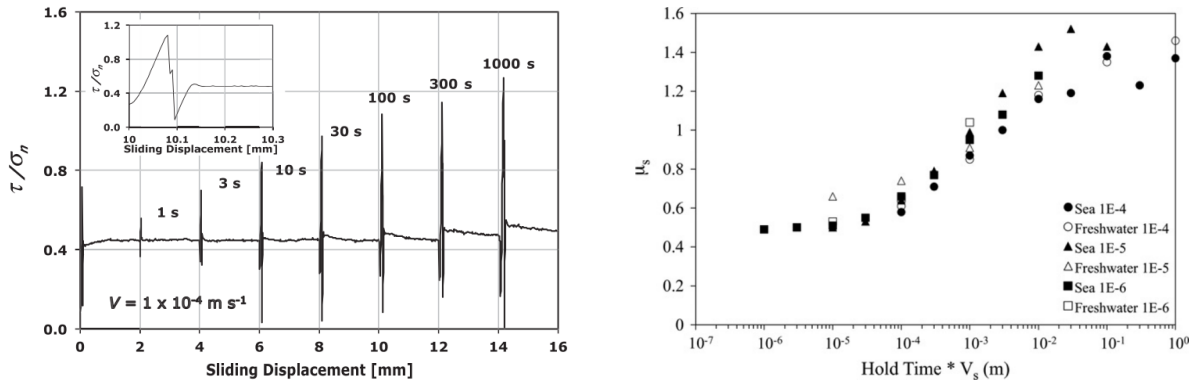

(a) Force versus hold time

(b) Influence of hold time to static friction of ice

Figure 2.14: Slide-hold-slide experiments [34]

2.5. Relationship between adhesion and abrasion

The adhesion of ice to concrete seems to be linked directly and indirectly to the abrasion of concrete. In a direct manner, the adhesive bond can create strong tensile stresses causing wear of the concrete surface and aggregate particles as described in section 2.2. Also, the rate of abrasion depends on temperature, contact pressure, relative velocity and the total sliding distance of the ice sheet along the concrete surface. So abrasion due to sliding is partly governed by the friction coefficients and in stick-slip sliding of ice along concrete, the friction seems governed by the adhesion. It is therefore useful to know more about the adhesion of ice to concrete in order to better understand the abrasion process. This study will therefore focus on investigating the adhesion using experiments which will be explained in the next chapter.

3

Apparatus design for shearing an adhesive ice-concrete bond

In order to examine the influence of variables: pressure, holding time, surface characteristics and submergence on the adhesive strength between ice and concrete, an apparatus has been designed to perform direct double shear tests. The goal has been to design a simple apparatus which can easily control the above mentioned variables. First some preliminary tests have been performed using a simple double shear pull-out apparatus which enabled the use of ASTM defined 6" diameter concrete cylinders. Based on the experience and results from this preliminary set-up, a newer apparatus has been designed and used to reduce friction-induced errors and handle uncertainties which arose from using the preliminary device.

3.1. Design considerations

The choice of equipment used for the apparatus and the main features of the design are based on a set of design considerations which will allow for relatively easy but controlled experiments. The design considerations are outlined in this section.

3.1.1. Standardisation

Standardisation is used widely to help maximize compatibility, repeatability, quality, safety and to reach more beneficial goals. Research on ice-concrete interaction has room to improve on this front and therefore, one of the focusses of the ICEWEAR project is to examine standardisation of test methods. This way, comparison with other studies will be better facilitated. Conventionally sized samples will be used according to the ASTM (American Society for Testing and Materials) International standard testing methods. This is one of the key drivers for the decisions on the dimensions of the concrete cylinders and ice puck and hydraulic actuator used for the shearing.

3.1.2. Scale of the apparatus

The apparatus has been designed in such a scale that it allows for representative cross-sectional area of ice-concrete contacts using standardized cylinder sizes, but still remain good portability. This is desired also to incorporate some other design considerations, such as the ability for submerged tests where the device has to be moved from one position to another.

3.1.3. Double shear versus single shear to eliminate machine friction and moments

To simulate a structure in a polar marine environment, where an ice sheet slides along a structure, a shear device will be used. In much of the research done on ice induced abrasion by concrete, the ice and concrete interact on one surface. In this research, a double shear device will be used which brings about two main advantages.

1. Elimination of moments

When trying to obtain pure shearing, it is difficult to not also induce a moment, since the actuator cannot

exert force on exactly zero distance from the interface without inducing machine friction. A solution to this is the use of double share to eliminate the moments induced when trying to shear off the ice. The assumption here is that the moments caused by the little distance between the ice holder and concrete surface is eliminated. It is assumed that the moments on both sides are of the same magnitude and opposite direction.

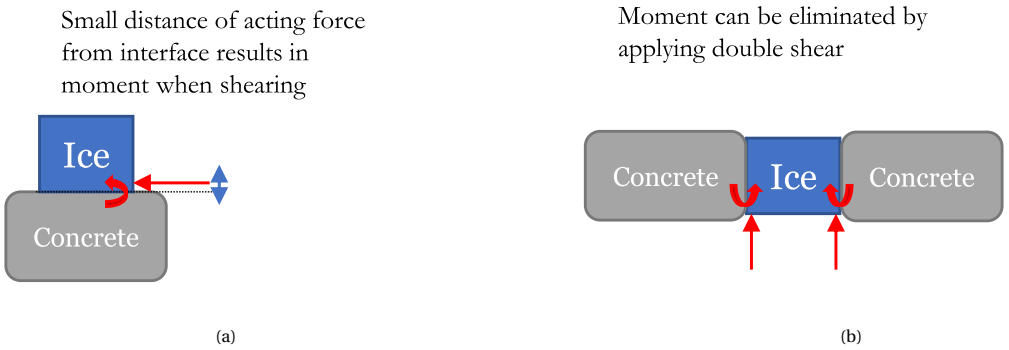

Figure 3.1: The advantage of double vs single shear by eliminating the moment

2. Removing machine friction

In a single shear setup, friction between two moving parts in a machine can be present in a situation where pure shear is desired. The red ellipse in Figure 3.2 indicates a set-up which pictures the idea where machine friction could become a problem. The measured force would then also include a friction force from moving machine parts.

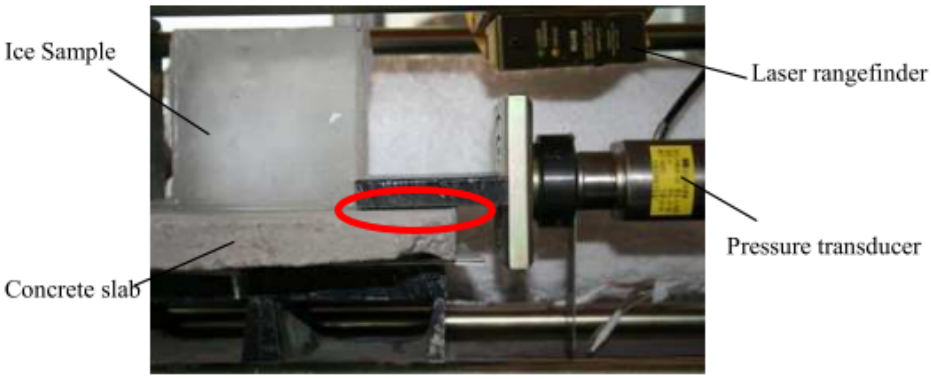

Figure 3.2: Ice adhesion strength test device [18]

The double shear will eliminate the possibility of machine friction in the pull out force.

3.1.4. Accurate and sustained application of normal loads

The device needed to be able to apply sustained loads on the ice-concrete contact in order to keep in control of the extrinsic parameters and perform reliable analyses. High accuracy of the load is also required to increase the repeatability of experiments.

3.1.5. Submergence of test set-up

The final design will have bottom and side enclosures so the whole set-up can be submerged to mimic real offshore conditions where wetted ice comes into contact with saturated concrete. The fact that submergence of the set-up has been one of the aims of this design has been the driving factor to use a mechanical lever-arm gravity system. Compared to an electrical induced actuator, it has the advantage of not having to submerge any electrical components, reducing risk of failure and increasing the overall simplicity.

3.1.6. Schematic representation of intended mechanism and forces in the set-up

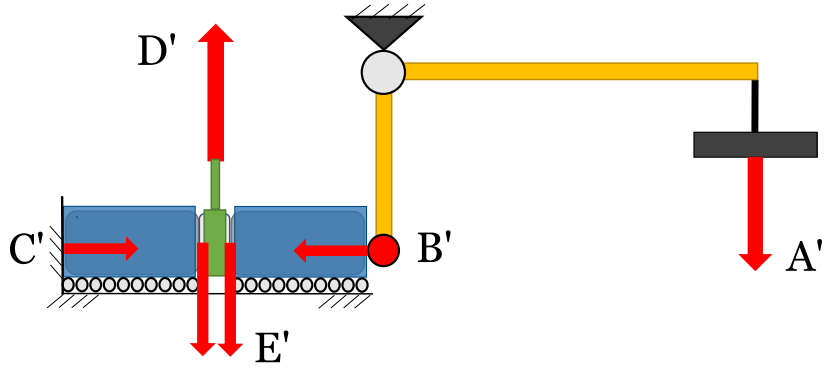

Figure 3.3: Final set-up for experiments

Figure 3.3 schematically shows the forces which are present in the set-up. Force A' is the gravity force which can be varied by adding or removing weights to a hanger which is attached to the lever arm. This gravity force will be translated to a horizontal orientated pushing force, force B', at the contact between the roller bearing and the concrete cylinder. C' is the reaction force which results from the normal force pushing back at the concrete cylinder from the side wall of the metal casing. Force D' is realised by activating the hydraulic actuator, which pulls the ice puck up. Force E's is the reaction force, consisting of the static friction between the ice and concrete and the force resisting the breaking of the ice-concrete bond. These forces are summarised in Table 3.1 below.

Table 3.1: Description of forces desired in the set-up

Component	description
A'	Gravity force of variable weights
B'	Pure horizontal force by lever arm and roller bearing
C'	Reaction force by a solid frame
D'	Force induced by pulling actuator
E'	Friction force at ice-concrete interface

3.2. Final design of apparatus

Taking into account the considerations of section 3.1 and findings of the preliminary design and its outcomes, a new design was made. The main features will be described in sections 3.2.1 to 3.2.2 below and makes the force scheme in Figure 3.3 achievable.

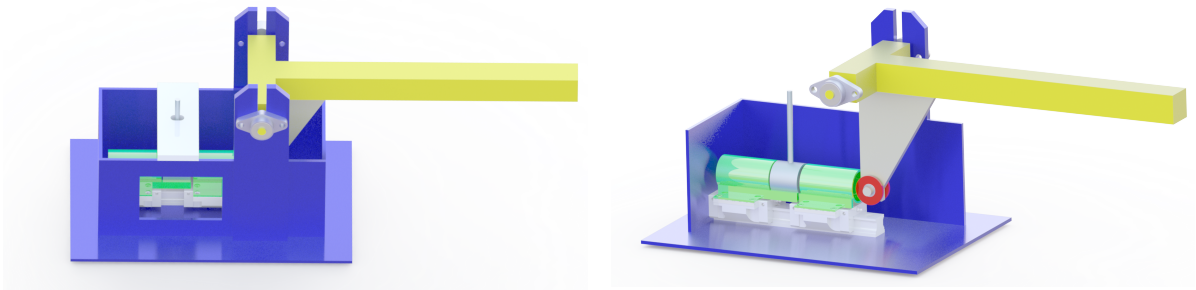

(a) Side view of the apparatus

(b) Side walls suppressed to show the inner parts

Figure 3.4: 3D SolidWorks images of the designed double shear apparatus

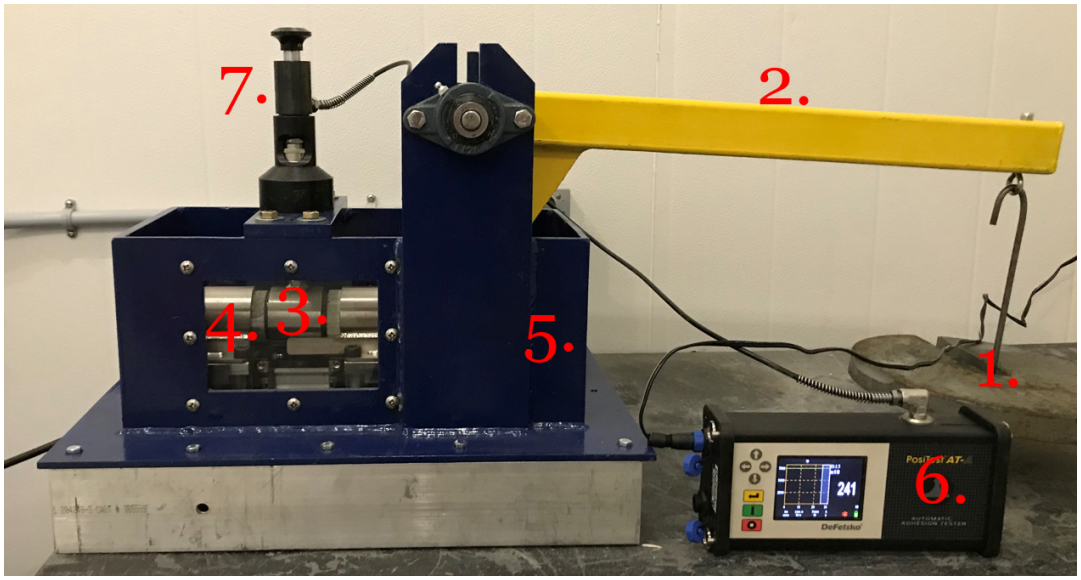

Figure 3.5: Final set-up for experiments

The items in figure 3.5 are described in table 3.2

Table 3.2: Parts of the set-up with their function

Part	Device	Function
1	Weight	Exerts force on the lever arm
2	Lever arm	Transfers load to apply pressure at ice-concrete interface
3	2" diameter ice puck holder	Positions the ice and exerts force on ice puck
4	2" diameter concrete cylinder holder	maintains position of concrete
5	Outer metal casing	To allow for submerged tests
6	DeFelsko Positest At-A	contains hydraulic system to actuate part 7
7	Actuator assembly	Pulls the ice-puck when initiated by part 6

3.2.1. Lever arm gravity system (parts 1 & 2)

The pressure is varied by changing the weights(1) hanging on the lever arm (2). A roller bearing is placed at the point where the lever arm touches the concrete to ensure only force translation and eliminates the possibility to transfer moments. The lever and weights will result in accurate and sustained load applications over extended periods of time.

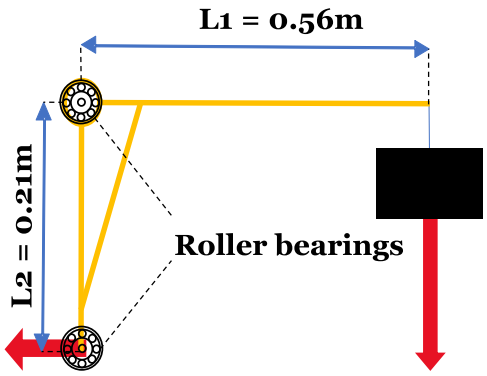

Figure 3.6: Dimensions of the lever arm

The force exerted by the weights on the concrete cylinder, F_{side} can be calculated by:

$$F_{side} = (W_{leverarm} + W_{hanging}) * g * (L_1 / L2) \tag{3.1}$$

Here, $W_{leverarm}$ is taken into account as weight required to keep the arm at a horizontal level and is measured by attaching a load cell at the end of the lever arm , at the same horizontal position as where the weights have been hanged. $W_{leverarm}$ was measured to be equal to 1.3kg. $W_{hanging}$ is then the part in the equation which allows for varying the pressure.

The diameter of the concrete and ice cylinders' surface, $D_{surface}$ is 2", which is 0.0508 m. The area $A_{surface}$ is then:

$$A_{surface} = \pi / 4 * D^2_{surface} \tag{3.2}$$

The pressure on one surface, $p_{surface}$, or normal load σ_n, is then calculated by:

$$\sigma_n = F_{side} / A_{surface} \tag{3.3}$$

The friction of the rotating bearings is neglected. Table 3.3 below shows the resulting pressures from the hanging weights:

Table 3.3: Pressures on the ice-concrete interface resulting form hanging weights

Weight (kg)	**Pressure (kPa)**
2.5	51
10	150
22.5	316
50	682

3.2.2. Ice puck holder and concrete cylinder holder (parts 3 & 4)

Part 3 is made from a stainless steel ring with a bolt welded on the top. A piece of threaded rod is used to attach part 3 to part 2 and when loaded up with an ice puck, it looks like Figure 3.7.

Figure 3.7: Part 3: stainless steel ice puck holder

Part 4 consist of a sliding bearing with a welded stainless steel cylinder to keep the concrete cylinders in place. Since this research aims to investigate pressures up to more than 600 kPa, a little design task has been done to predict the maximum force and resulting bending moment on the sliding bearing.

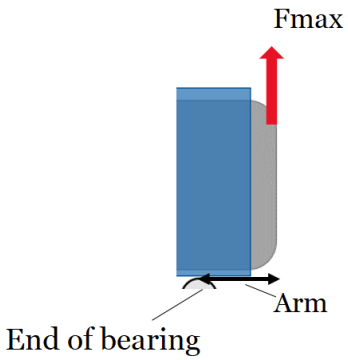

Figure 3.8: Arm resulting in bending moment in part 4

The weight of the stainless steel cylinder has been calculated to be less then 1/250th of the maximum force and has therefore been neglected in the capacity calculation of the sliding bearing. The maximum force which the DeFelsko Positest can exert is 7550N. With an assumed maximum arm of 0.05m, as seen in Figure 3.8, the maximum moment which the sliding bearing should withstand is than 377.5 Nm. Combining this with the dimensional desires to hold a 2" concrete cylinder, the McMaster-carr 9184T55 Maintenance-Free Ball Bearing Carriage has been chosen. It has a pitch moment capacity of over 555 Nm, which is sufficient to endure the moment resulted by the maximum force from the DeFelsko.

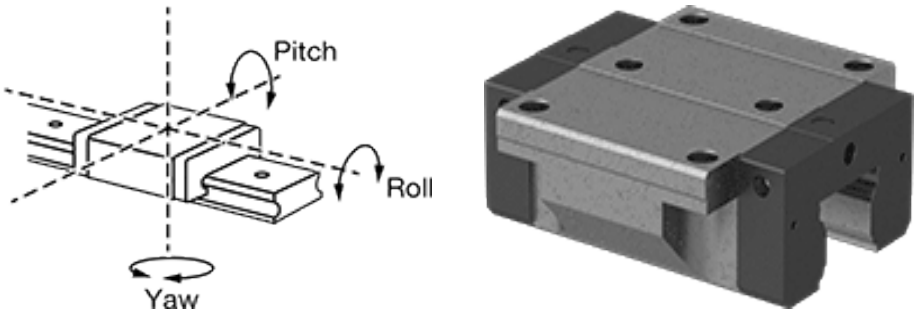

(a) Schematic illustration of the sliding bearing

(b) 3D CGI of the sliding table

Figure 3.9: Sliding bearing and sliding table system

3.2.3. Box shape metal casing

The box shaped metal casing is designed to enable for submerged tests. The offset of the lever arm gravity system permits submergence while keeping the data acquisition equipment dry. It has a window for viewing and filming for both the submerged and dry tests to compensate the decrease in visibility the metal casing brings about. The lever arm has a slotted attachment so the bearing can be adjusted to ensure perfect line-up with the lower part of the roller bearing with the concrete cylinder.

3.2.4. Hydraulic actuator system to pull out the ice (Parts 6 & 7)

The hydraulic actuator pulls out part 3 in vertical direction. The actuator is driven by part 6, which is the DeFelsko PosiTest At-A Pull-off adhesion tester. Normally used for testing the adhesive strength of coatings to metal, wood, concrete and other rigid surfaces, now modified to use in this experiment. The device conforms to international standards including ASTM C1583/D4541/D7234/D7522, ISO 4642/16276-1, EN 1542/12004-2, AS/NZS 1580.408.5 and others. The use of this device enforces the goal of standardisation.

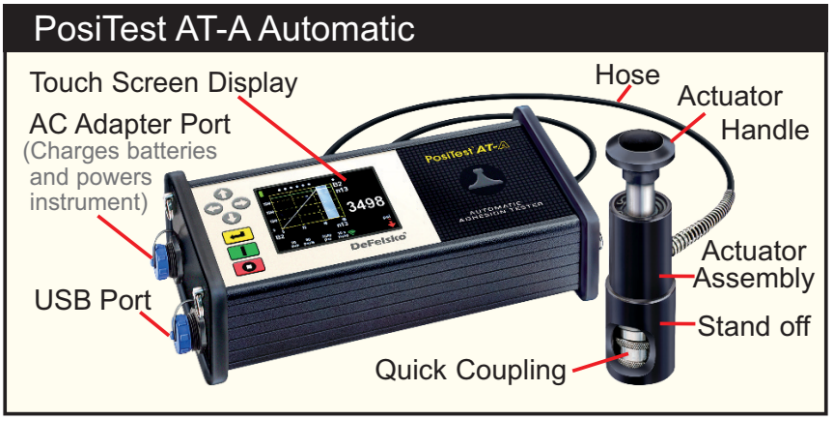

Figure 3.10: DeFelsko Positest AT-A adhesion tester

It is calibrated to apply force with a 1% accuracy. The device's manual states to pull with a constant rate of 300N/s after a build-up range until 220N. By pressing a button, the device initiates the pull and part 2 will start pulling with a steady rate. As an output, the device gives the force at which the devices measures a 'fail', which is when the adhesive bond breaks. How the software of the device measures a 'fail' is not clear, but probably it measures a sudden change in voltage in the internal load cell or it measures a sudden acceleration.

3.2.5. Data collection

In order to obtain force measurements throughout the whole pull motion, the DeFelsko Positest has been set-up for continuous data stream mode and is connected to a computer using a USB cable. On the PC, HyperTerminal software has been used to open a serial port in order to receive information from the DeFelsko Positest. The DeFelsko Positest now sends the readings from its inner load cell to the computer which can record the data in text files using HyperTerminal software. The results of a preliminary test can be seen in Figure 3.11 below.

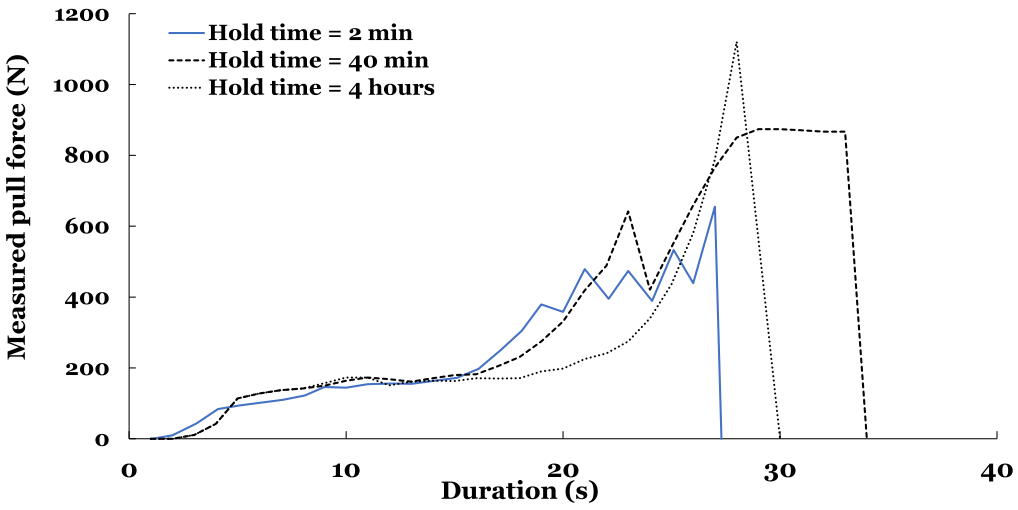

Figure 3.11: Results measured from DeFelsko data stream

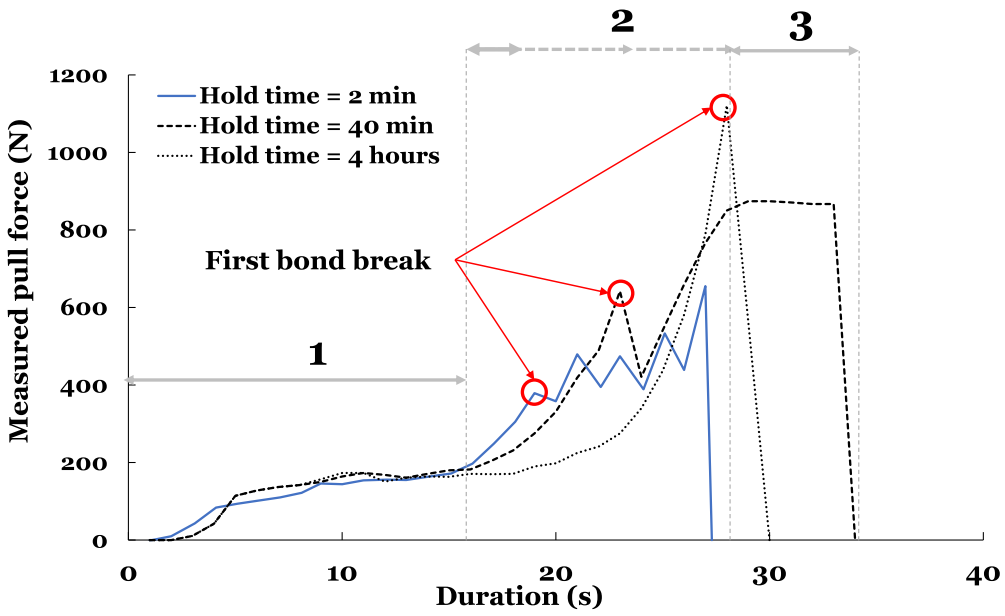

Figure 3.12: Results measured from DeFelsko data stream with interpretation

The three different regions in the graph in Figure 3.12 describe three different regions in the process of pulling out the ice puck. In region 1, the load is building up slowly until it reaches a threshold of about 220N. Stage 2 is the main pulling stage, where the actuator pulls at the programmed rate. At stage 3 the device registers a 'fail' of the bond and stops pulling and, unfortunately, stops measuring.

When analysing the data from the DeFelsko data stream, the sampling rate of the DeFelsko data stream appeared to be about 1Hz, which can also be noticed when looking at the curves in Figure 3.11 above. It is unclear what happens exactly at region 2 in the graph and the resolution seems low. Also the device stops measuring after it registers a fail, while it could be interesting to see what happens after the bond breaks. Therefore, an adjustment to the set-up has been made and a load cell has been added between part 1 and part 2 which can be seen in Figure D.1. The load cell is then connected to a Data Acquisition Center (DAC), which consist of a National Instruments USB interface and a C-series Universal Analog Input Module, which converts the analog voltage from the load cell to a digital signal. The DAC's sampling rate is set to the maximum of the module, which is 99Hz.

An overview of the set-up is given in Figure 3.13 of which the parts are described in table 3.2. Parts 8 and 9 are the 500kg capacity load cell and part 9 is the DAC.

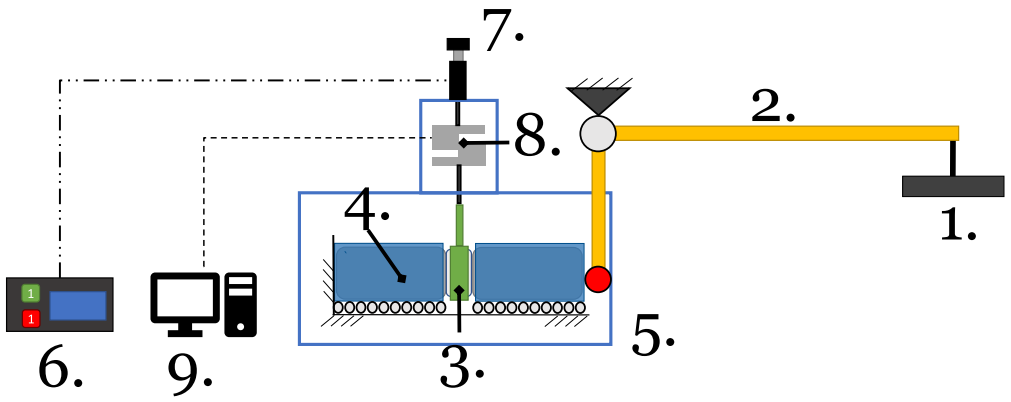

Figure 3.13: Schematic set-up for experiments

The load cell gives a much higher resolution than the data from the DeFelsko Positest as can be seen in

Figure 3.14. Here, a direct pull has been performed using 682 kPa pressure on either sides of the ice. LabView software is used to record the voltage and converts it to Newtons using the parameters from the Load cell data sheet. The output of the recording is then 1 column with the measured force on the load cell and the time at which this force is measured.

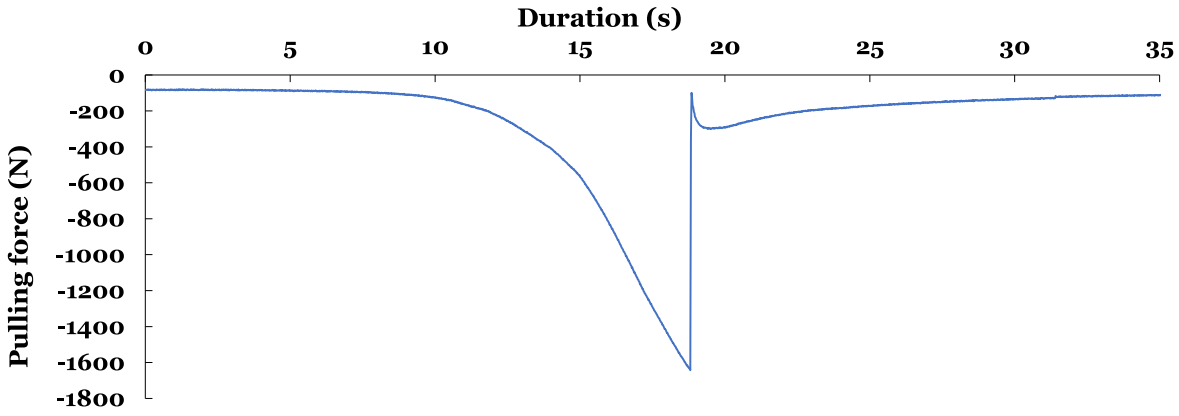

Figure 3.14: Data acquired from load cell

3.3. Validation of the load cell measurements and the hydraulic actuator

To test if the measured outcomes from the load cell into the Data Acquisition Center are valid, and to check if the hydraulic pulley pulls with a constant rate, two types of tests have been designed and performed. The test have been done using weights with known mass, and are outlined below.

3.3.1. Hanging weights with known mass to load cell

The set-up used for this test is illustrated in Figure 3.15. The measurements from the load cell can be seen in Figure 3.16 and the values in the fourth column of Table 3.4 are obtained by averaging over the flat sections of the graph which are indicated by numbers 1 to 6.

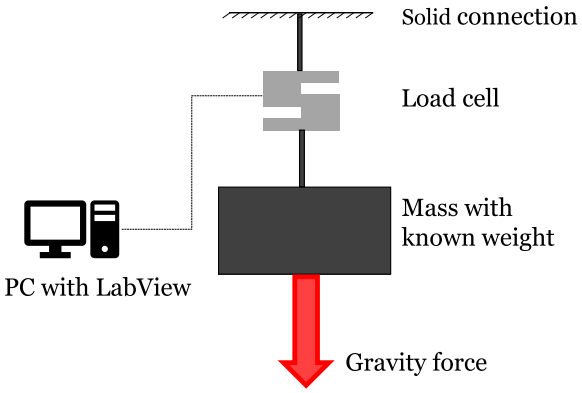

Figure 3.15: Schematic set-up used for verifying the load cell's measurements

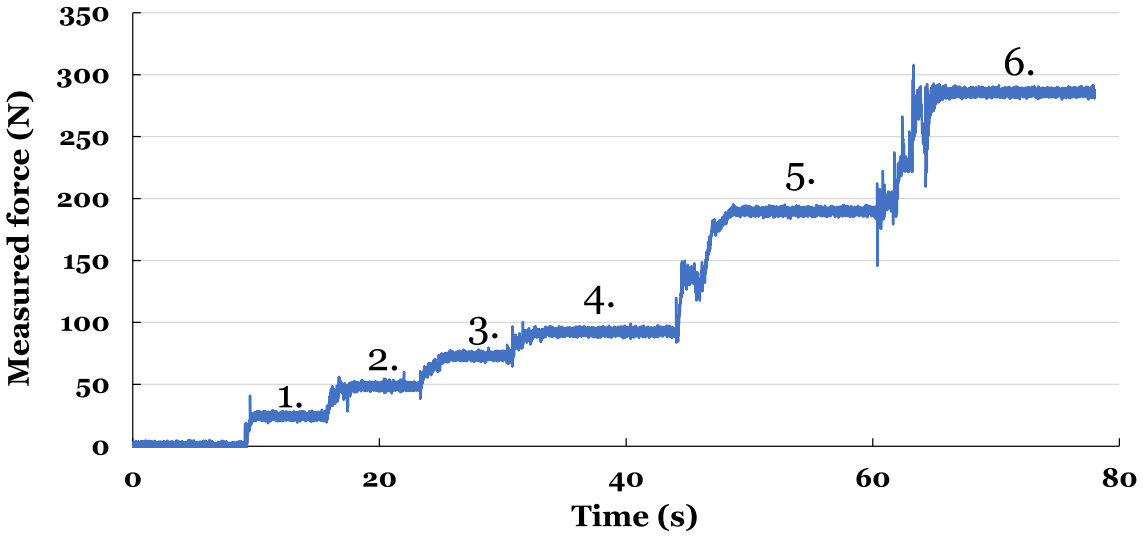

Figure 3.16: Graph obtained from the verification procedure

The error is than calculated by taking:

$$Error = 1 - \frac{Measured force}{Theoretical gravity force} * 100\% \tag{3.4}$$

Table 3.4: Values used in load cell calibration, measured output, and error

# in graph	Weight (kg)	Resulting gravity force (N)	Measured force (N)	Error (%)
1	2.5	24.5	24.3	0.9
2	5	49.1	48.5	1.1
3	7.5	73.6	72.9	0.9
4	10	98.1	93.14	5.1
5	20	196.2	189.7	3.31
6	30	294.3	285.6	2.96

The average error is 2.4% which is far below the fluctuations one could obtain when doing experiments with ice. It is therefore assumed that the load cell measurements are accurate enough to use in the analysis.

3.3.2. Dead weight pull

To verify the pull-rate of the hydraulic actuator, a dead weight pull has been performed. The weights pulled are first supported by a frame after which the actuator will be activated and the pulling starts. The output of the measurements can be seen in Figure 3.18. The pull rate is then calculated by equation 3.5.

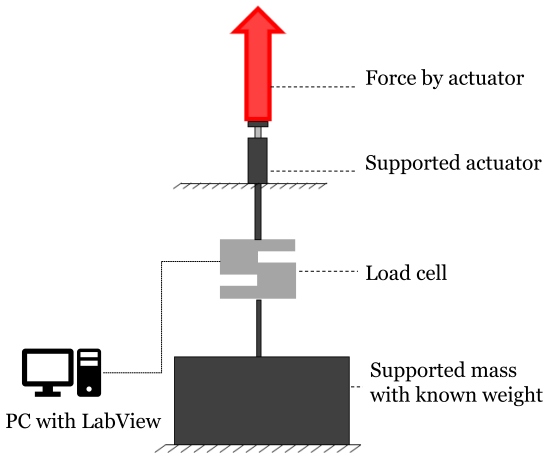

Figure 3.17: Schematic set-up used for checking the pull characteristics

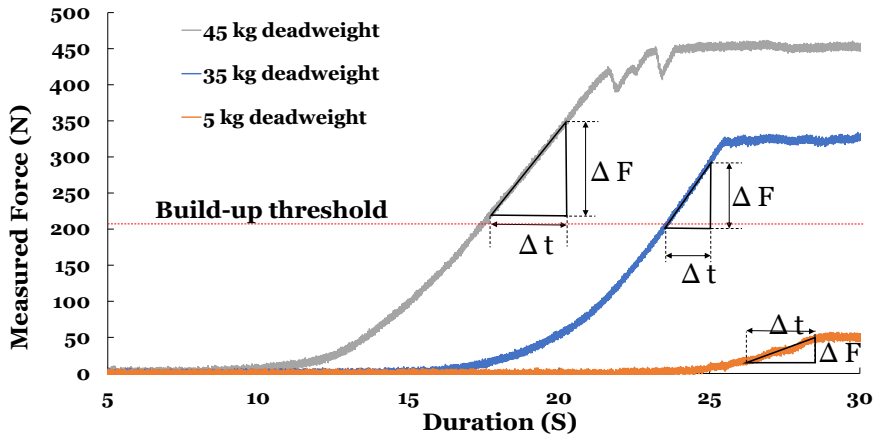

Figure 3.18: Graph obtained from the dead weight pull

$$Pullrate = \frac{\Delta F}{\Delta t} \tag{3.5}$$

where ΔF is the difference in force of a section throughout the steady pull (where the slope is highest in the graph and is steady) and Δt is the difference in duration for that section.

Table 3.5: Values used in load cell calibration, measured output, and error

Weight (kg)	**5**	**35**	**45**
Pull rate (N/s)	18.1	58.3	51.8
Measured force (N)	49.8	340.9	459.5
Theoretical gravity force (N)	49.1	343.4	441.5

It can be noticed that the pull rate of the low weight is significantly lower than of the higher two weights. This can be explained by the fact that the DeFelsko Positest device has a build-up pull-rate up to about 220N after which the pulling at the designed rate starts. This can also be seen from the graphs of the 35 and 50 kg pulls where the slope gradually increases until it reaches about 220N, where the slope is the highest. This threshold is indicated with the red dashed line in the graph.

4

Experimental procedure followed for gathering data on ice-concrete bond strength

4.1. Test sequence design

According to Tatinclaux [37] ,conditions which influence friction at centimeter scale are the: normal stress, roughness of the structure and the sliding velocity. Direct contact pressures between undamaged ice and a structure can be as high as 10 MPa [28], but existing measurements of ice forces on offshore structures seldom exceed 1 MPa. For crushed ice this contact pressure can be as high as 1 MPa. [30]. Firorio [12], who did a double shear sliding experiment, pressures ranged from 25Kpa to 800 Kpa. In this research, both short and long holding periods will be chosen as a preliminary definition. Several test sequences have been performed in order to examine the influence of pressure, time, different surfaces and submergence on the adhesion between ice and concrete. These sequences are:

1. The influence of holding time and pressure on the pull-out force while maintaining pressure
2. The influence of holding time and pressure on the pull-out force after releasing pressure
3. The memory effect of adhesion
4. Different surfaces and ice-adhesion
5. The influence of submergence: saturated concrete in contact with ice.

For all test sequences, several options for the variables pressure and time have been chosen. Their considerations of the choices are described in the subsections below.

4.1.1. Sequence 1: maintaining pressure before pull-out

In this sequence, the pressure applied on the interface is maintained before the pull is initiated. This way, the pull-out force exists of a static friction component and of an adhesion component. The primary goal is to find out what the effect of varying pressures and holding times will be on the pull-out force. To compare, a sequence of very short holding time has been done to 'simulate' pure static friction. It is unfortunately almost impossible to directly pull out the ice after the pressure is applied due to the delay of the DeFelsko Positest. Therefore, a 6 second holding time is used for the shorter holding time.

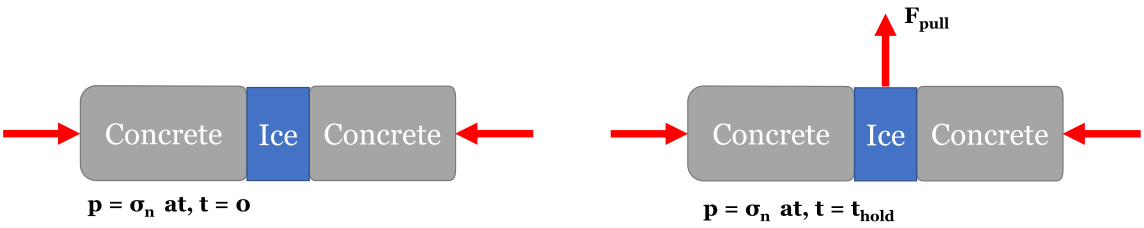

Figure 4.1: Illustration of the idea used in test sequence 1: remaining pressure when initiating pull.

Due to limitations on available weights, it has been decided to use 50kg as a maximum weight, which corresponds to a pressure of 682kPa. The holding time ranges from very short to overnight. Longer holding times can be achieved, but due to sudden occurrence of a defrost cycle of the freezer, there is a high risk of a failed experiment when trying to do so. Taking into account the above, the following parameters for the variables have been chosen for test sequence 1:

Table 4.1: Chosen hold times for test Sequence 1

Hold time (min)	0.1	2	5	20	60	180	overnight

Table 4.2: Chosen hold times for test Sequence 1

Pressure (kPa)	51	316	682

The following steps have been followed for this test sequence:

1. Position cooled concrete cylinders in concrete holders
2. Freeze shaped ice cylinder in the ice puck holder and wait 5 minutes
3. Position ice puck holder in line with concrete cylinders
4. Attach the actuator of the PosiTest device and the load cell to ice puck holder
5. Slide concrete towards the ice and hang weights on the lever arm and start timer
6. Wait for the described holding time and press button on the DeFelsko Positest to initiate pull
7. Let LabView record the voltage of the load cell

4.1.2. Sequence 2: removing pressure before pull-out

The decisions for the experiments of sequence 2 is based on the same rational as for sequence 1. A very short holding time however showed no measurable adhesion in the current set-up so those tests have been eliminated for this sequence. Also, due to the occurrence of many defrost cycles of the cold room overnight, only one overnight experiment has been successfully done for this sequence. For the rest, the values of the variables chosen in the experiments of sequence 2 are the same as in sequence 1.

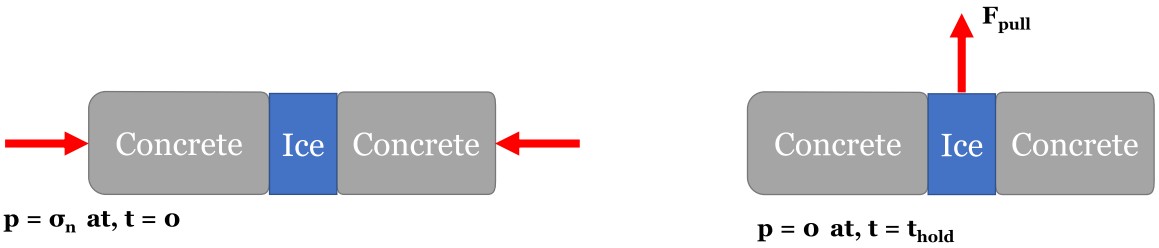

Figure 4.2: Illustration of the idea used in test sequence 2: releasing the pressure before initiating pull.

Table 4.3: Chosen hold times for test Sequence 2

Hold time (min)	2	5	20	60	180	overnight

Table 4.4: Chosen hold times for test Sequence 2

Pressure (kPa)	51	316	682

4.1.3. Sequence 3: The memory effect of adhesion

During this test sequence, the pressure will be released before pulling out the ice puck. Where in sequence 2 the pull was initiated almost straight after releasing the pressure, in sequence 3 the time before pulling after releasing the pressure will be varied from 5 minutes to 180 minutes for a pressure of 682 kPa. The highest pressure is chosen in an effort to achieve bigger differences in outcome.

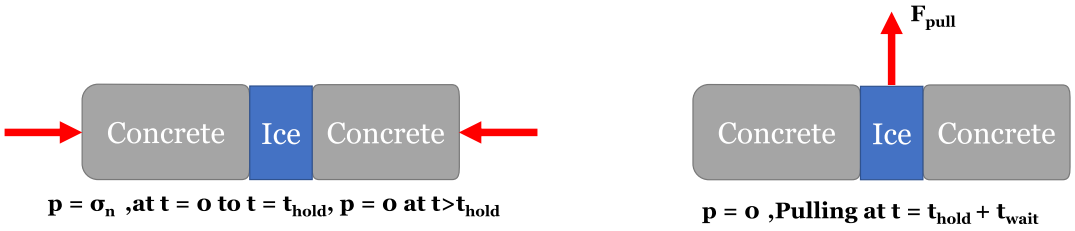

Figure 4.3: Illustration of the idea used in test sequence 3: waiting a certain time before initiating pull.

Table 4.5: Chosen parameters for test sequence 3

Pressure (kPa)	Hold time (min)	Wait time before pull (min)					
682	20	5	10	20	30	60	180

4.1.4. Sequence 4: Different surfaces

The effect of different surfaces will be investigated by using different materials instead of the grounded concrete cylinders. The chosen materials are:

- Pure sandstone rock core samples
- A regular concrete cylinder with a smooth paste surface, representing the outermost layer of concrete of a structure without any exposure of aggregate
- Grounded concrete cylinder as used in all the other tests.

The pressure will be remained and released before initiating the pull. The pressure will be 682 kPa and a hold time of 20 minutes has been chosen based on sufficient repeatability of the 20 minutes hold time and 682 kPa test. (see analysis) A picture of the surfaces used in this test sequence can be found in the figures below.

(a) Red sandstone rock core sample surface

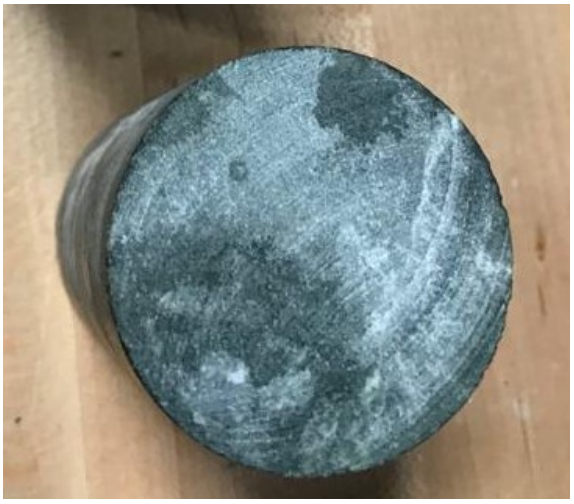

(b) Green sandstone rock core sample surface

Figure 4.4: Rock cores used in test sequence 4

(a) Surface of the paste

(b) Grounded concrete surface

Figure 4.5: Concrete cylinders used in test sequence 4

4.1.5. Sequence 5: The influence of submergence

A smaller version of test sequence 1 has been repeated for sequence 5 but now when the entire concrete-ice interface is submerged in water at 0 °C. The water is cooled down before added into the set-up and ice cubes ae added to remain a cold temperature of the water. All test were performed outside the cold room with an ambient temperature of about 20 °C. Because the ice puck also seemed to melt in this set-up, the maximum hold time was set to 20 minutes. Holding times of an hour or longer tests have been performed, but the results were poor because the ice puck was molten to much to obtain comparable results. The variables chosen for this sequence can be found in Tables **??** and 4.6. Figure D.2 shows an image of the set-up used for performing these tests.

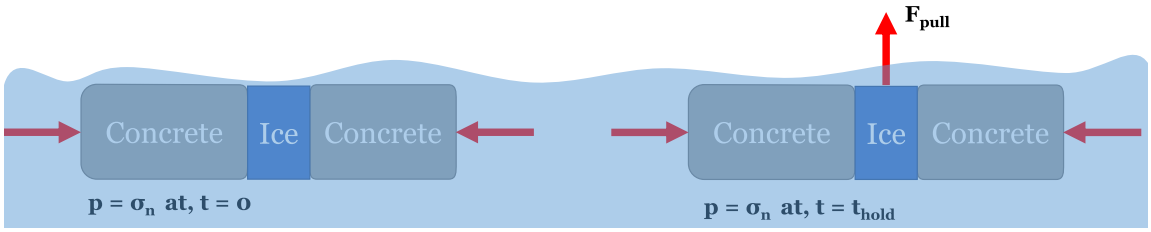

Figure 4.6: Illustration of the idea used in test sequence 5: submerged set-up, and same principle as test sequence 1.

Table 4.6: Chosen hold times for test Sequence 5

Hold time (min)	0.1	2	5	20

Table 4.7: Chosen hold times for test Sequence 5

Pressure (kPa)	51	316	682

4.2. Environment

All but the submerged experiments have be done in a cold room, a large freezing room which aims to have a constant temperature of around -9 °C. Temperatures sometimes vary due to other activities occurring in the same space but remain relatively stable throughout the day. Sometimes, the freezer starts performing a defrost cycle, in which it increases the temperature and highly decreases air humidity causing all the ice to evaporate and therefore disturbing the experiments. This usually happens some days overnight, but on a very unpredictable schedule.

4.3. The concrete used in the experiments

The concrete used for the experiment is produced according to the ASTM C192: Standard Practice for Making and Curing Concrete Test Specimens in the Laboratory, which covers the procedure for making and curing test specimens of concrete in the laboratory under accurate control of materials and test conditions.

4.3.1. Concrete mix

The cement, sand and aggregate are added to the mixer for a dry mix. Water is added slowly while the mixer is on. Then, Adva 190 is added, which a polycarboxlate-based high-range water-reducing admixture. This helps to produce concrete with extreme workable characteristics which is referred to as 'high slump'. The amount of the materials used in the mix can be found in table 4.8.

[11] Shows that the size of the aggregate of the concrete and, in particular their size is related to the wear of the concrete. We therefore chose to keep the aggregate size constant to ensure informative comparison.

Table 4.8: Concrete mix properties

Ingredient	**Amount**
Cement	18.0 kg
Sand	35.3 kg
Fine aggregate (<10mm)	42.3 kg
Water	7.2 kg
Ratio's	
Cement Factor C/F	1.2
Water to binder ratio	0.4

4.3.2. Concrete surface

All the concrete surfaces will be smoothed using a grinding machine. This way, the aggregate and the paste will both be in contact with the ice. The grounding machine will cause visible grooves across the diameter of the cylinder.

Concrete surface roughness

This may however result in different shear pull-out forcers for different orientations of the cylinder. And as [18] concluded that adhesion strength was larger for a higher roughness in his experiments, the orientation of the concrete cylinders during the experiments could matter. To foresee whether the orientation of the concrete cylinder could cause a problem in the experiments, the roughness of the surface is measured along the grooves and perpendicular to the grooves using a Starrett SR400 roughness measuring device. Figure 4.7 (a) shows the surface of a grounded cylinders and (b) shows the approximate measurement paths used for measuring the roughness. The diameter of the cylinders is 2".

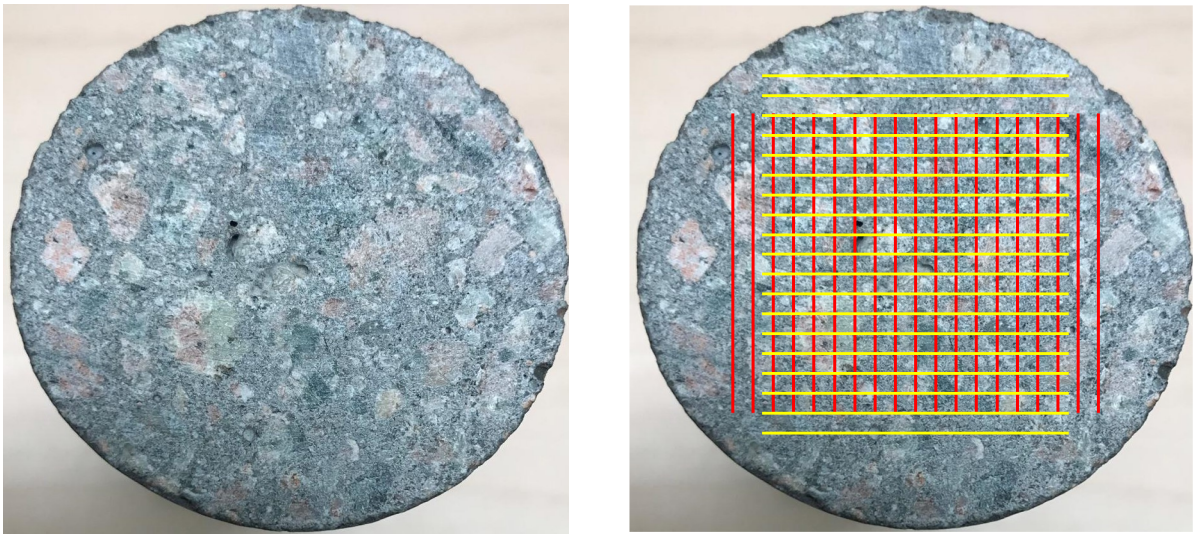

(a) Grounded surface 1 (b) Grounded surface with measurement paths

Figure 4.7: The average and standard deviation of critical parameters: Region R4

Firstly, roughness was measured in a direction perpendicular to the groves, and secondly the roughness was measured along the groves of the surface. This resulted in an average roughness of 8.21 when measuring across the groves and 8.025 when along the groves. The very small difference of the average direction between the two directions which, after performing a t-test, shows no statistical significance. The results of the roughness measurements can be found in Appendix D.

Concrete surface aggregate over paste ratio

In order to find the average ratio of aggregate over paste of the cut concrete surface used in the tests, Image J software has been used to analyse 20 surfaces of the concrete by performing the steps below:

1. Load image
2. Select only the concrete surface with the circle tool and clear outside
3. Measure the circle in pixel amount
4. Enhance the contrast of the image
5. Convert image to 16-bit image (Black and White)
6. Threshold the image to only select the aggregate or paste parts
7. Let the software count the area of the masked pixels

The resulting average Aggregate over paste ratio of the 20 analysed concrete surfaces is found to be 1.3.

Figure 4.8 shows the original image versus the masked image of which the software determined the area of aggregate. From comparing the pictures, the software seems to pretty accurately determine the aggregate particles.

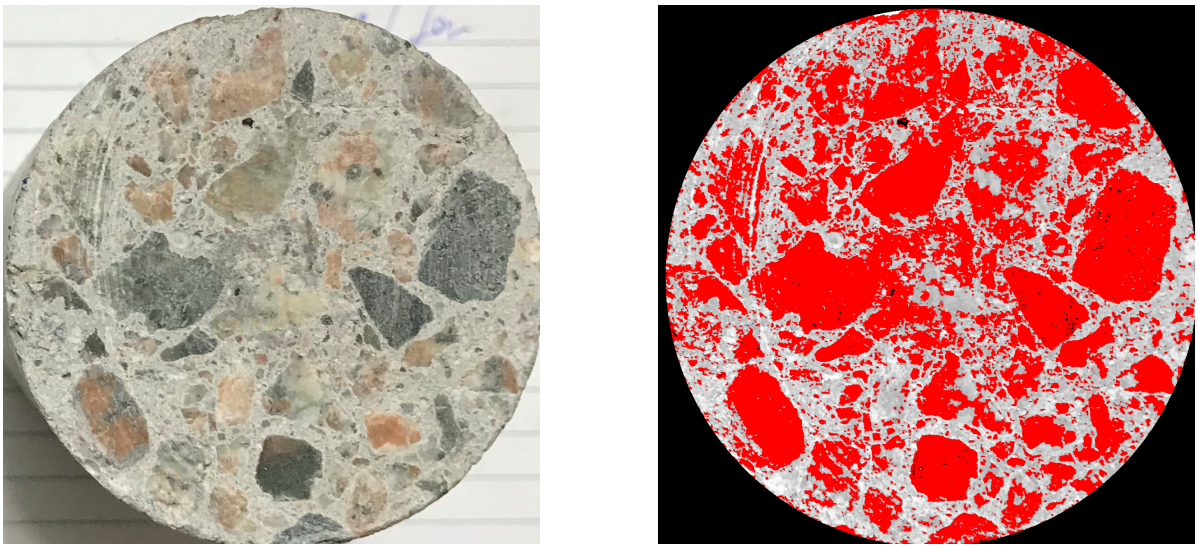

(a) Original image of surface

(b) Masked surface by image threshold

Figure 4.8: Image of typical cut concrete surface and masked image using ImageJ software.

4.3.3. Concrete strength

A UCS test has been performed after 28 days of curing, which resulted in strengths of 66.13, 68.2 and 66.49 Mpa with an average strength of 66.94 Mpa. All the concrete cylinders used in the experiments in this thesis are from the same batch.

4.4. The ice

The ice used in the experiment is made according to a standard procedure used by many researchers working at the ICEWEAR project and is made as described in 'Bruneau et Al. (2013)'. The aim is to obtain granular polycrystalline freshwater ice with a grain size of about 4-10mm. This is important, as the grain size of ice will influence the transition strain rate from ductile to brittle behaviour and therefore the compressive strength of the ice [2]. Figure 4.9a shows an average distribution of the grains used when making the ice. The grains of the ice are obtained by crushing ice cubes in an ice crushing machine. These grains will be inserted 2" diameter plastic cylinders and water will be added while stirring with a rod. The water is first distilled, than ran through an purifying device which de-ionizes the water. The water is than de-aerated using a de-aerator machine and a vacuum pump. When the water and the ice grains are mixed, the plastic cylinders are inserted in a styrofoam insulation box. Using this insulation box, as seen in Figure 4.10a, will make sure the water-grain mix will freeze from the bottom up. This way the water can escape when freezing which will reduce the risk of cracks and internal stresses when the water freezes. After freezing the cylinders for more than 24 hours, the cylinders are demolded using an air compressor. They are then placed in the cold room to acclimatise to the cold room temperature where the apparatus is placed. The cylinders are first cut to size using a bend saw in the cold room and are then smoothed using an aluminium heat sink. The cylinders are shaped using a v-shape plastic frame to ensure squareness of the cylinder. This v-shape is illustrated in Figure 4.10b.

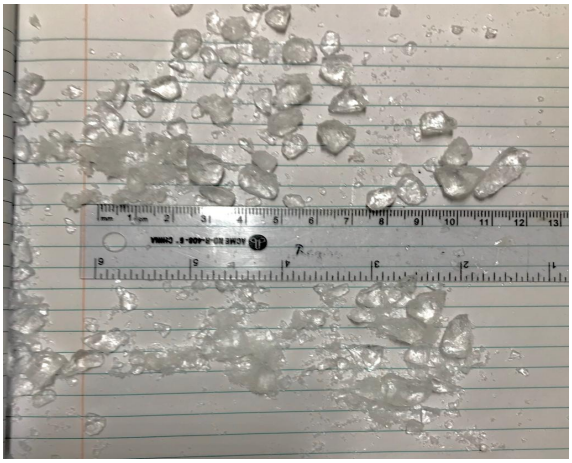

(a)

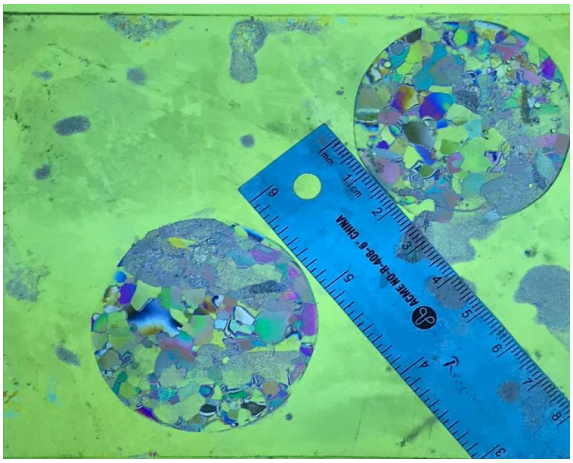

(b)

Figure 4.9: (a) A scoop of ice out of the crushing machine. (b) Thin section of ice used in the experiments

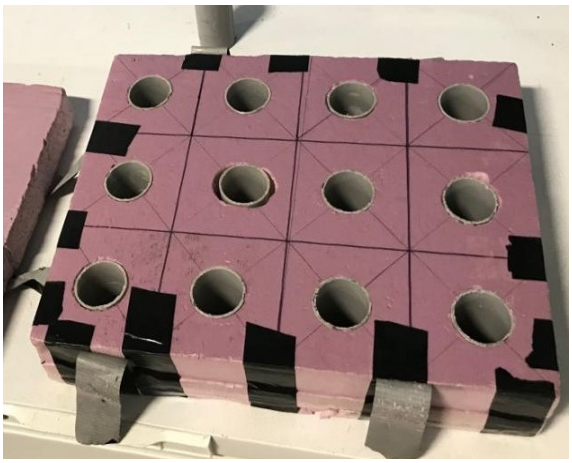

(a)

(b)

Figure 4.10: (a) The insulation box used for making the ice samples. (b) Alluminium heat sink with V-shape frame to create straight cylinders

5

Results of the experiments

After performing the experiments as outlined in section 4 much data is gathered. This section describes the method by which the raw data is processed and presents the results. An analysis of the results can be found in chapter 6.

5.1. Data processing

The results obtained from the tests are in the form of .TDSM files which, when opened, turn into excel files with two columns of data. The first column shows the time-step at each sample, and the second column shows the sampled value of the load cell's voltage multiplied by the pre-set coefficient, which converts the voltage to Newtons. When plotting the recording time on the x-axis and force on the y-axis, a typical graph looks like the one in Figure 5.1, which is from a test of sequence 1, for 316k Pa pressure and a 2 minute hold time.

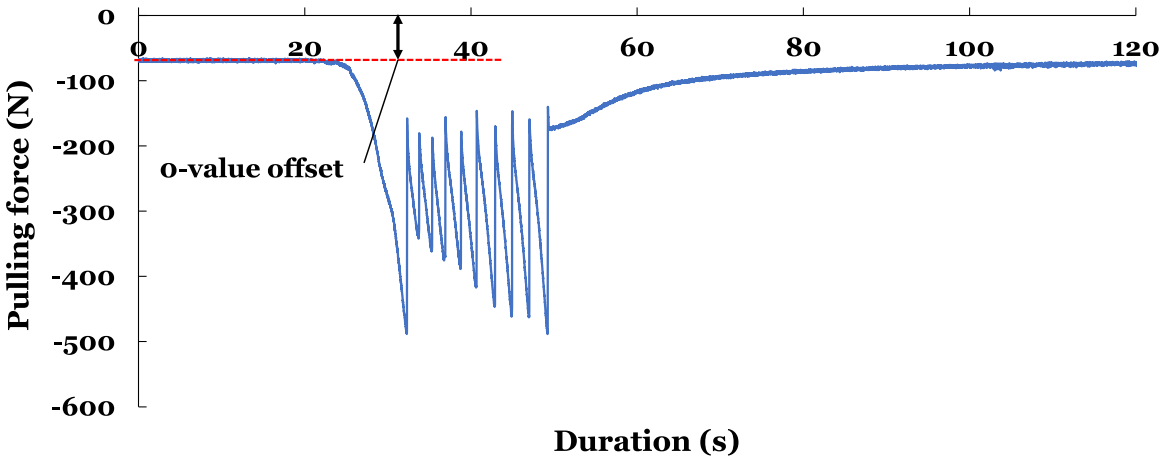

Figure 5.1: Typical pull-curve from raw data. Pressure: 316kPa, hold time: 2 minutes

5.1.1. Shifting and noise filtering

The graph shows an offset of the 0-value of the force and can sometimes include high frequency noise. The following procedure has been followed to shift the graph to delete the offset and flip it so it is easier to read:

1. The average of the first 300 samples, which represents the zero-level of the load-cell's output, is calculated.
2. This average value is than subtracted from the x-values and multiplied by -1 to flip the graph over the x-axis.

The graph in Figure 5.1 will after these steps look like the graph in Figure 5.2.

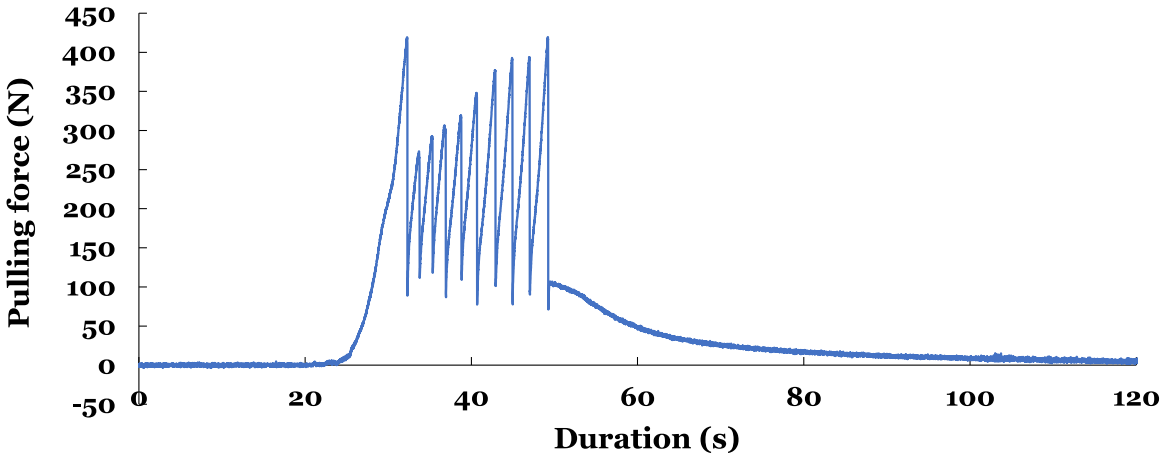

Figure 5.2: Typical pull-curve from processed data. Pressure: 316kPa, hold time: 2 minutes

Figure 5.3 shows an example where the forces are relatively low and one can see from the graph that the signal from the load cell is„ relatively noisy. To filter out this noise and obtain more clear plots, the moving average of the first 10 samples is taken, which for a sampling frequency of 99Hz, is the 0.09s Moving Average and calculated by:

$$F_{n+10,filtered} = \frac{F_1 + F_2 + ... + F_n}{n} \tag{5.1}$$

Where F_1 is the first data point from the experiment and $n = 10$ samples.

The result is that the high frequency noise is filtered out and the graph becomes more clear. An example of a filtered graph can be found in Figure 5.4.

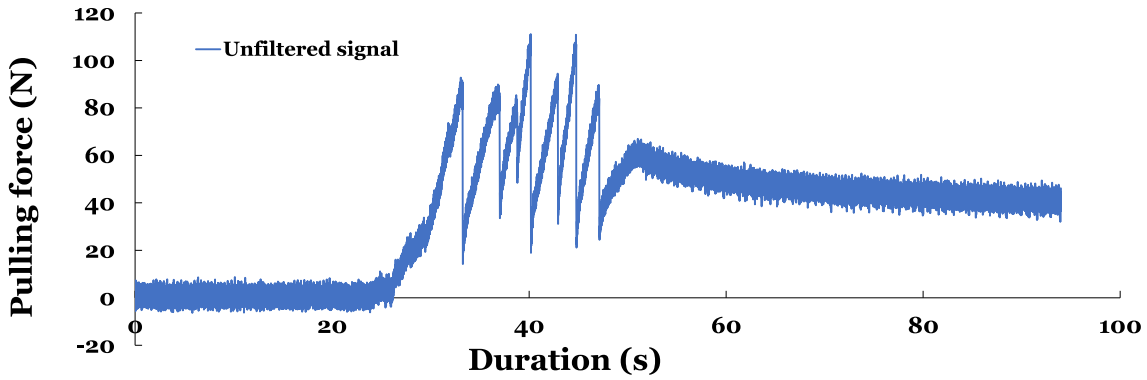

Figure 5.3: Unfiltered signal after steps in section 5.1. Pressure: 51kPa, hold time: 2 minutes

5.1.2. Graph interpretation

For this research, the interesting value is the value of the first peak, where the bond between the ice and the concrete breaks. At this time, the ice puck moves which results in a lowering of the tension in the rod attached to the ice puck and is measured by the load cell as a decline in force. To store the value of interest, indicated by the red circle in Figure 5.5, the following procedure has been followed: The maximum of the graph is found using MAX(Range) in Excel, where Range is from the first data point to just after the first peak. This corresponds to the maximum adhesion force, indicated in graph in Figure 5.5. These values are stored in tables which are defined in sections

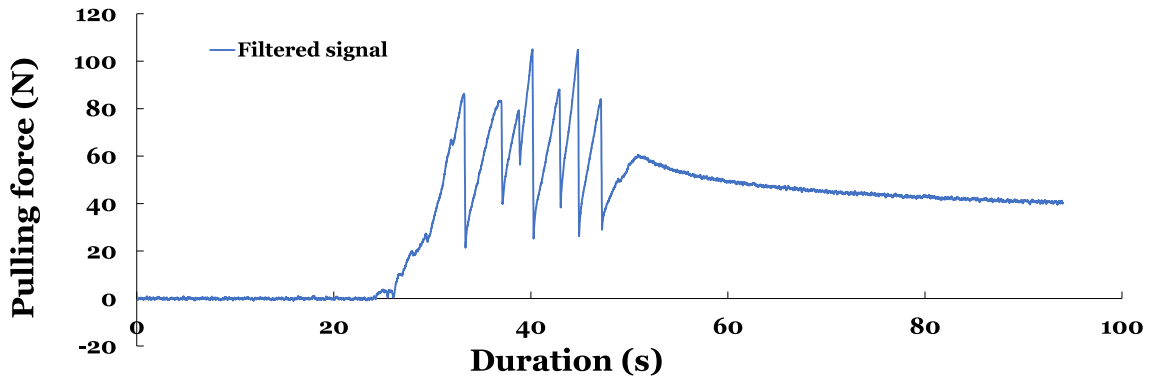

Figure 5.4: Same signal, but with 0.1 s moving average. Pressure: 51kPa, hold time: 2 minutes

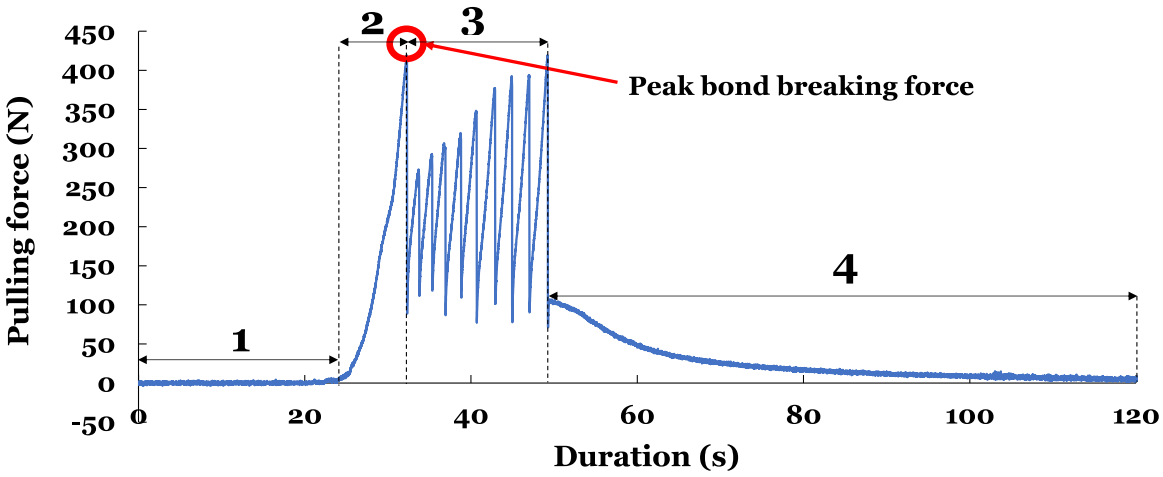

Figure 5.5: Sequence 1 pull-test. Pressure: 316kPa, hold time: 2 minutes. Indicating different regions in the graph.

Further interpretation of the graph is explained below, where the graph has been divided in four different sections.

1. This part of the graph represents the steady state of the set-up. The actuator hasn't been activated yet and nothing is moving so the load cell does not measure a force.
2. At this stage, the actuator starts pulling the ice puck and the tension in the rod which connects the ice puck to the load cell increases. The load cell measures throughout the pull an increasing force, until the graph reaches its peak force. Here, the bond between the ice and the concrete is broken and the tension in the rod suddenly drops resulting in the decline in the graph.
3. In this section, the force increases until it breaks the bond again and repeats this cycle until region 4. When this happens
4. At region 4, the actuator stops exerting force. The force in the load cell gradually decays until it reaches a steady-state level.

5.2. Test sequence 1: remained pressure

Figure 5.6 plots all the bond breaking forces of the different tests (4.1.1) as performed by the method described above. The values of the data points can be found in Appendix A and the pull-curves in Appendix B. The x-axis of Figure 5.6 gives the holding time (as defined in section 5.1.2) and represents the duration of the applied

pressure before pulling out the ice. The different pressures are indicated by the different colours and shapes, as highlighted in the legend box in the top left of the graph. A general increasing trend of bond breaking force versus hold time can be seen for all the different pressures, but there seems to be a little dip from the 5 to 20 minutes hold time. The highest pressure results in the highest pull-out force. Some of the repeated tests are closer to one another, but all remain in the same order of magnitude.

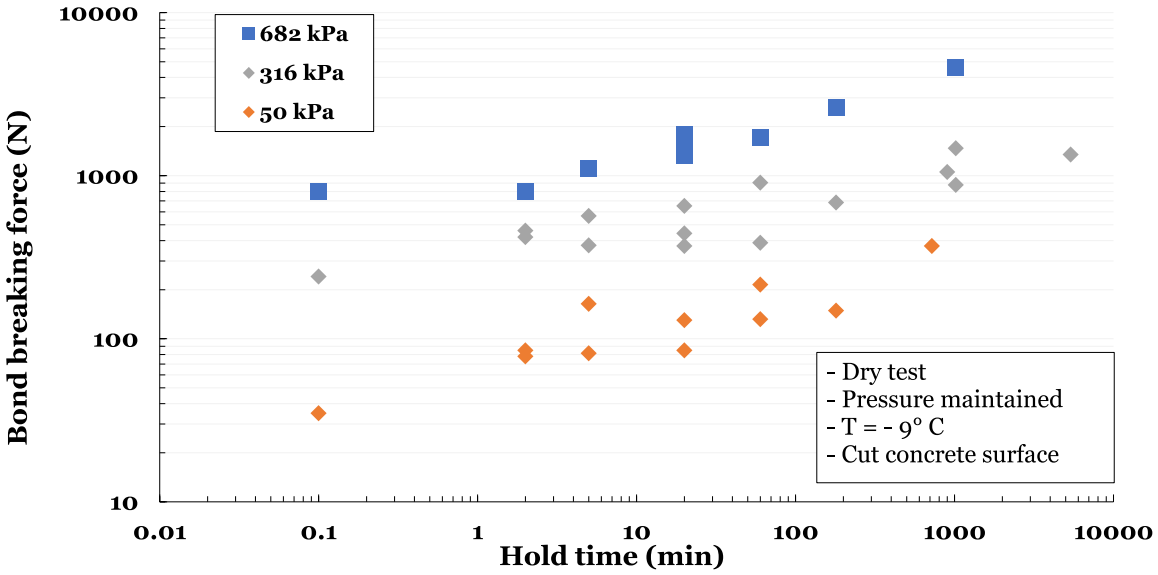

Figure 5.6: Peak adhesion force for tests in sequence 1 plotted versus hold time

5.3. Test sequence 2: pressure released

Figure 5.7 shows the bond breaking force as obtained in the procedure followed in section 5.1.2. The results are significantly lower than in sequence 1 and the same trend of increasing bond break force versus longer holding times is observed. There seems to be no clear difference between the influence of different pressures on the bond breaking strength when looking at this graph.

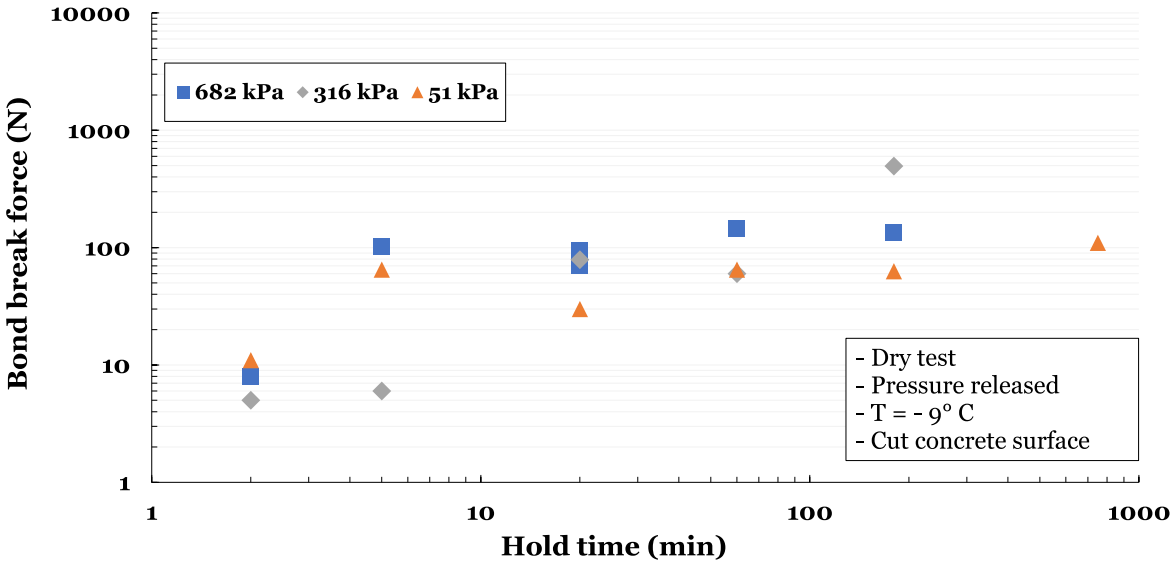

Figure 5.7: Peak adhesion force for tests in sequence 2 plotted versus hold time

5.4. Test sequence 3: The memory effect of adhesion

Figure 5.8 shows the force required to break the ice-concrete bond, represented by the squares in the plot, with their values in Newtons, after releasing the applied pressure and waiting a variable amount of time. The amount of time waited before pulling out the ice is showed on the x-axis. A general trend of increasing pull-out force is observed for longer waiting times, with a discontinuity of the trend at a waiting time of 20 and 30 minutes. The pull-out force for breaking the bond can, apparently, be 3 times higher when waiting for a certain amount of time compared to no waiting time. The result of the experiment with the shortest waiting time has an outcome which is close to the outcome of the same experiment from test sequence 2, but for no waiting time.

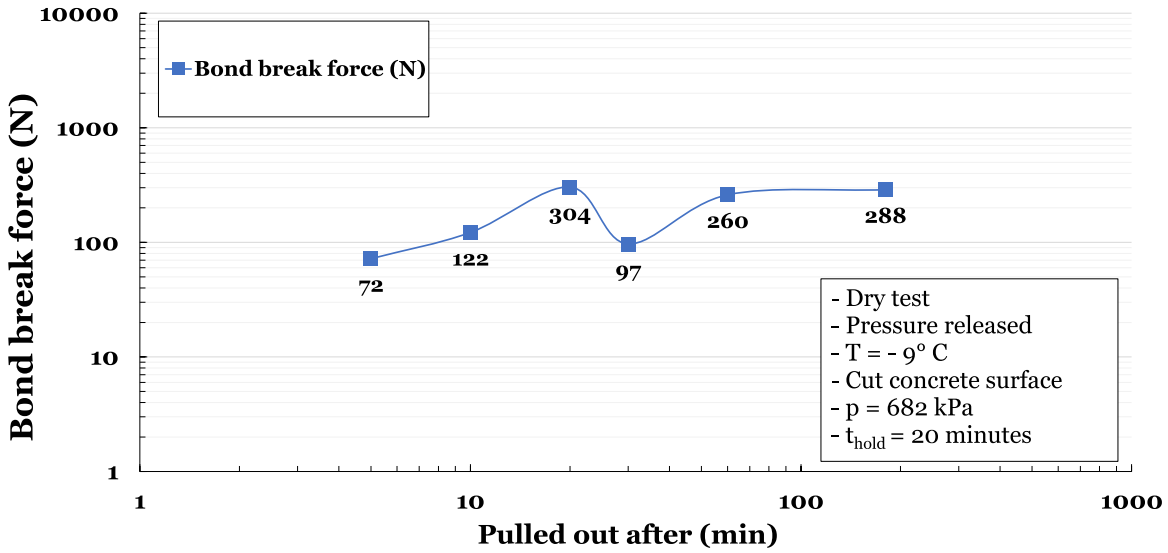

Figure 5.8: Peak adhesion force of 682 kPa pressure and 20 minutes hold time plotted over waiting time before pulling.

5.5. Test sequence 4: Different surfaces

The test results of the different surfaces are shown in Figure 5.9 and show the outcomes of bond breaking force in Newtons. The pressure for all tests was 682 kPa and the hold time has been set to 20 minutes. The triangle shaped plots are for tests which share the same principle as Sequence 1, where the pressure is maintained when pulling out the ice. Sequence 2 tests, where the pressure has been released before pulling out the ice are indicated in the graph by squares the squares. The maintained pressure results show higher bond breaking forces than the pressure released tests. This is in line with the outcomes of comparing sequence 1 to sequence 2.

5.6. Test sequence 5: the influence of submergence

In this test sequence, the test set-up has been submerged and the outcomes are shown in Figure 5.10. Like all other tests, the holding time has a positive influence on the bond breaking force. The outcomes are significantly lower than the same tests in dry conditions. The failure mode for all tests is pure adhesive as no ice pieces stuck on the concrete surface have been observed. There is a clear difference between the outcomes of different pressures, although it seems that the difference between 682 kPa and 316 kPa for holding times longer than 10 minutes result in almost the same bond breaking force. The ice at the end of the 20 minute holding time tests has visibly decreased in size, most likely due to melting processes.

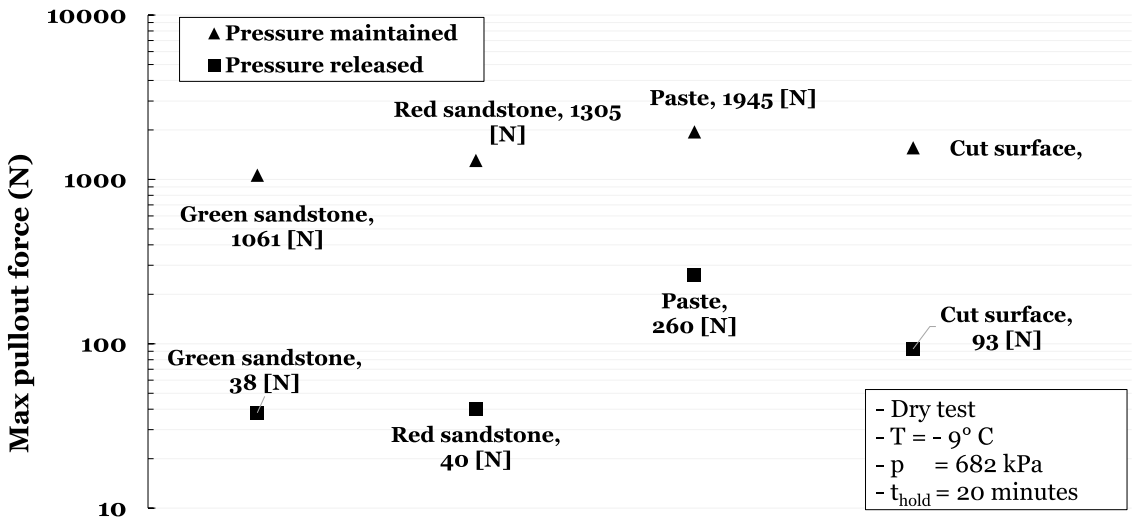

Figure 5.9: Peak adhesion force plotted for different surfaces

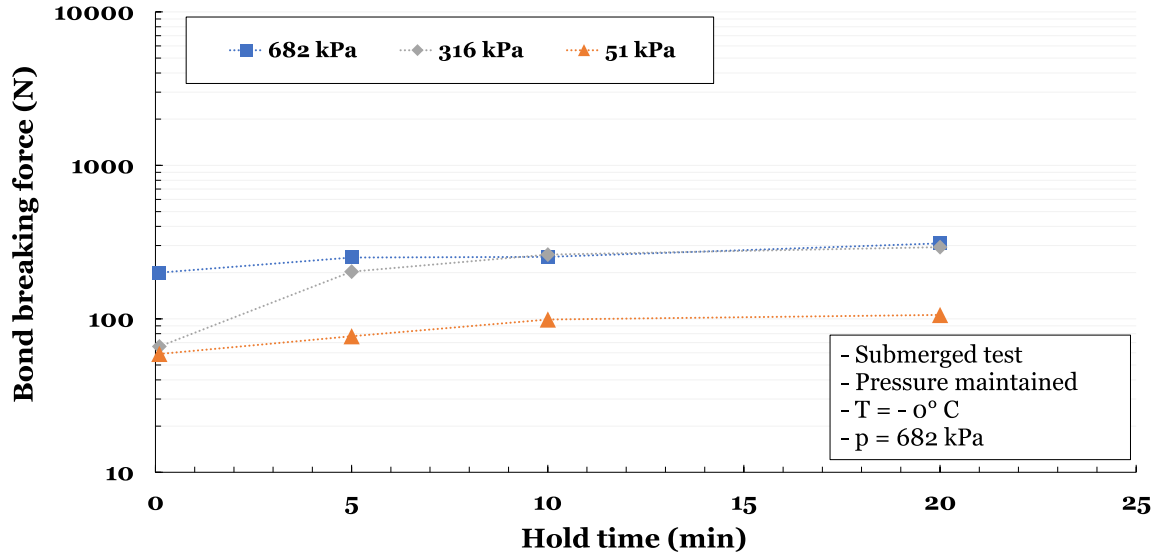

Figure 5.10: Peak adhesion force for tests in sequence 5 plotted versus hold time for submerged tests

5.6.1. Challenges in the submerged set-up

The main challenge in this set-up has been the perfect alignment of the ice and concrete cylinders. The visibility on the interface is highly decreased and the ice puck camouflages very well in the ice containing water. Multiple times, miss-alignment has been observed during several tests and the tests had to be done again to assure a valid outcome. Figure C.5 shows an ice puck after a test where the alignment of the ice puck and concrete cylinder was insufficient to ensure a constant pressure on the interface. The ice-puck also got pushed out if its position. Only successful tests have been taken into account and are shown in Figure 6.12.

6

Analysis and discussion of the results from the experiments

6.1. The influence of holding time on ice-concrete bond strength

The results from the experiments show that the holding time generally positively influences the adhesive bond strength. This has been observed in most tests of sequence 1, 2 and 5. This section will present an analysis of the results and concludes there is indeed a positive influence of holding time on the ice concrete bond strength after performing a simple statistical analysis.

6.1.1. Static friction coefficients

To compare the results of the different tests, a value for a static friction coefficient, and later the dimensionless bond breaking force, will be used. The static friction coefficient μ_s is calculated using formula 6.3 and the values for test sequence 1 are showed in Table A.1b in Appendix A. Using this parameter allows for comparison between different pressures and will also be used for discussing the influence of pressure on the bond strength in different situations. The static friction component is calculated by rewriting equation 6.1:

$$F_{pullout} = \mu_s * F_n \tag{6.1}$$

where F_n is the normal load, calculated by:

$$F_n = \sigma_n * 2 * A_{surface} \tag{6.2}$$

in which σ_n is the applied pressure by hanging the weights to the lever arm resulting in the pressures according to table 3.3, to:

$$\mu_s = \frac{F_{pullout}}{2 * A_{surface} * \sigma_n} \tag{6.3}$$

Here, $F_{pullout}$ is the shear force required to break the ice-concrete bond in Newtons, which has been measured by the load cell and is stored in a table by the described method. Actually seeing μ_s as static friction resulting from the tests in this experiment might not be exactly correct. The reasoning for this is because, as can be seen in the pictures in Appendix C, the failure is not really just pure adhesive failure, but also partly cohesive failure by the breaking of small ice pieces.

In order to prevent confusion about static friction and dimensionless pull-out force, μ_s in equation 6.3 will be called $\mu_{pullout}$ instead and is thus calculated by:

$$\mu_{pullout} = \frac{F_{pullout}}{2 * A_{surface} * \sigma_n} \tag{6.4}$$

It represents the dimensionless pull-out force required to break the break the adhesive bond between the largest mass of the ice puck and the concrete cylinder. The values of the tests of the different pressures and hold times of sequence 1 are plotted in Figure 6.1. The same increasing trend can be seen as in Figure 5.6. And for longer holding times, there is a larger difference in the outcomes of $\mu_{pullout}$ for the different pressures.

To check if the outcomes are reasonable, they have been compared with similar tests in literature.

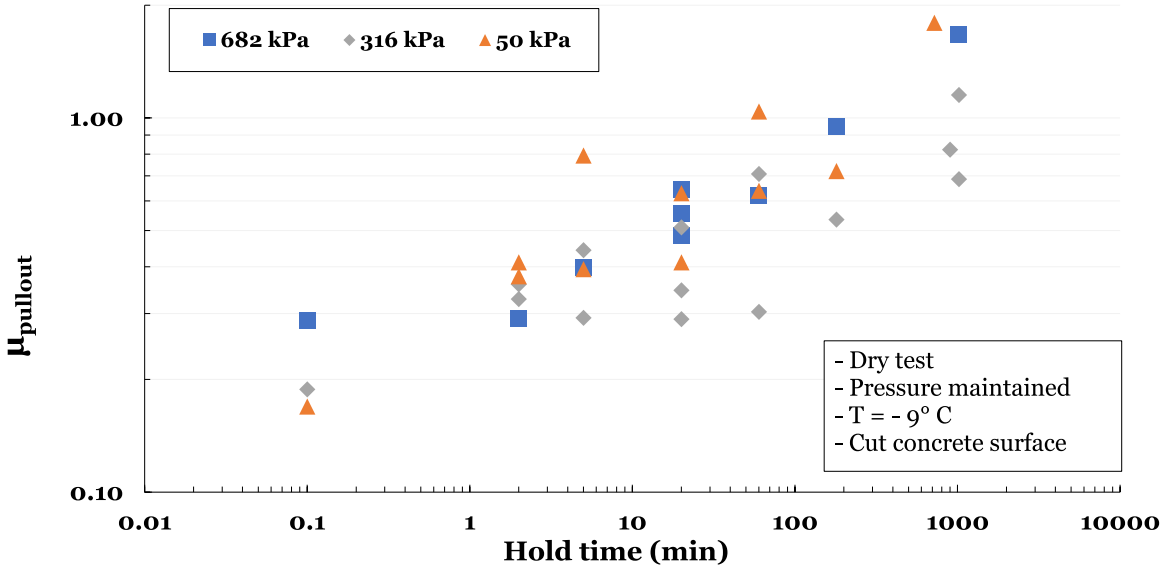

Figure 6.1: Calculated static friction coefficient

Figure 6.2 shows results of slide-hold-slide test of ice on ice for $\sigma_n = 60$ Kpa. The results of the ice-concrete bond show somewhat smaller static friction coefficients, and the results from the experiments in this thesis are not far off from the slide-hold-slide tests, which partly verifies the results of the experiments in this thesis.

6.1.2. Correlation between holding time and bond break force

There is a strong positive correlation between the holding time and the bond break force for all applied pressures. Table 6.1 shows the correlation between holding time and the bond break force which is proven to be statistical significant. The linear correlation is calculated using:

$$r = \frac{n(\Sigma t_{hold} F_{pullout}) - (\Sigma t_{hold})(\Sigma F_{pullout})}{\sqrt{[n\Sigma t_{hold}^2 - (\Sigma t_{hold})^2][n\Sigma F_{pullout}^2 - (\Sigma F_{pullout})^2]}} \tag{6.5}$$

Although the relationship might not be linear in nature, it does show a very strong correlation and therefore it can be stated that the bond breaking force strongly depends on holding time.

The dimensionless force will provide the ability to investigate the correlation between the holding time and bond break force of all the pressures. In formula 6.5, $F_{adhesion}$ is then replaced with $\mu_{pullout}$, as calculated in formula 6.4. The correlation between the dimensionless forces of all pressures and the holding time turns out to be 0.70.

Table 6.1: Correlation between holding time and bond break force for different pressures in test sequence 1

Pressure (kPa)	51	316	682	μ_s
Observations	11	14	9	34
r	0.88	0.82	0.94	0.70
r^2	0.77	0.68	0.88	0.50
Significance	0.00037	0.00016	0.00028	3.31E-06

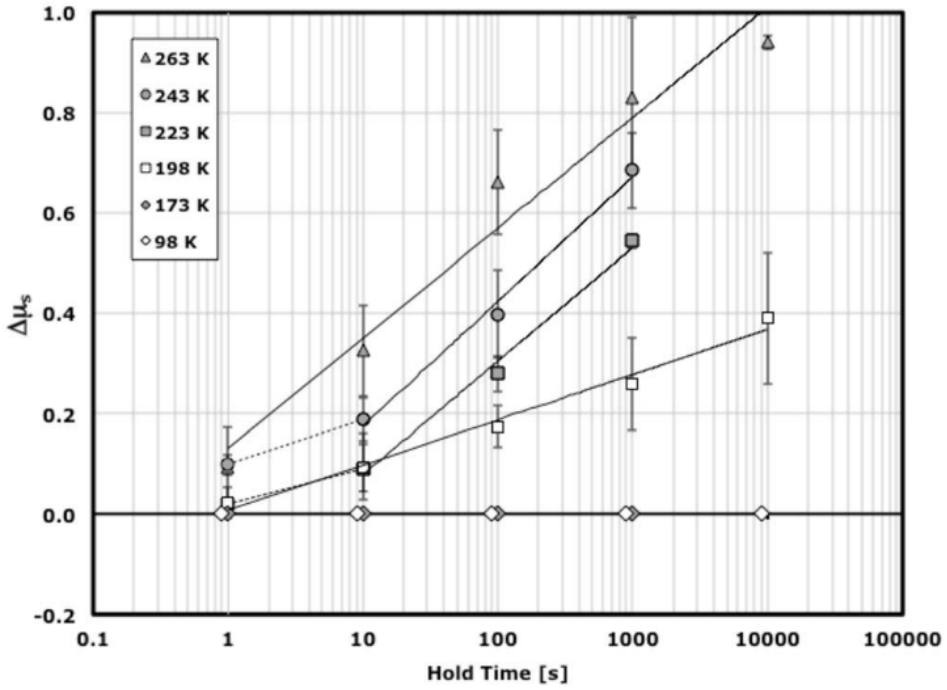

Figure 6.2: Change of coefficient of static friction versus hold time for varying temperatures and σ_n = 60 kPa

Looking at the output from table 6.1, it can be seen that all the Significance values are lower than 0.05, which means the result can be accepted as statistical significant.

These findings are in line with the findings of the Slide-hold-slide experiment from [34], which found that increasing the holding time would increase the force to re-initiate sliding. *"Slide-hold-slide experiments revealed that the coefficient of static friction increases by an amount that scales logarithmically with holding time"* [34].

The indication that an increasing hold time results in increasing adhesive bond strength can be supported by the tests from sequence 2, which show the same behaviour. Because in these tests the pressure is released before pulling, and thus σ_n is zero, the theoretical shear force is pure the adhesive bond strength.

The relation of $\mu_{pullout}$ versus the hold time is plotted in Figure 6.3, where the results from test sequence 2 have been used and σ_n is the normal pressure which has been applied before releasing. Because in test sequence 2 the normal load σ_n before pulling is in fact zero, the dimensionless force would be infinitely high when considering formula 6.4. This means that Coulomb's friction model is not sufficient for analysing adhesion. The graph in Figure Figure 6.3 indicates, like the tests from sequence 1, a positive correlation between hold time and bond break force, but when analysing the statistics, only the results of the 316kPa tests are statistical significant when using a linear correlation analysis. This can be explained because of the low number of observations in this test sequence, or because there just is not really a clear relationship when performing shear tests after releasing the pressure. But when analysing the correlation between μ_s and the hold time, which combines the outcomes of all the pressures, a statistical significant correlation has been found, meaning that also for these tests, the bond break strength is positively dependent on the holding time.

Table 6.2: Correlation between holding time and bond break force for different pressures in test sequence 2

Pressure (kPa)	51	316	682	μ_s
Observations	6	5	5	16
r	0.81	0.97	0.64	0.72
r^2	0.66	0.94	0.41	0.52
Significance	0.0504	0.00609	0.243	0.00168

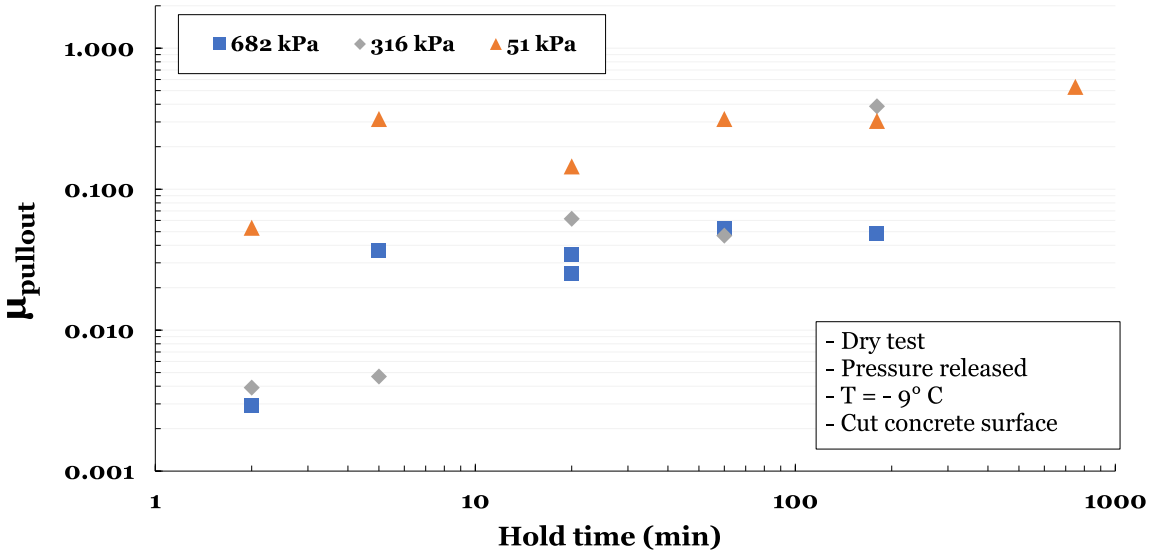

Figure 6.3: Calculated static friction coefficient for tests from sequence 2

6.1.3. Visual observations

Visual observations have shown that for longer holding times, more ice will stuck on the concrete after shearing, which strengthens the idea that longer holding times result in more ice-concrete adhesion. Figures C.1 in Appendix C shows images of the ice and concrete after performing shear tests from the procedure of test sequence 2. The fact that more ice damage and more ice on the concrete surface can be seen, supports the outcome of the results and could be hinting to an explanation of what is going at the interface. This will be further investigated in section 6.6.

6.1.4. Explaining the odd results

In a few instances, the adhesion force is lower for an experiment with a longer holding time. An example for such a case is for the 51kPa test where an experiment with a holding time of 5 minutes shows, in 1 case, a higher bond breaking force than an experiment of 20 minutes. The red circles in Figure 6.4 highlights this example.

This could be caused by the randomness of the ice or difficulties of the positioning of the ice puck in between the concrete cylinders at exactly the same manner every time. Due to the inhomogeneity of the concrete and ice surfaces, it is almost impossible to exactly generate the same pattern of stresses for each experiment done. Also, large stress concentrations of unknown magnitude may be produced by discontinuities and residual stresses, possibly originated by the actual forming of the interface, may play a role in the observed adhesive strength. This could explain the deviations which are found in the tests.

Perhaps an explanation can be found when looking at the pull curves. It can be seen clearly that the pull behaviour is odd for the lower peak forces in a test with the exact same pressure and holding time. The pull-rate is lower, which could indicate that the ice is already moving a bit or perhaps breaking a bit before the critical bond failure. In Figure 6.5, just before the pull rate declines, a little peak is observed. This can only happen if the ice puck moves a bit, so most likely a little ice piece already broke before reaching the peak bond break force.

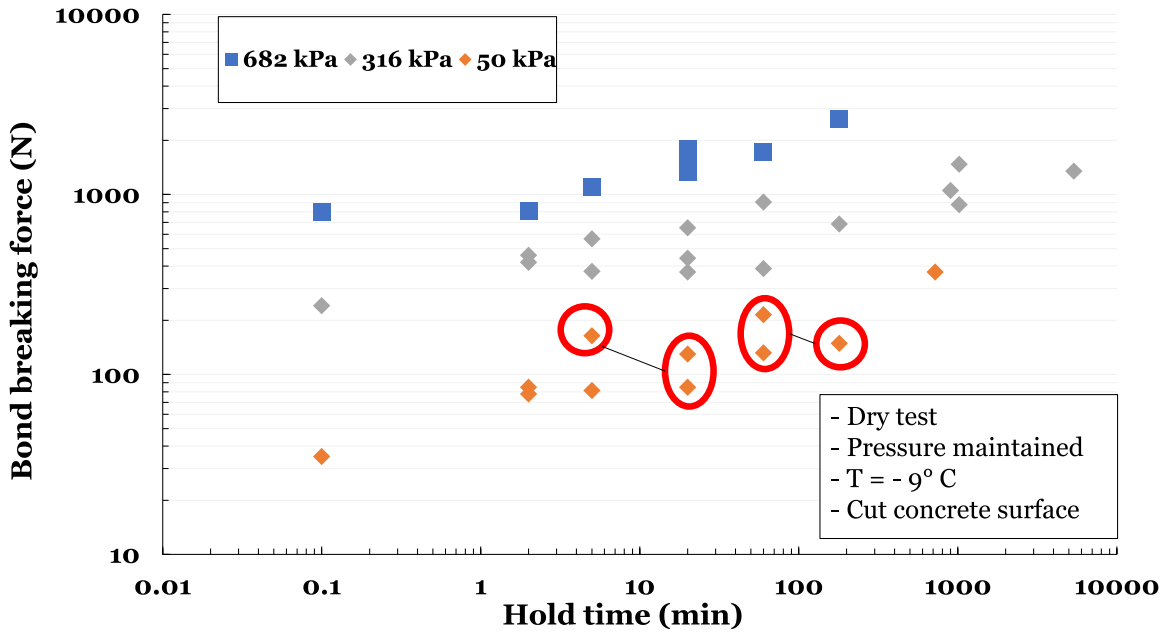

Figure 6.4: Red circles indicate odd instances

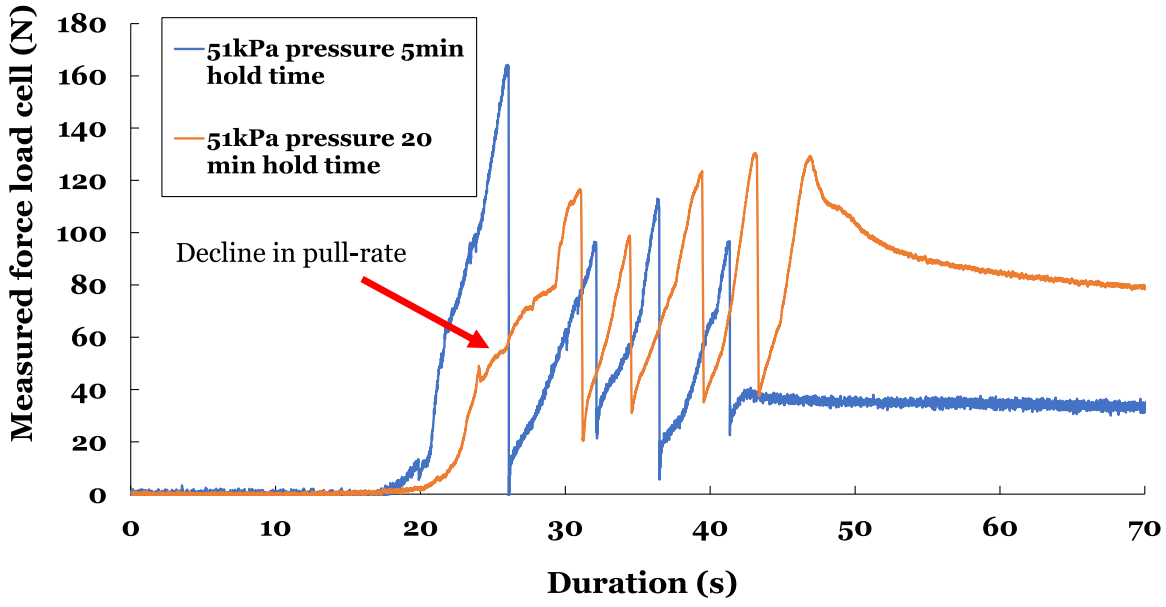

Figure 6.5: Pull curves show different behaviour for longer vs shorter holding time

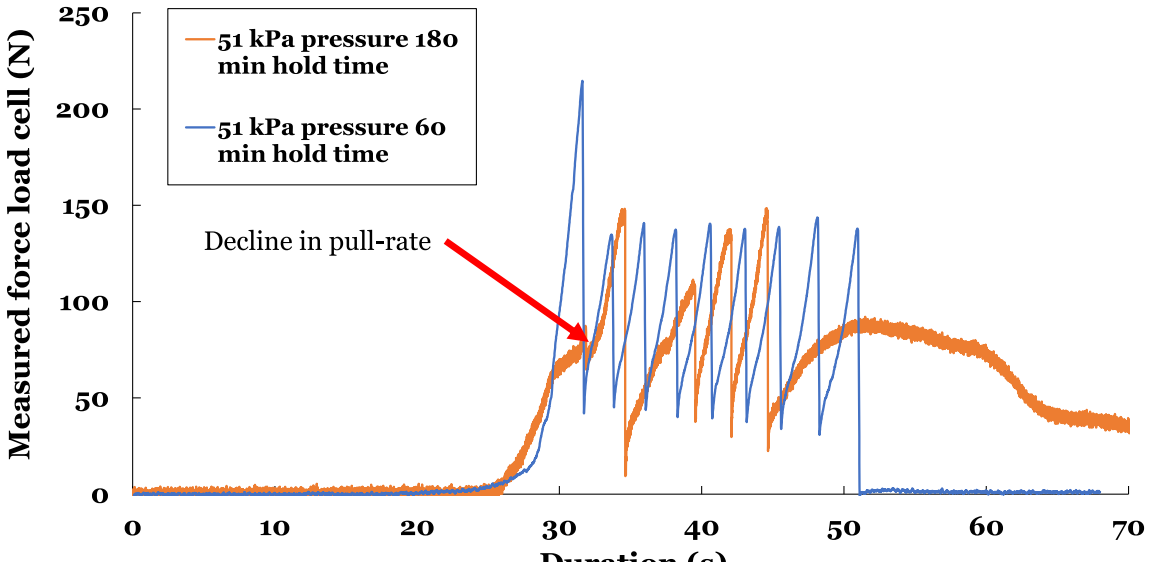

There is also a difference in stick-slip frequency of when comparing the two different tests. It is however unsure if this is in fact caused by the ice-concrete interaction or by the a different pull rate of the hydraulic actuator. As shown in section 3.3.2. This difference in frequency can be seen when looking at the saw-tooth shapes of the graph in Figure 6.6.

6.2. The influence of pressure on adhesive bond strength

It is clear from looking at Figure 5.6 that an increase in pressure, results in an increase of force required to shear the ice. This can be partly understood by considering Coulomb's friction law (formula 6.3) where a higher pressure results in a higher pull-out force. But the question is how the adhesive strength is affected by a change in pressure. In order to compare the test results of the different pressures from sequence 1, the maximum pull-out force has to be made dimensionless using equation 6.3.

Looking at the pictures could provide useful information on the influence of pressure on the ice-concrete bond strength. It does seem that the higher the pressure, the more ice will stick on the concrete. But when looking at Figure 6.3, the highest coefficients are seen for the highest lowest pressures.

Why then does the bond break force seems to decrease with increasing pressure, while there is more ice on the concrete? This can perhaps be explained by the fact that for a higher pressure, more dislocations in the crystals occur which decreasing the strength of the ice. Then when pulling out, the weakened ice breaks off easier, leaving more ice on the concrete and causing the pull-out force to be lower.

6.3. The memory effect of adhesion

When looking at the outcomes of the results of test sequence 3, again a positive relationship between waiting time and bond break force has been observed. It seems that the bond strength between the ice and concrete increases after releasing the pressure. [21] Did a finite element numerical analysis which shows an uneven stress distribution when doing shear tests. The visco-plastic behaviour of ice could cause this uneven distribution to even out more, resulting in less high stress concentrations and a larger overall bond strength.

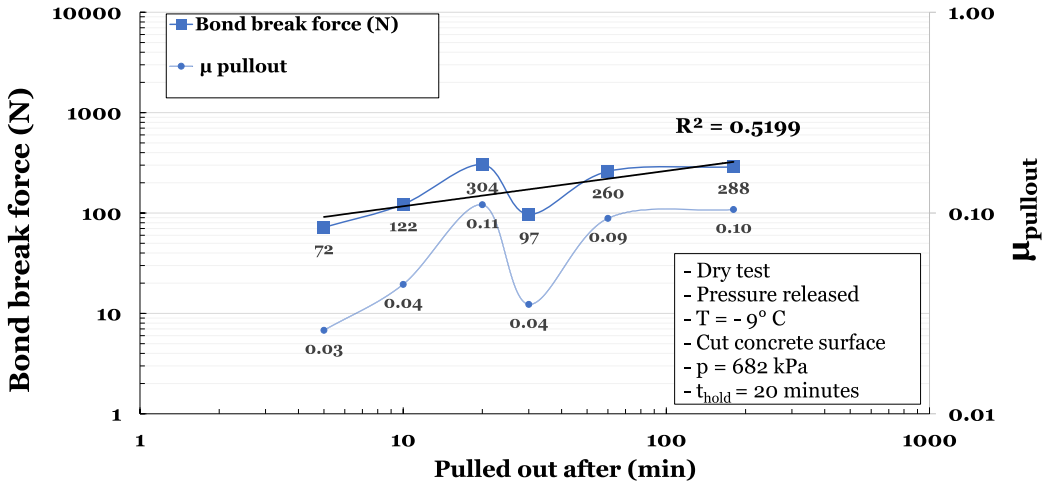

Figure 6.7: Bond breaking force of 682 kPa pressure and 20 minutes hold time plotted over waiting time before pulling.

6.3.1. explaining the outliers in the results

There are two noticeable big outliers in this sequence, indicated by the red circles in Figure 6.7. It is unlikely that these are measurement errors and looking at the pull-curves of the tests could help explain the outliers. When comparing the pull- curves, which can be found in Appendix B, Figure B.6, some differences in the behaviour can be noticed. The pull curves of the 5, 10, 20, and 30 minute waiting time can be seen in Figure 6.8.

In all but the 20 minute wait time curve, a small dip has been observed before pulling the ice. When assuming the hydraulic actuator performs a pull with an alwasy increasing force, which has been validated in section 3.3.2, the little dip can only be explained by a small movement of a part in the system. It is not

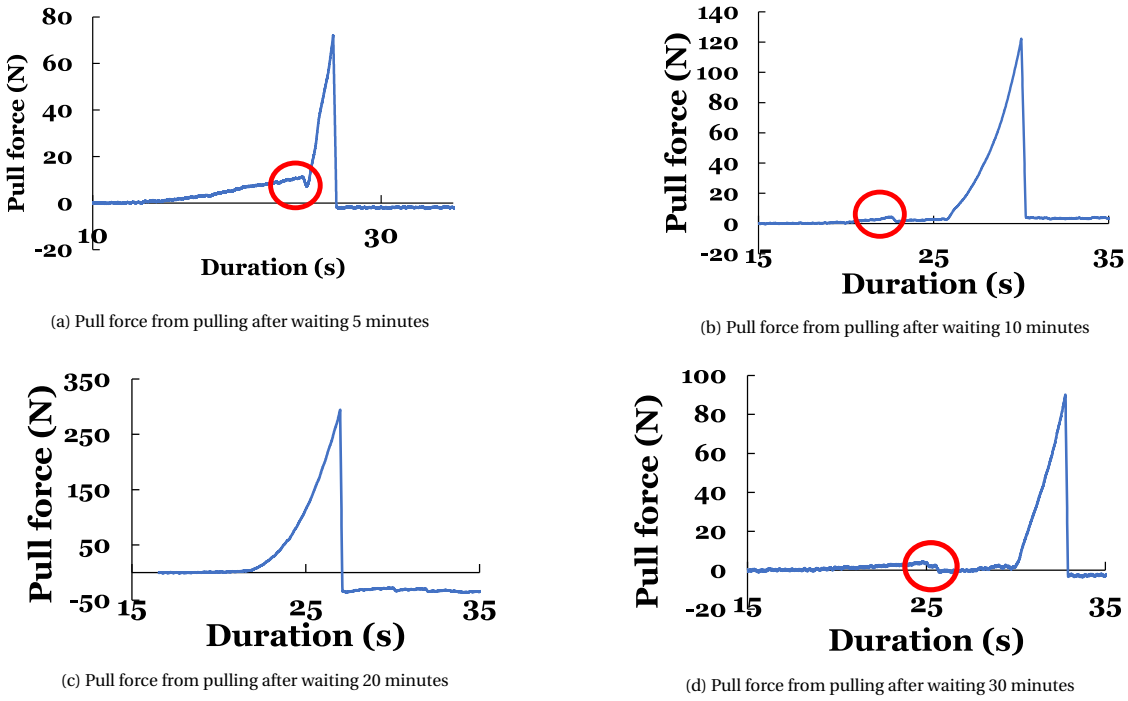

(a) Pull force from pulling after waiting 5 minutes

(b) Pull force from pulling after waiting 10 minutes

(c) Pull force from pulling after waiting 20 minutes

(d) Pull force from pulling after waiting 30 minutes

Figure 6.8: Pull curves of 682kPa 20 minutes hold time test, pulling after certain waiting time.

clear where this motion happens exactly, but it could be in the ice puck, or the ice inside the ice puck holder itself .This could mean that perhaps a tiny bit of the bond already broke, or that the bond broke on 1 of the concrete surfaces before building up large forces and breaking the other bond. This could explain the high outlier of the 20 minute test or perhaps the underestimation of the other three tests. To explore if this would result in a smaller outliers of the dimensionless force, equation 6.4 is adjusted to:

$$\mu_{pullout} = \frac{F_{pullout}}{A_{surface} * \sigma_n} \tag{6.6}$$

For the holding times which show a little dip in the pull curve and only 1 surface is now considered when calculating the area and its related dimensionless force. The adjusted results are plotted in Figure 6.9 below.

An increase of $\mu_{pullout}$ from 0.03 to 0.05 is the result for a waiting time of 5 minutes before pulling out. The values $\mu_{pullout}$ of waiting 0 minutes before pulling out, as has been done twice in sequence 2, are 0.025 and 0.034 (from Appendix B, Table **??** using formula 6.4) which are around the same as after waiting for 5 minutes.

The results indicate that waiting longer on pulling out the ice puck will indeed result in an increasing force, but no statistical significance has been reached and further research will need to be done in order to that confirm the indication.

6.4. Comparing different surfaces

The tests from sequence 4, where different surfaces have been used in the same tests, show a significant difference in outcome. The error bands in the graph shows a 5.1% error which could be caused by an error in the load cell. The differences in bond breaking force are significant when considering the error ranges of the results. The sandstone shows significantly lower bond breaking forces, both when the pressure is released and maintained. To compare, the pure paste surface, as shown in Figures 6.10 and 6.11 shows the highest bond breaking force. Both cohesive as substrate failure has been observed after the test, indicating either very strong adhesive force or poor coherence of the concrete cylinder. A photograph can be found in Appendix C, Figures C.7a and C.7b. The cut surface, which has an aggregate to paste ration of about 1.3, lies somewhere in between. This indicates that some properties of the different surfaces will result in varying bond

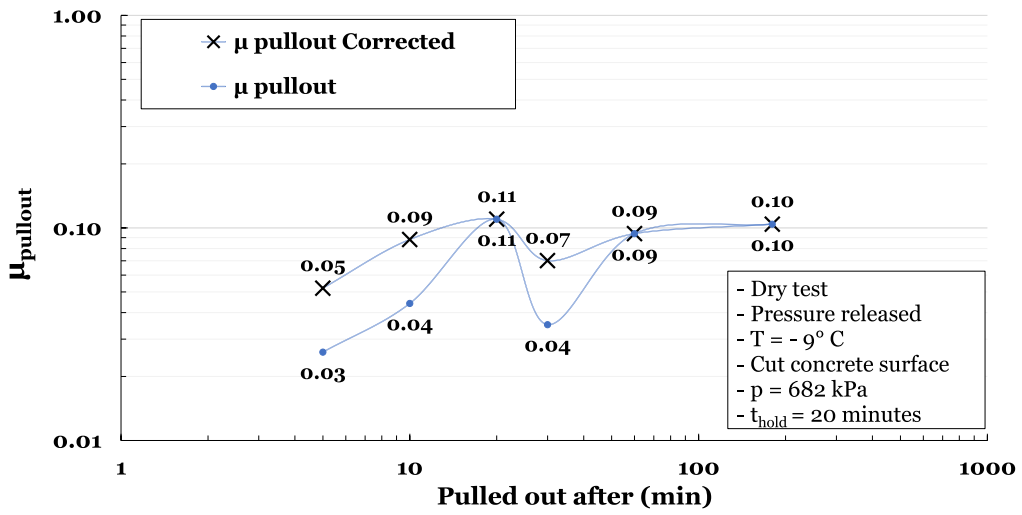

Figure 6.9: Dimensionless pull force from 682 kPa pressure and 20 minutes hold time test plotted over waiting time before pulling.

breaking forces. Factors such as: surface roughness, permeability, porosity, chemical composition might all be influencing the bond strength. Literature suggests that surface roughness is an important property determining the outcome when comparing results of the same material. It would be interesting to compare different surfaces, while keeping surface roughness constant and look at the influence of different compositions and permeation properties.

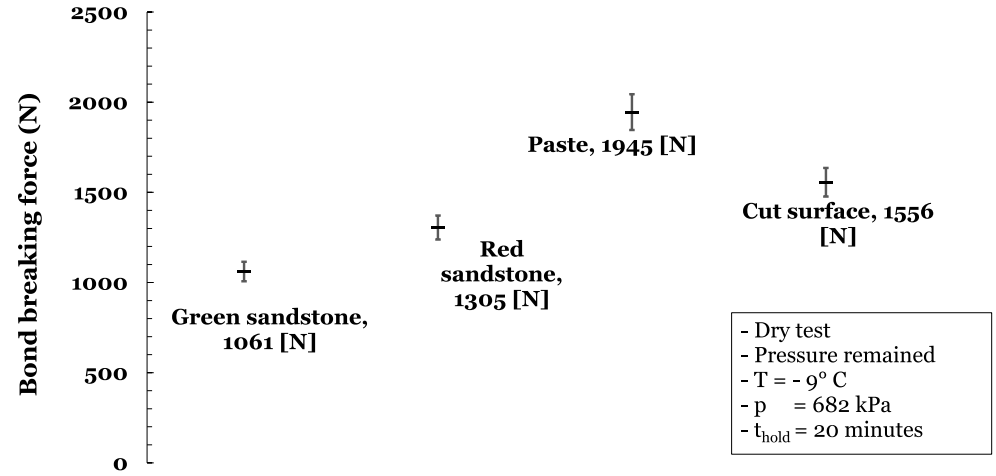

Figure 6.10: Bond breaking force for different ice-concrete shear test with different surfaces. Pressure is remained before initiating pull.

The main conclusions from this test sequence are:

- The sandstone rock core samples show lower adhesive strengths than the cut surface and the paste. This could be because of differences in surface roughness, permeability, porosity. This however needs more research to be confirmed.
- The paste surface is more likely to undergo substrate failure and also has seen the highest bond breaking forces. This indicates that the adhesive bond between ice and the paste is stronger than the cut surface and the granite rock core samples. It could also indicate that the coherence of the outer layer of the concrete is not very strong, which allows for exposure of the aggregate.

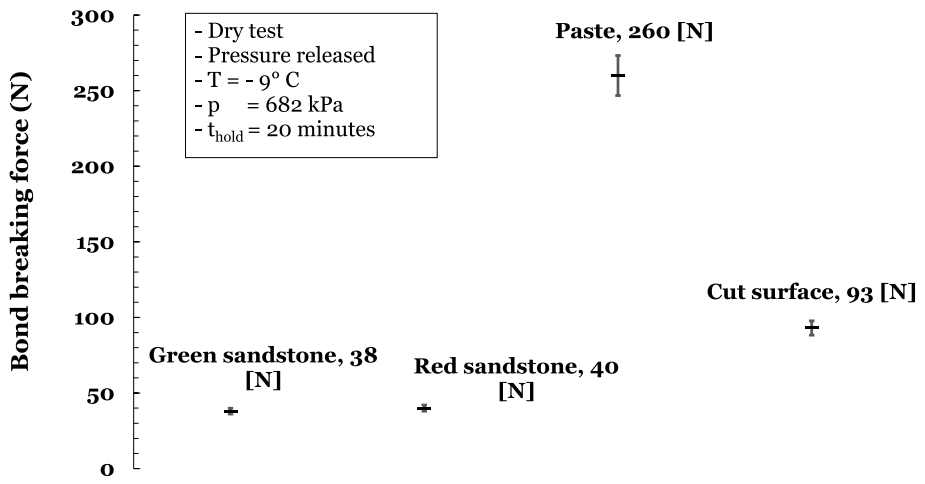

Figure 6.11: Bond breaking force for different ice-concrete shear test with different surfaces. Pressure is released before initiating pull.

- From these tests, it is not possible to determine which property of the material causes the difference in bond breaking strength.
- The observation that the pure paste has been abraded away in this test supports the theory of [17] of concrete abrasion, where at the initial stage of general wear, first the concrete paste is abraded away.

6.5. The influence of submergence on ice-concrete bond strength

The submergence tests showed a similar positive influence of holding time on bond strength as can be seen in Figure 6.12. When comparing the different pressures, it generally seems that a higher pressure results in a higher bond strength, however when comparing the static friction coefficients, an increase in pressure results in a decrease of static friction coefficient, as can be seen in Figure 6.13a.

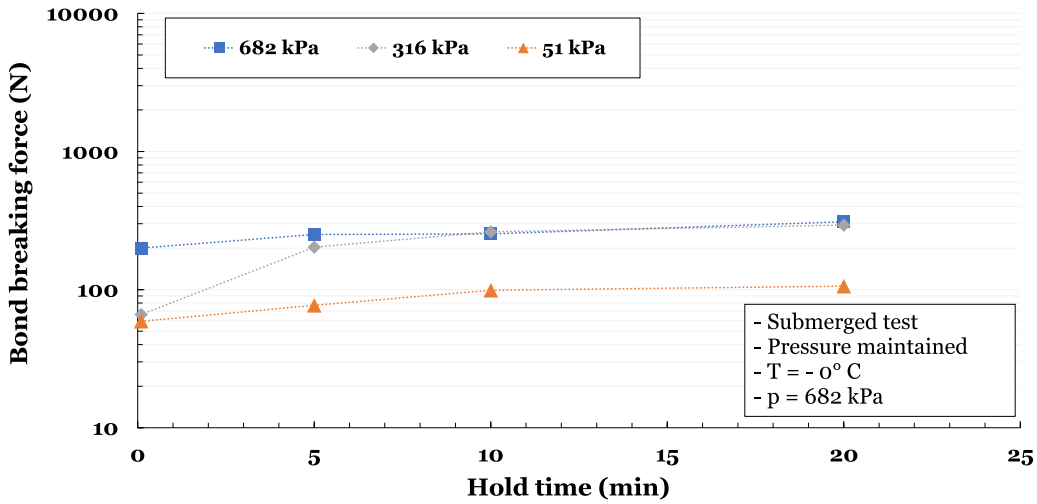

Figure 6.12: Peak adhesion force for tests in sequence 1 plotted versus hold time for submerged tests

The fact that the shear force required to break the bond increases for an increasing pressure, but noting that the static friction coefficient μ_s decreases, can be explained by looking at formula 6.1 and realizing that σ_n increases more than μ_s decreases.

It can be seen very clear from Figure 6.13a that the friction coefficient is lower for higher pressures. [12] found similar results for his cyclic friction tests using laboratory grown columnar ice and micro-concrete

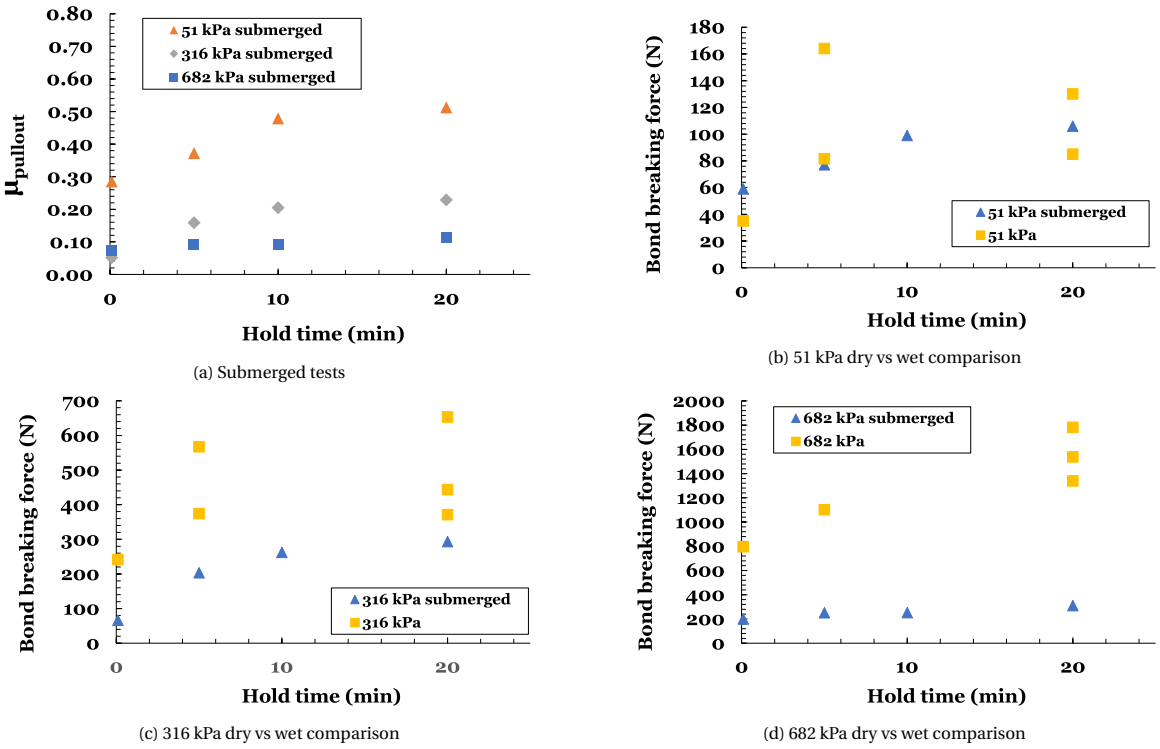

(a) Submerged tests

(b) 51 kPa dry vs wet comparison

(c) 316 kPa dry vs wet comparison

(d) 682 kPa dry vs wet comparison

Figure 6.13: (a) t/m (c): Submerged versus dry test, (d) static friction coefficients of submerged test

plates at similar temperatures.

6.5.1. Comparison of wet versus dry adhesion

As can be seen from Figure 6.13b, for more than half of the instances of the 51 kPa pressure test, the dry bond is stronger than the wet bond, but the results are not sufficient to draw any conclusions. However for the 316 kPa (Figure 6.13c) and 682 kPa (Figure 6.13d) pressures, the bond strength of the wet test is significantly lower than that of the dry test. The fact that the submerged ice cylinder is surrounded by water of about 0 °Celsius could have significant influence on the bond strength.

Effect of temperature

[27] Found that for adhesion strength of ice to uncoated steel, the adfreeze bond strength is higher for lower temperatures. This can be seen in Figure 6.14. The shear strength is a physical property of the ice which depends on the temperature. When the temperature increases, the shear strength decreases resulting perhaps in easier breaking of the adhesive bond.

Effect of undrained concrete

During the submerged tests, the concrete cylinders have been underwater the entire time. This results in a fully undrained situation where the pores of the concrete are fully filled with water. Mechanical adhesion theory suggests that the adherend will replace the air in the pores and cavities of the concrete. The presence of a water layer or water molecules in the concrete pores may reduce the mechanical bonding mechanism. It could also be that the ice melts, reducing the creep rate into the concrete.

Liquid like layer

It is hard to tell what exactly causes the adhesive bond strength to decrease, but concluded can be that many factors can be responsible and that the effects on a structure will be reduced when the interface is (partly) wet.

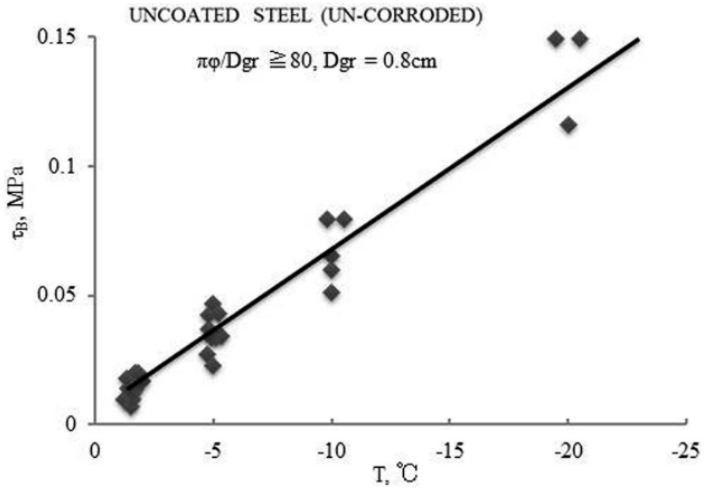

Figure 6.14: Effect of temperature on adfreeze bond strength for uncoated steel [27]

6.6. What could happen at the interface

Now that it is clear that the holding time has a positive influence on the bond breaking strength, it is interesting to see how this can be explained. An effort is done by looking into literature and theorising about the possible mechanisms responsible for the observed phenomenon.

6.6.1. Increase in real contact area

In literature, it is widely accepted that the actual contact area of two solids is only a small fraction of the nominal contact are[5]. Because of ice's ability to perform dislocation creep, the area of micro-contacts during holding is likely to increase. The shear force required to break the bond the increases with proportion to the contact area. [5] has shown that the contact area scales logarithmic with time. [21] states that it is reasonable to assume the following: The adhesion strength depends linearly with the effective contact area. Thus adhesion strength scales logarithmic with time.

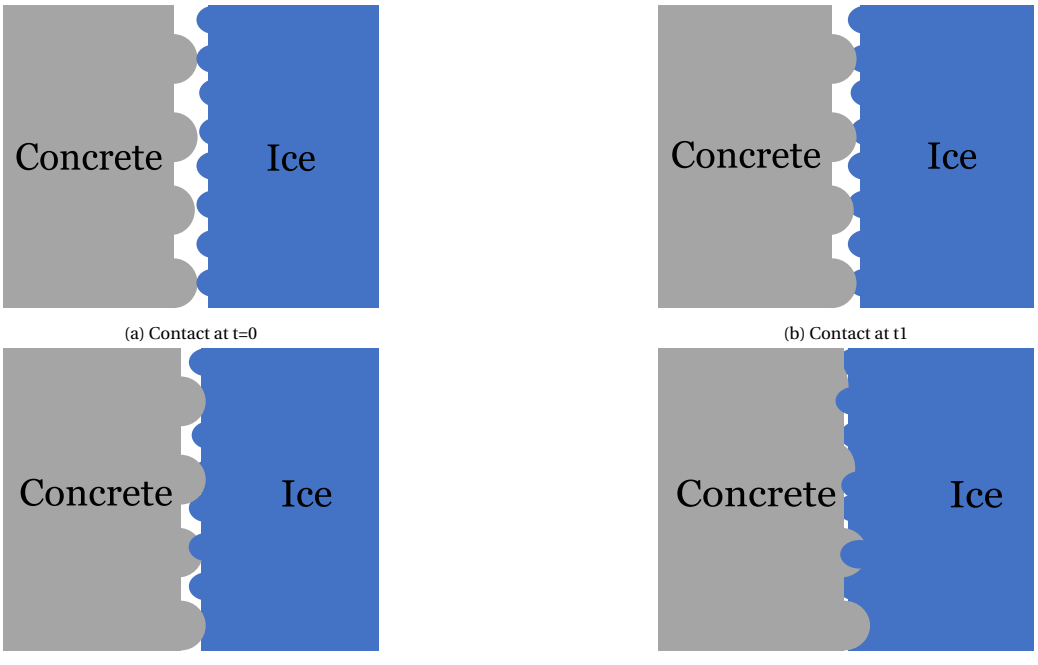

(a) Contact at t=0

(b) Contact at t1

(c) Contact at t2

(d) Contact at t3

Figure 6.15: Theoretical representation of increase of real contact area over time

6.6.2. How the bond is formed

As is observed from the research in this thesis , as well as in research from others, a longer holding time will result in a stronger ice-concrete bond. This could be because the real contact area between concrete and ice asperities increases over time due to the viscous-plasticity of ice.

It is known that ice behaves viscous-plastic and that when under pressure, ice can deform and by dislocations in the crystal structure the ice will creep. Therefore, during the experiments, the ice asperities may creep into the concrete asperities and later creep its way into the pores of the concrete. This hypothesis can be supported by the visual observations, which show that for longer holding times, the amount of ice which is stuck on the concrete after breaking the bond is significantly higher. Figure 6.16 shows deformation of the ice after 3 hours of 683kPa pressure.

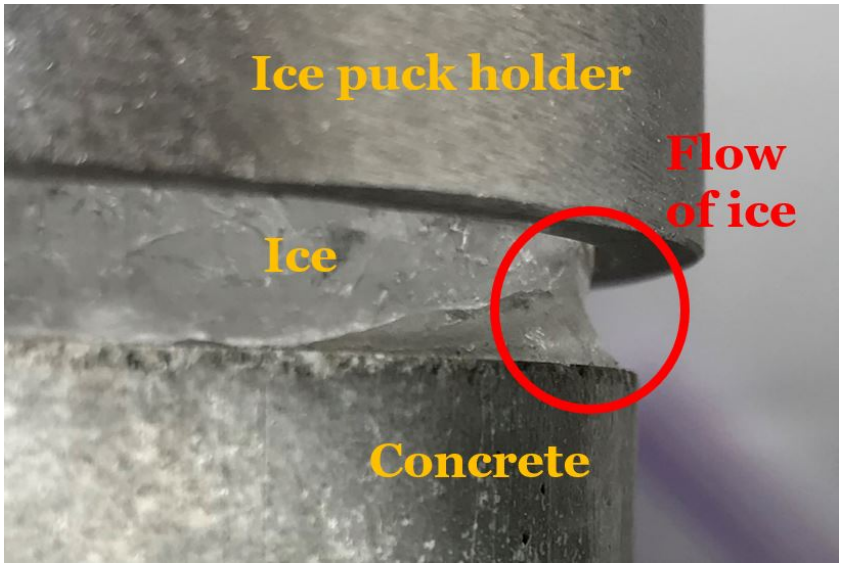

Figure 6.16: Deformation of the ice overnight after 682 kPa pressure

From visual observations it seems that water molecules creep into the concrete pores. If this happens, there is no clear interface anymore which means the failure is both adhesive and cohesive. Comparing the pictures in Figures C.2a and C.2b with C.4, one can see that perhaps multiple adhesive bonding mechanisms and different failure modes are present. The first pictures show clear wetting of the concrete surface and very little to no damage to the ice, indicating adhesive failure. But for both longer holding times and higher pressures, mechanical adhesion theory, where the adhesive penetrates the pores of the ice, seems to apply. The failure mode then becomes mostly cohesive (mode (b) in Figure 6.17) and a significant portion of ice is stuck on the concrete.

6.6.3. How the bond is broken

There are three different types of bond failure which are considered and observed in this research. In Figure 6.17, (a) shows the illustration of pure adhesive failure. The bond breaks exactly at the interface and the surfaces of the two materials remain fully intact. This mode is referred to as: adhesive failure. At (b), the bond at the interface is stronger than the strength of the material itself resulting in cohesive failure of the adhesive, the ice. Failure mode (c) represents failure in coherence of the concrete, where the substrate, in the case of this research the concrete, fails. If this happens in an ice-concrete interaction, this type of failure would directly result into concrete abrasion.

From all experiments with a holding time longer than 6 seconds, a clear layer of water has been observed on the surface of the concrete. This indicates that the breaking of the bond is never pure adhesive failure. The adhesive bond seems stronger than the ice itself and during many tests, and confirmed by video, the critical failure of the bond starts with the propagation of tiny cracks, followed by a critical failure of the ice.

All three failure modes from Figure 6.17 have been observed during the experiments. with a clear adhesive failure for low holding times and low pressures, an overlapping region where either cohesive, or adhesive failure occurs and full cohesive failure for the longer holding times and higher pressures. Cohesive failure has been observed the most throughout all the tests. Table 6.3 shows the failure modes observed for the different

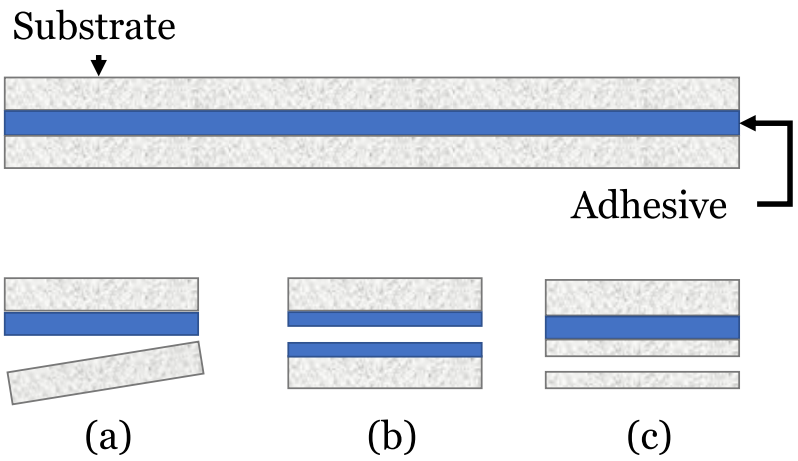

Figure 6.17: Three different failure modes: (a) Adhesive failure, (b) cohesive failure of ice, (c) Substrate failure of concrete

pressures and holding time.

Table 6.3: Failure modes observed in tests

		Pressure (kPa)		
		51	316	682
Hold time (min)	0.1	A	A	C/A
	2	A	C/A	C
	5	C/A	C/A	C/S*
	≥ 20	C	C	C

A= Adhesive failure
C = Cohesive failure
S = Substrate failure

Figure 6.18 shows an illustration of the influence of holding time on the observed bond failure and the result on both the concrete's and ice's surface.

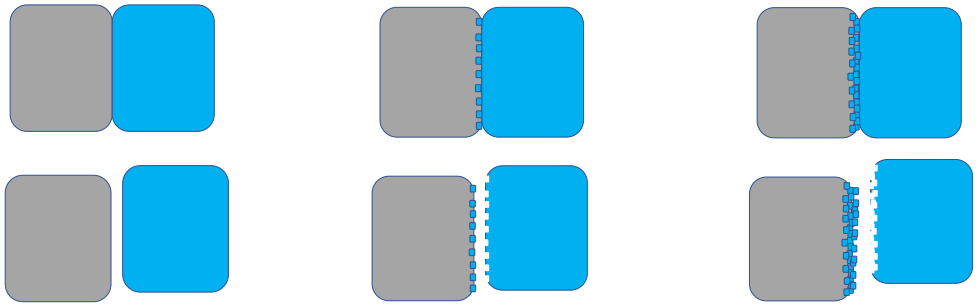

(a) Bond failure after short hold time (b) Bond failure after longer hold time (c) Bond failure after longer hold time

Figure 6.18: Theoretical representation of influence of holding time on ice destruction

Although there is a clear dependence of the bond breaking force on holding time, still however, many uncertainties arise when breaking the bond and the peak bond breaking force can be influenced by some uncontrollable factors such as:

Stress distribution when performing shear tests
The finite element numerical analysis by [21] shows an uneven stress distribution when doing shear tests. Although the double shear is designed to eliminate moments which could cause normal stresses on the ice, its very hard to be sure that only shear stresses are present when shearing off the ice. This could cause preliminary cracking of the ice resulting in lower adhesion strengths.

Fluctuating temperature on bond strength

Thermally induced stresses [21], caused by quickly cooling down the ice samples after shaping them, could cause micro cracks in the ice. The thermal expansion coefficient of ice is, on average, 5 times higher than that of concrete ($50 * 10^{-}6/$ °C [21] of ice versus $9.6 * 10^{-}6/$ °C of an average concrete [3]) So when temperature is fluctuating, the differences in thermal expansion or contraction will cause stresses in the ice, affecting its strength and therefore the adhesive bond or cohesive internal strength of the concrete. Also, [27] showed that the adhesive bond strength increases for a decreasing temperature, because of an increase of shear strength of ice for a decreasing temperature.

6.7. Empirical model for predicting the adhesion force for dry ice-concrete interaction

During the Slide-hold-slide experiments performed by [32], the increment of static friction to re-initiating sliding following holding, increases logarithmically with time as:

$$\Delta\mu_s \propto \beta \log_{10} t \tag{6.7}$$

Where β is defined as the static strengthening coefficient and has the value $\beta = 0.23 \pm 0.02$. Static strengthening is defined as an increase in static friction coefficient, $\Delta\mu_s$, for increasing holding times [31]. Alternative to equation 6.7, the increment of μ_s may be described by the power law, in the form of:

$$\Delta\mu_s = At^m \tag{6.8}$$

Where, A is a constant, t is the holding time, and m is a coefficient.

The formula for the static friction coefficient describes the outcomes of a σ_m =60 kPa test with ice-ice interaction. When fitting a curve to the data, it fits best using a power-law formula, which has the same shape as formula 6.8.

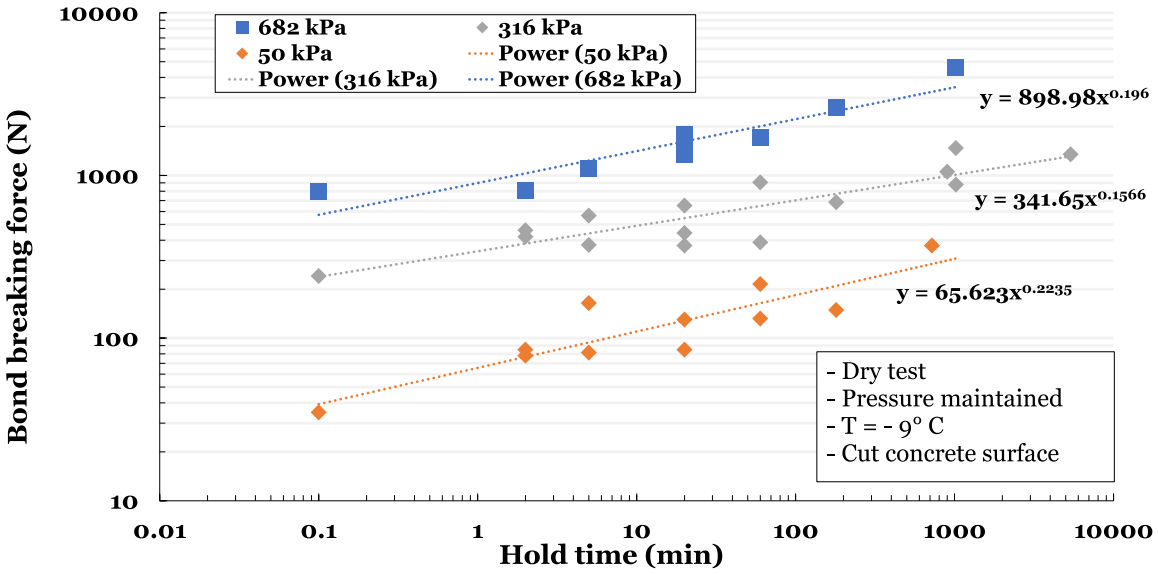

Figure 6.19: Sequence 1 with power-law curves

Instead of having A as a constant, it seems best to have this as a variable depending on the pressure and m in the formula can be derived from the experiments and turns out to be about 0.2. The fitted curves almost take the shape of the following form:

$$F_{bondbreak} = p_{applied} * t_{hold}^{0.2} \tag{6.9}$$

The correlation between the predictive formula and the actual experimental data is calculated to be 0.945 for the pull-out force. Equation 6.9 could be used to estimate the force required to break an ice-concrete bond using the pressure and holding time as predictors.

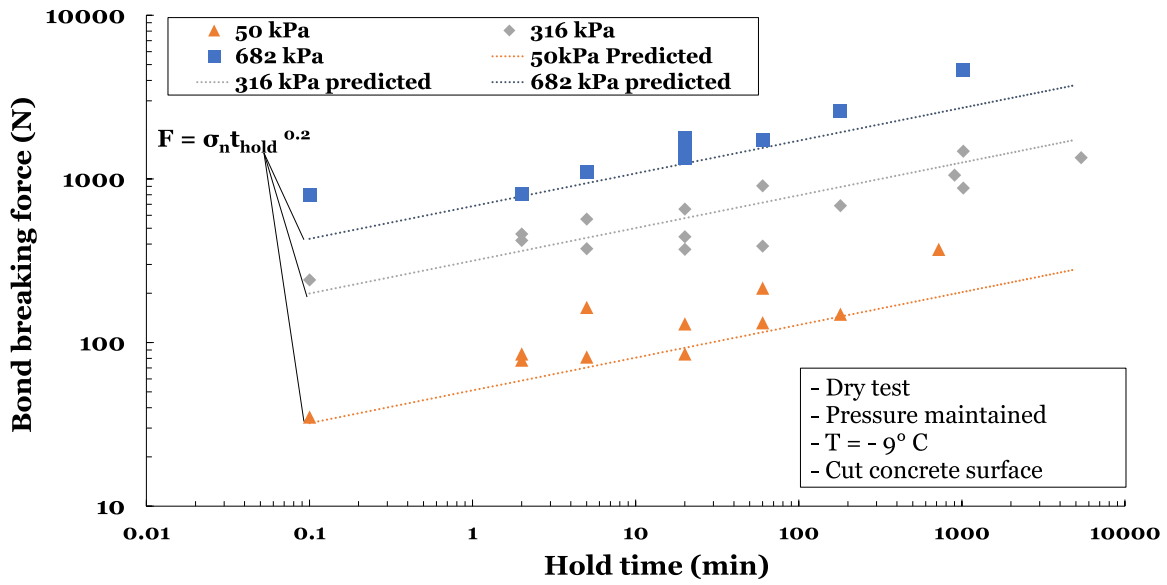

Figure 6.20: Sequence 1 with power-law curves from model 6.9

6.8. Theoretical mapping of possible abrasion mechanisms by adhesion

Adhesion of ice to concrete can contribute to abrasion in many different ways. It seems unlikely that adhesion only plays a role in just one mechanism at the time. This is already obvious when thinking about the first division in the diagram of Figure 6.21, and realizing that in real-life situations, both wet (1) and dry(2) adhesion can occur at the same time. The diagram gives an overview of how several mechanisms of concrete abrasion relate to ice-concrete adhesion and when to expect which mechanism. Many of the mechanisms involved are related to each other. As has been concluded from the experiments and literature review, the failure mode of the ice-concrete bond depends heavily on the surface characteristics, pressure and holding time (3). Depending on the conditions, either adhesive (4), cohesive (5) or substrate failure (6) can occur. When adhesive failure occurs, The loosening of sharp abrasive particles (7) could increase the wear rate (11) until, after general wear (16), a state of catastrophic wear (17) is reached.(2.2). Incorporated with this change of state in mechanism is a change in surface characteristics, which, as shown by the experiments from tests with different surfaces, could changes the outcome of adhesive strength. Micro cracks (13) can be caused by high tensile stresses, but also because of a difference in thermal expansion/contraction coefficient (12) between ice and concrete. These microcracks will then allow more water to enter the concrete and high pressures could propagate these cracks. This leads to increased porosity (14) and changes in permeation properties of water [24]. This could lead to stronger adhesion but also the weakened concrete could lead to increased probability of substrate failure by lowering the freeze-thaw cycle resistance (15). When substrate failure occurs, the aggregate of the concrete can be exposed (10) resulting in a change of surface characteristics which may lead to another bond failure type.

6.9. Application for full-scale ice-interaction from results

The results from the experiments are obtained when measuring in a laboratory where many factors were remained constant. This allows for systematically exploration of several factors. It s however important to think about how this would be in a full-size ice-structure interaction situation and if the interpretations from the experiments are applicable on a larger scale.

The effect that ice adhesion has on full-scale ice-structure interaction, when considering abrasion, is influenced by many factors. It is very difficult to relate the outcomes of the experiments to reality because of the many uncertainties that arise in real-life situations. In the lab, many factors can be controlled more easily and many factors such as the ice composition en the constant ambient temperature have been simplified. The outcomes of test sequence 1 and the empirical model can be used to roughly estimate the forces exerted by the ice on a structure in contact region 2 (illustrated in Figure 2.1). The other outcomes can be used to

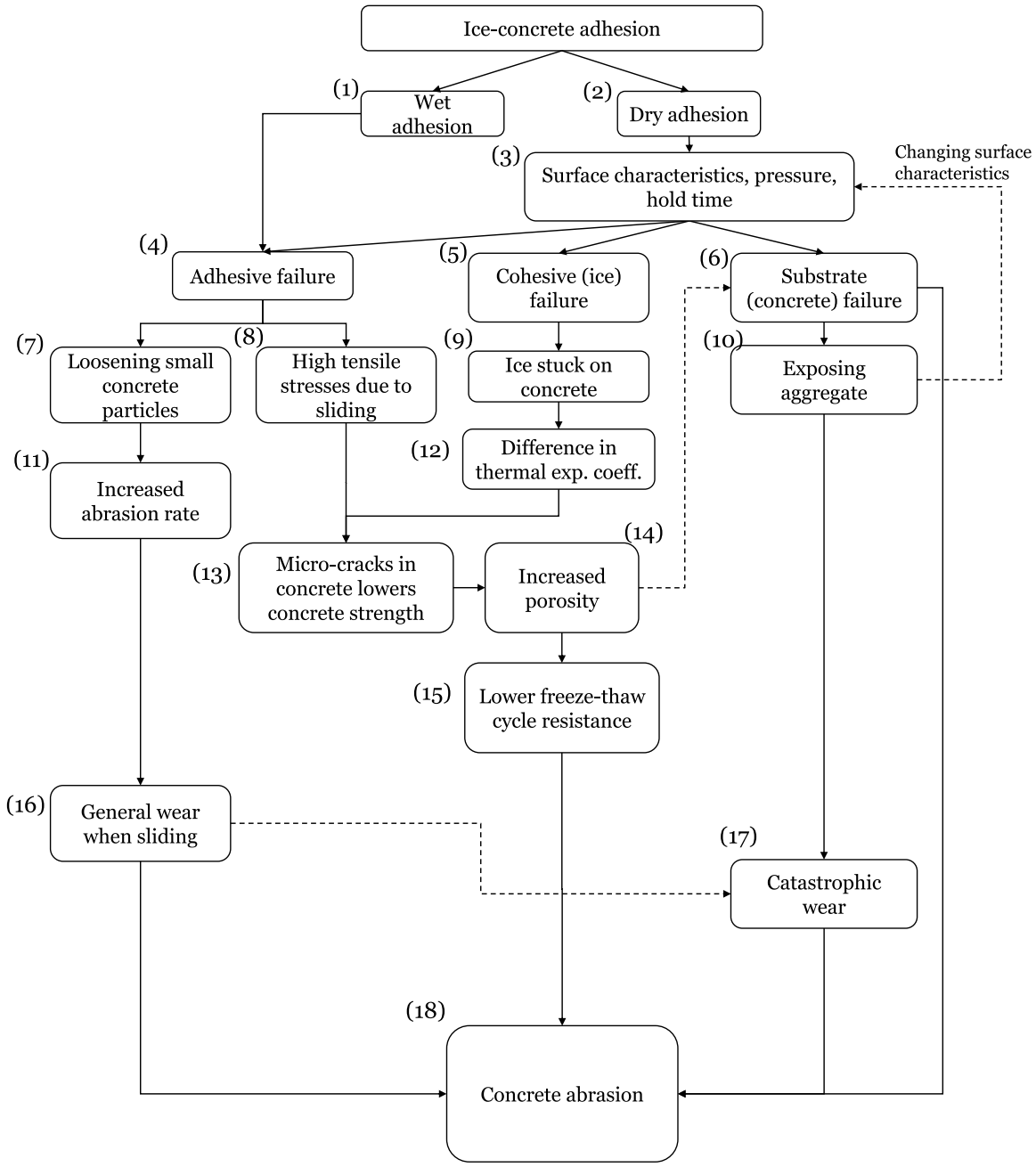

Figure 6.21: Theoretical options for concrete abrasion by ice adhesion

further investigate the boundaries for when certain abrasion mechanism can be present during interaction. To apply this outcome in a full-scale situation, one should consider the following:

6.9.1. Surface of concrete in experiments versus tests

The surfaces of all the concrete cylinders used in the test have been prepared by performing the same procedure for every cylinder which would result in a highly constant roughness. [12] observed however when performing his cyclic friction tests (2.3) that plates with equivalent average roughness, could still give differences in frictional behaviour.

6.9.2. Effect of water salinity

The adhesion of all materials is affected by impurities and chemical effects. In real-life applications, the majority of ice encountered by structures is formed from sea ice. Because the NaCl crystals won't fit in the crystal structure of hexagonal ice, they are wedged out when the ice is formed leaving behind brine pockets. The existence of brine pockets reduces de adhesion strength of ice which, apparently is caused by a reduction of real contact area at the ice-concrete interface. [21] Created a model where brine pockets were modelled as vertically orientated cylinders, but the model predicted much higher adhesion forces than observed. [30] Has found that a liquid salt solution layer exists at the interface causing the adhesive strength to decrease. It is thus expected that adhesion of highly saline ice causes lower adhesion forces. It does require further investigation and the only thing the author can say is that a thicker brine layer will result in lower ice adhesion strength. [**?**] observed that in the case of low temperature sea water, solid salts accelerate abrasion. In fresh water conditions, the same effect is expected when the ice can be contaminated with small than, clay or powdered concrete particles etc.

6.9.3. Wet or dry surface

In reality, most of the surface of the ice is, due to waves and the surrounding water, wetted when interacting with a structure. The tests from Sequence 5 have shown that wetting dramatically reduces the strength of the ice-concrete bond. In reality, part of the ice will be wet and the upper part will be dry. To really examine whether this effect is true on real-life applications, measurements of abrasion should be done when also monitoring the water level and the wetting of the surface. But from literature, and illustrated in Figure 2.7, the effect of a water layer between the ice and the concrete could result in high internal stresses and form micro cracks in the concrete reducing its strength and leaving it more vulnerable to abrasion.

6.9.4. Size effect

Although the brine pockets present in sea ice do not significantly change the friction of ice [20], it will affect the shear strength of ice. Because generally speaking, the strength of ice is that of the weakest link. There is a smaller chance of a defect in an ice sample when it is smaller. Therefore the average strength of small ice samples will be higher than that of real life situations where massive ice samples will very likely have several defects.

6.9.5. Abrasion by shearing versus crushing

In a case of a real life ice-structure interaction, sliding is not the only mechanism by which the ice and concrete will interact. At the high pressure zone (region 1 in Figure 2.1) mainly ice crushing will occur and the question is whether this could play a role in the abrasion by adhesion and how it influences the abrasion mechanisms. The formation of a layer of crushed ice particles between the ice-concrete interface may very well have an effect on the adhesion and abrasion. A state of the art study by [22] however concluded that sliding is more detrimental for abrasion than crushing. Perhaps because a normal load, in the case of a crushing situation, would push aggregate parts into the concrete's past instead of shearing them out when ice slides along concrete in a case of catastrophic wear. Probably many factors will influence the mechanism responsible for abrasion and in the region where ice crushing occurs, the movement of a broken ice piece could also cause tensile stresses when being squeezed by the concrete surface and the incoming ice sheet.

7

Conclusions and recommendations

7.1. Conclusion

During this master thesis, we have successfully completed the design and construction of a double shear test apparatus, which can simulate simplified ice adhesion in ice-structure interaction whilst controlling several extrinsic parameters.

This resulted in the ability to perform multiple test sequences in order to explore the impact of several extrinsic conditions on the bond strength between concrete and ice. It also enabled us to investigate the role adhesion can play in the abrasion processes and to explore the failure modes.

From these experiments, it can be concluded that the adhesion of ice to concrete and the achieved bonding strength is heavily dependent on the holding time and the surface characteristics of the materials involved. The duration of applied pressure and time before shearing is initiated have a strong positive influence on the bond strength. It is unclear what role exactly pressure plays on the bond strength. These conclusions have, together with literature, been incorporated into a method which can help asses which role adhesion could play in the abrasion of concrete by ice. It shows the multiple connections between several abrasion mechanisms and in which way they can affect each other. Additionally, concluded from this research can be that:

- From the experiments in this research, mechanical bonding seems to be the main mechanism of the ice-concrete bond, but it is impossible to assess how hydrogen bonding and wetting theory are involved in the bonding processes by the experiments in this research.
- The ice-concrete bond experiences adhesive, cohesive and substrate failure. The type of failure is dependent on holding time and pressure.
- Although the ice-concrete bond strength can be approximated by a power-law formula, no direct link to prediction of concrete abrasion by adhesion has been found.
- The degree of abrasion rates by ice on concrete is still not well understood, but this research identified the possible roles adhesion can play in concrete abrasion processes.
- Holding time has a positive influence on the ice-concrete bond strength under the conditions of this research. Submergence has a negative influence on holding time, possibly because of fully draining the concrete air pores.
- The influence of pressure on the bond strength has not been identified in this research and requires more varying parameters to be identified.
- The work done is relevant because it identifies different mechanisms by which adhesion could contribute to concrete abrasion.

It is clear that adhesion is governing bond strength, but how do we distinguish adhesion force from friction force? From the tests in sequence 1, it is not possible to distinguish adhesion from static friction. And because there is still a significant amount of force needed to break the ice-concrete bond after releasing the pressure, as has been done in sequence 2, it can be concluded that adhesion cannot be assessed by Coulomb's friction model, because the 0-value of the normal load would result in zero force.

The results from the released pressure tests also suggest that there is no influence of pressure on the bond strength. But is the adhesion then unrelated to the applied normal load?

The data from test sequence 2 does not show any clear relationship between pressure and bond breaking force. The fact that adhesive strength increases after waiting for a certain amount of time also suggests that pressure application is not the main driver for the bond strength. But if this is true, then why won't the data from test sequence 1 converge? Also, visual observations have shown that more ice will be stuck on the concrete for higher pressures. So the question is then, what happens at the interface and in the ice when the pressure is released which influences the bond strength? Is there a limit in the bonding force or breaking force of the ice when the ice is not confined? And why then is the difference between wet and dry adhesion tests larger for higher pressures?

It is unclear which physical mechanism is responsible for this behaviour. If it's true that ice penetrates concrete when bonding, and will penetrate concrete more when under higher stresses, then water filled pores of concrete may reduce the penetration of the concrete which explains the higher differences.
When considering real life applications, it is expected that dry adhesion will cause more abrasive damage to the concrete compared to the wet adhesion because higher bond breaking strengths have been observed and in dry situations, water can act as a lubricant. This however has to be confirmed by field studies where there has been a constant monitoring of the waterline to conclude if this is true. If adhesion changes with pressure, how much does this tell us for the full situation?

7.2. recommendations

To further understand the influence of adhesion to abrasion processes, and to get more accurate results, some recommendations are stated below.

7.2.1. Improvements in experimental set-up and procedure

To further investigate the specific mechanisms which could play a role in concrete abrasion by ice, several improvements are suggested.

- Using a different hydraulic actuator when analysing stick-slip behaviour
  Although the DeFelsko Positest is an ASTM machine, it does have a drawback. The pulling will stop as soon as the device measures a 'fail'. It could however be interesting to see how a continuation of pulling effects the resulting measured force.
- Tests with a longer holding time could be held to investigate an upper limit on the bond breaking strength. Longer holding time tests require a more consistent cold room and Schulson [32] states that static strengthening has its dependence up to 10^5 seconds.
- Perform visual observations using optical microscopes at lower pressures
- Using a thermal camera to monitor heat fluxes
- Measure the displacement of the hydraulic actuator so the work done can be calculated which enables the use of energy balance analysis.

7.2.2. Recommendations for further research

- **Microcracks and adhesion** Further investigation of microcracks and adhesion in order to investigate the effect of micro cracks on adhesive strength. Identify which crack type is present when the ice fails to identify ductile-to-brittle failure regime.
- **Investigate Permeability versus adhesion** To investigate if the differences in outcome of different materials can be attributed to a specific material property.

- **The role of aggregate size in adhesion** The role of aggregate size and it's contribution to wear and to ice-concrete bond strength.
- **Explore ice-concrete interaction with a numerical model** In order to accurately predict the abrasion of concrete by ice including adhesion, the mechanisms in section 6.8 should be modelled by introducing different phases of the abrasion process and linking the different mechanisms together. Fiorio [12] stated that modelling contact between ice and concrete is complex and would require a 3D numerical model including an accurate description of the concrete's surface topography and the non-linear viscous-plastic behaviour of ice over this topography.

A

Data from experiments

(a) Data obtained by test sequence 1, table showing force in Newtons

Hold time (minutes)	Pressure		
	51 kPa	316 kPa	682 kPa
0.1	35	241	796
2	78	420	806
2	85	460	
5	164	374	1101
5	82	567	
20	85	653	1538
20	130	443	1339
20		371	1782
60	215	388	1714
60	132	907	
180	149	685	2614
720	371		
900		1053	
1020		1474	4609
1020		878	
5376		1347	

(b) Calculated dimensionless forces from sequence 1

Hold time (minutes)	Pressure		
	51 kPa	316 kPa	682 kPa
0.1	0.17	0.19	0.29
2	0.38	0.33	0.29
2	0.41	0.36	
5	0.79	0.29	0.40
5	0.39	0.44	
20	0.41	0.51	0.56
20	0.63	0.35	0.48
20		0.29	0.64
60	1.04	0.30	0.62
60	0.64	0.71	
180	0.72	0.53	0.95
720	1.79	0.00	
900		0.82	
1020		1.15	1.67
1020		0.69	
5376		1.05	

Table A.2: Data obtained by test sequence 2, table showing force in Newtons

Pressure	Hold time (minutes)						
	2	5	20	20	60	180	750
51 kPa	11	65	30		65	63	110
316 kPa	5	6	79		60	496	
682 kPa	8	102	70	95	145	135	

Table A.3: Calculated dimensionless forces from sequence 2

Pressure	Hold time (minutes)						
	2	5	20	20	60	180	750
51 kPa	0.053	0.314	0.145		0.314	0.305	0.532
316 kPa	0.004	0.005	0.062		0.047	0.387	
682 kPa	0.003	0.037	0.025	0.034	0.052	0.049	

Table A.4: Data obtained by test sequence 3, table showing force in Newtons

Pressure	Hold time	Waiting time (minutes)					
		5	10	20	30	60	180
682 kPa	20 min	72	122	304	97	260	288

Table A.5: Calculated dimensionless forces from sequence 3

Pressure	Hold time	Waiting time (minutes)					
		5	10	20	30	60	180
682 kPa	20 min	0.03	0.04	0.11	0.04	0.09	0.10

Table A.6: Data obtained by test sequence 4, table showing force in Newtons

p = 682 kPa t_{hold} **= 20 min**	Surface type			
	Green	Red	Paste	Cut
Pressure remained	1061	1305	1945	1556
Pressure released	38	40	260	93

Table A.7: Calculated dimensionless forces from sequence 4

p = 682 kPa t_{hold} **= 20 min**	Surface type			
	Green	Red	Paste	Cut
Pressure remained	0.384	0.472	0.704	0.563
Pressure released	0.014	0.014	0.094	0.034

Table A.8: Data obtained by test sequence 5, table showing force in Newtons

Pressure	Hold time (minutes)			
	0.1	5	10	20
51 kPa	59	77	99	106
316 kPa	66	203	262	293
682 kPa	200	251	253	310

Table A.9: Calculated dimensionless forces from sequence 5

Pressure	Hold time (minutes)			
	0.1	5	10	20
51 kPa	0.29	0.37	0.48	0.51
316 kPa	0.05	0.16	0.20	0.23
682 kPa	0.07	0.09	0.09	0.11

B

Pull curves

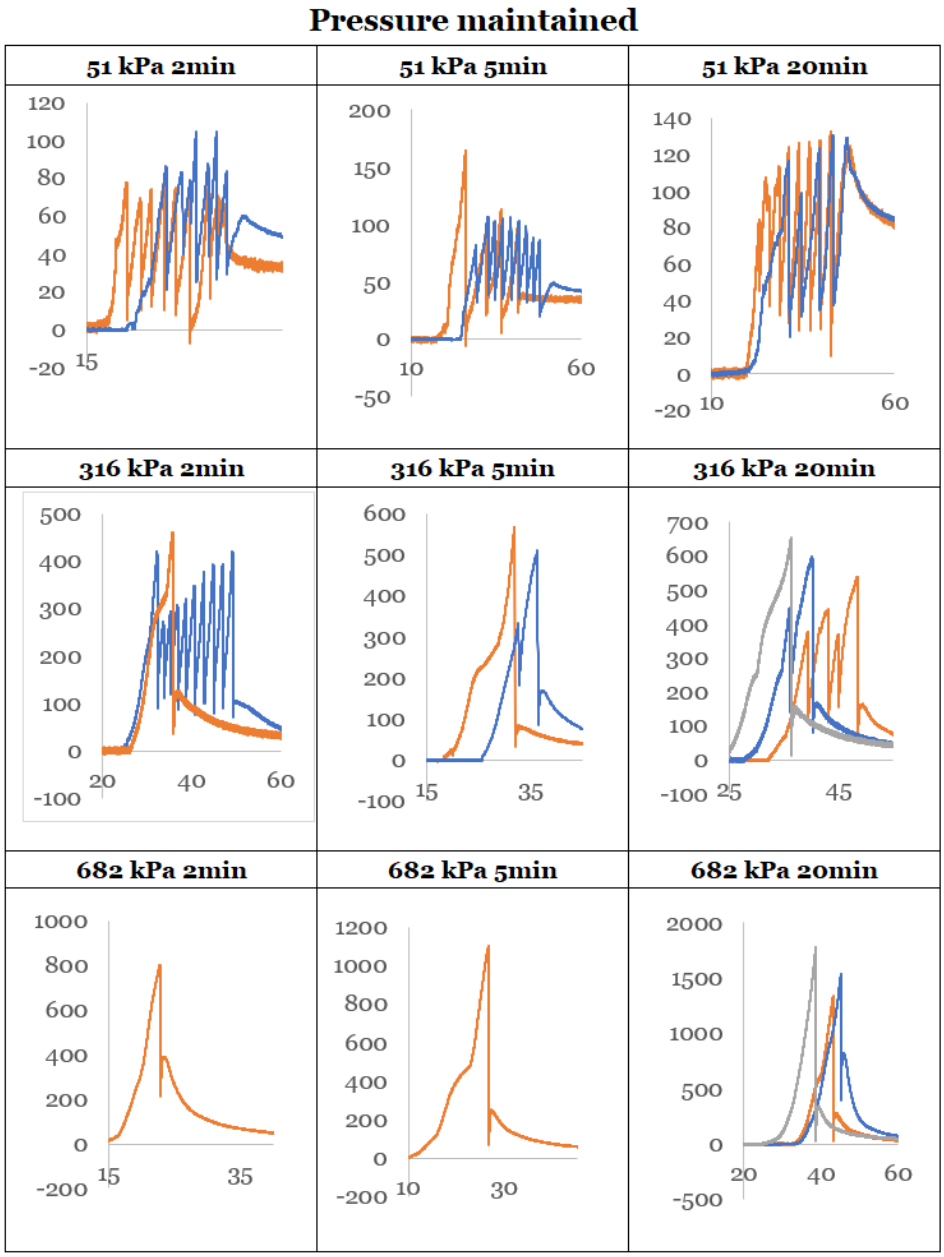

Figure B.1: Pull curves test sequence 1. Duration on x-axis and force on the y-axis

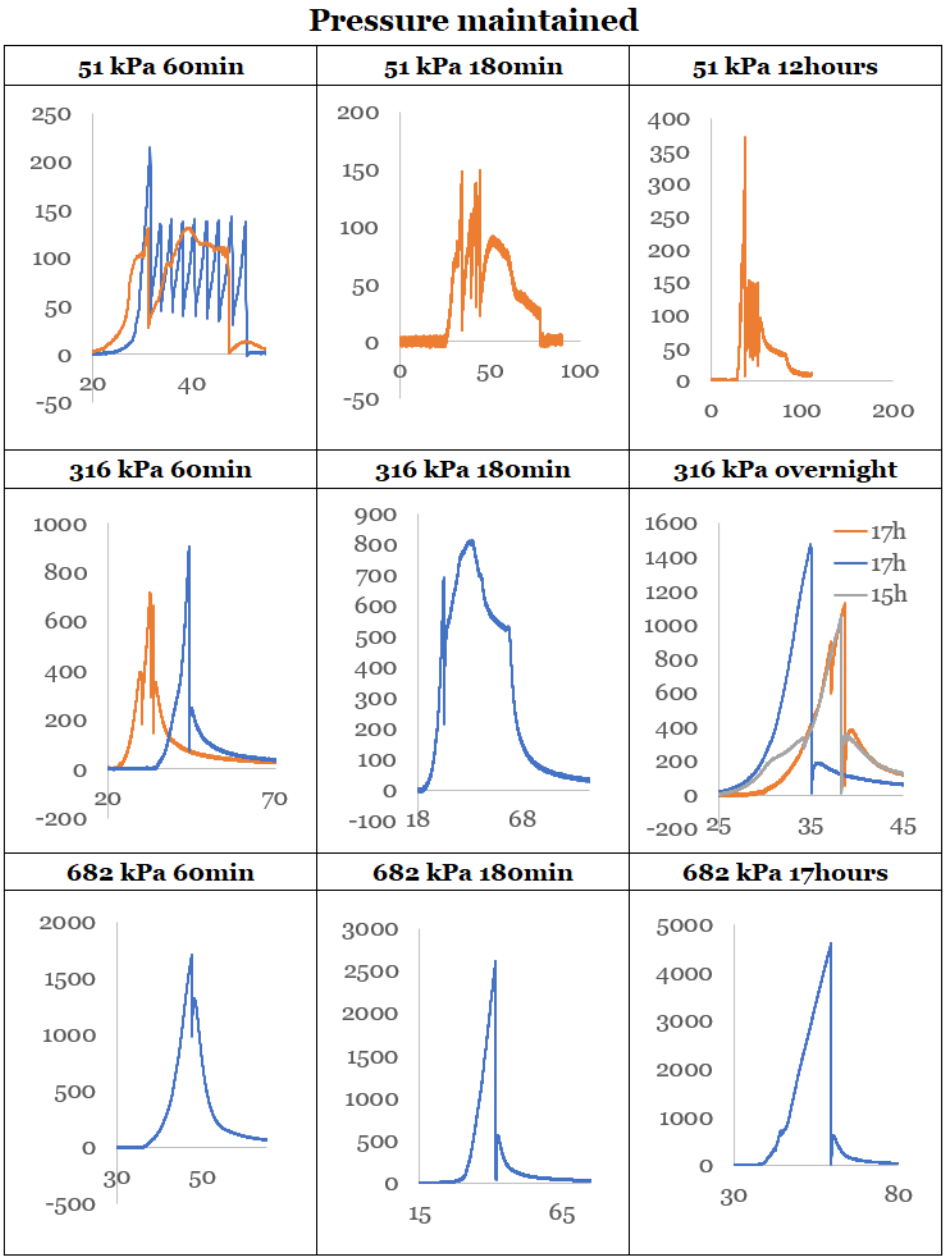

Figure B.2: Pull curves test sequence 1. Duration on x-axis and force on the y-axis

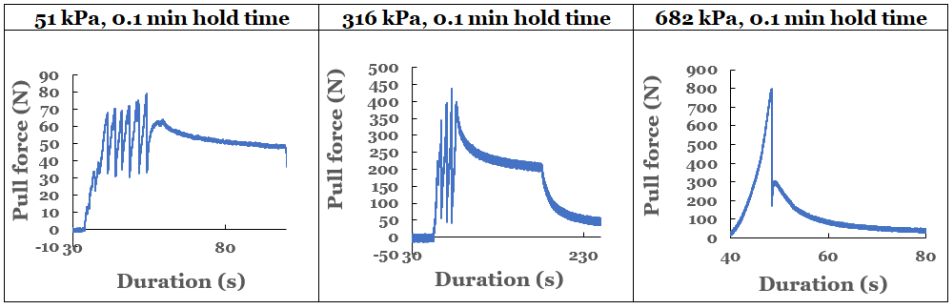

Figure B.3: pull curves of test sequence 1: 0.1 minute hold time test

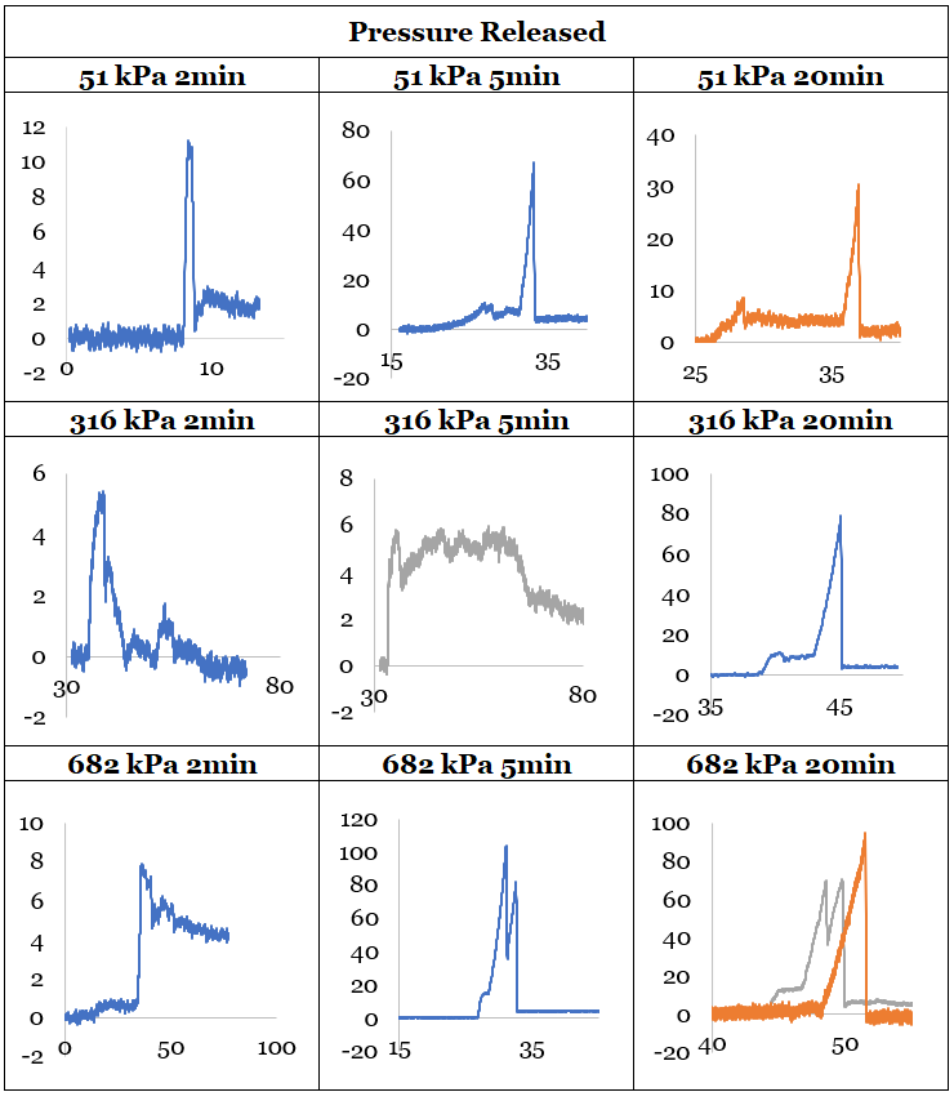

Figure B.4: Pull curves test sequence 2. Duration on x-axis and force on the y-axis

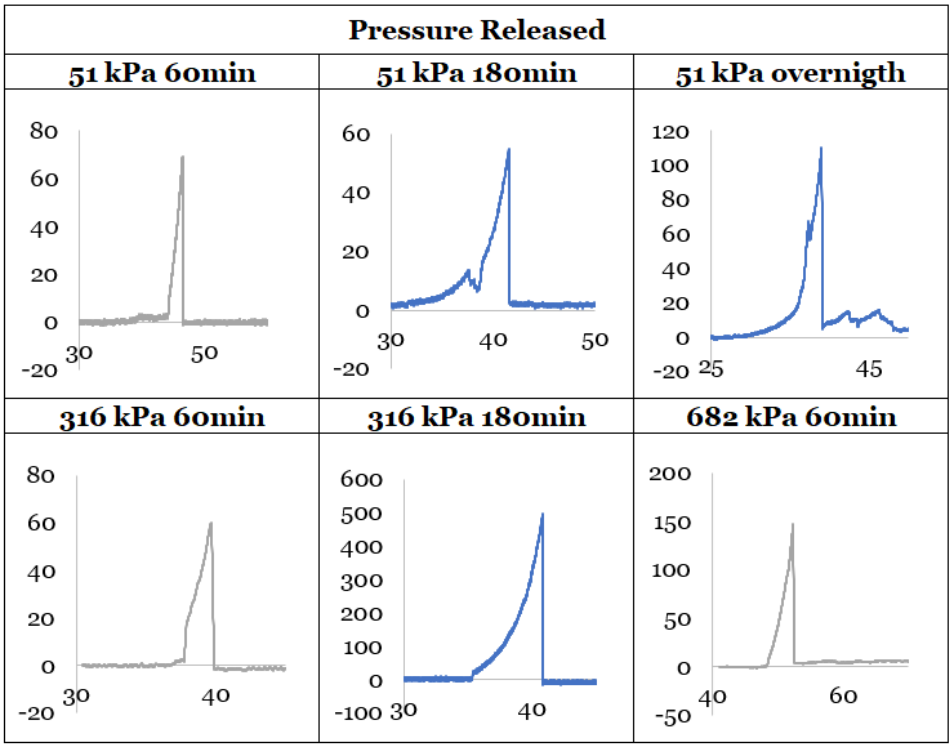

Figure B.5: Pull curves test sequence 2. Duration on x-axis and force on the y-axis

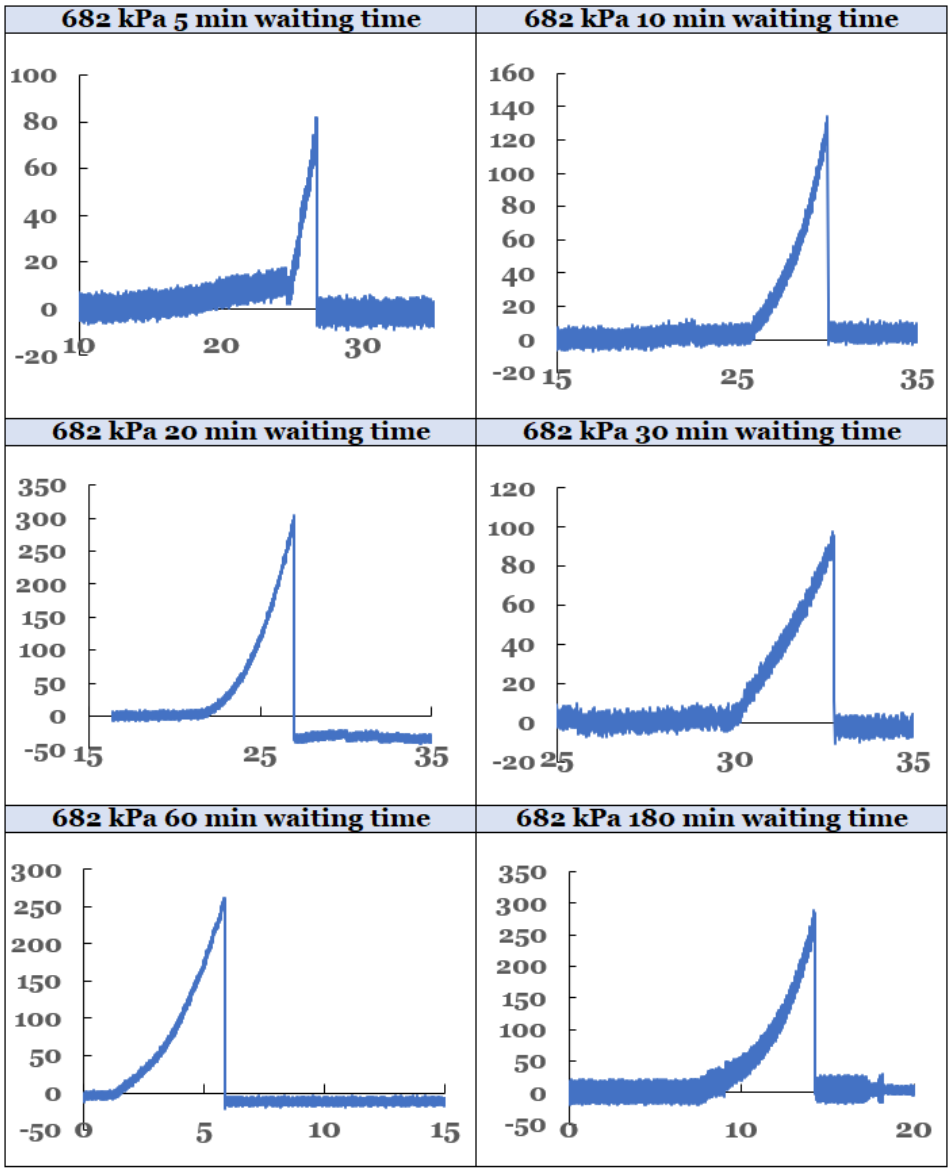

Figure B.6: Pull curves test sequence 3. Duration on x-axis and force on the y-axis

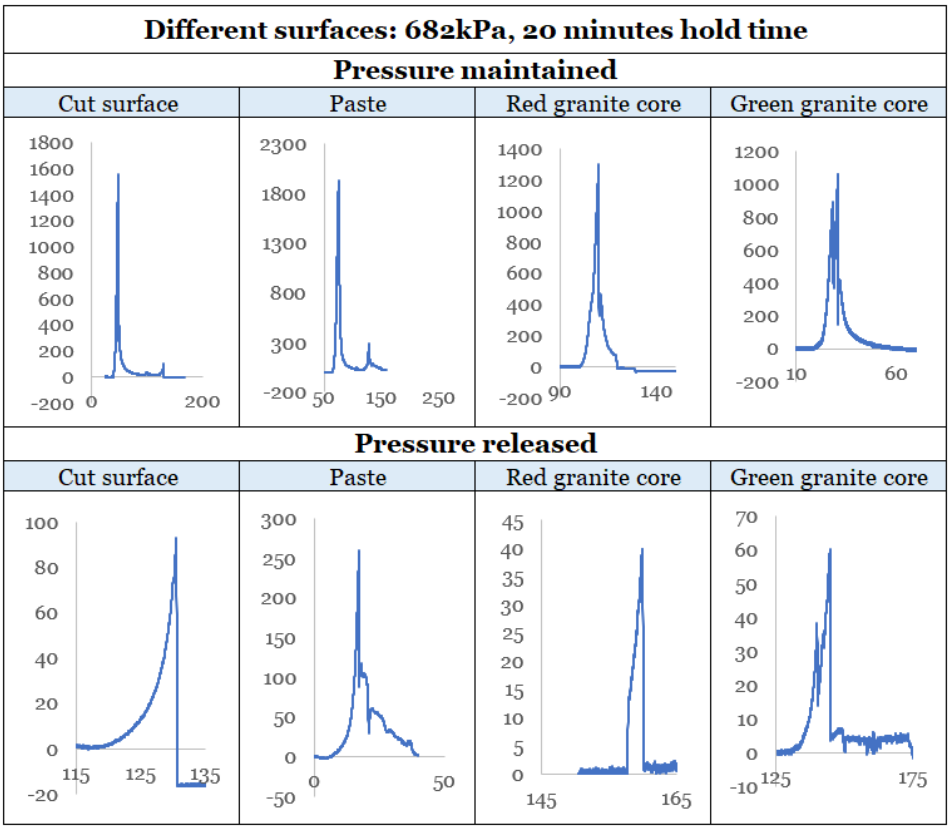

Figure B.7: Pull curves test sequence 4. Duration on x-axis and force on the y-axis

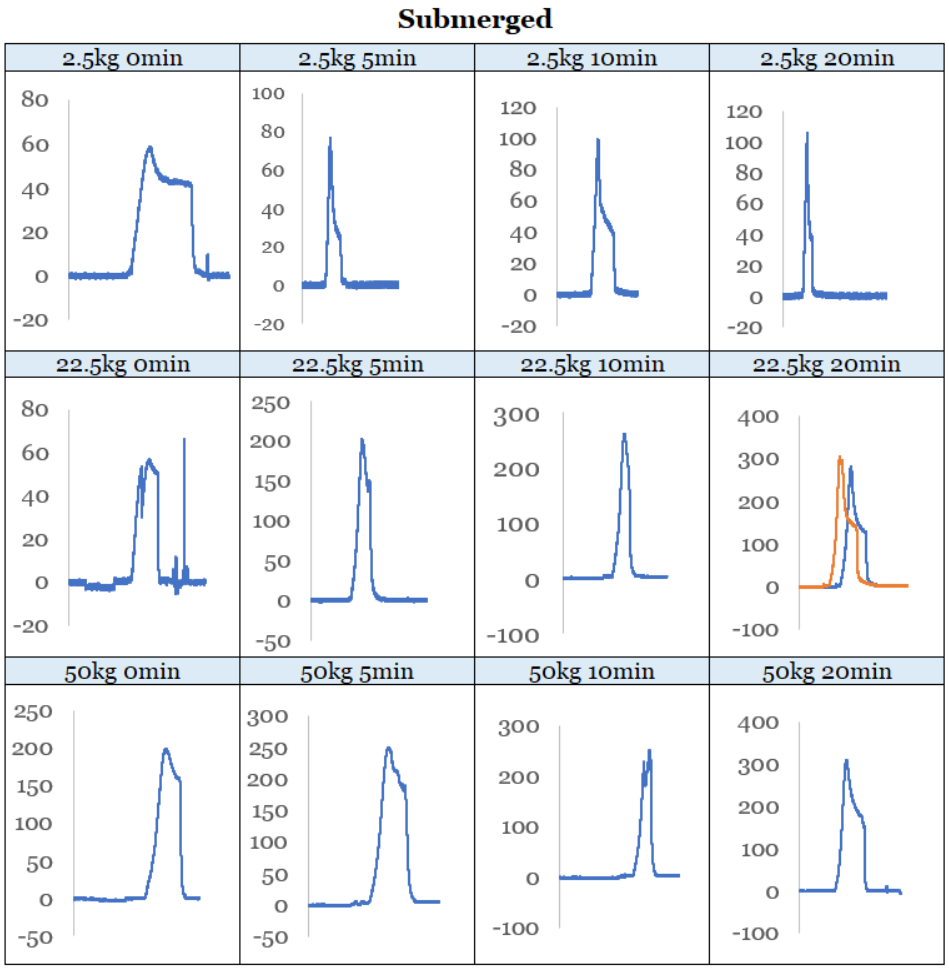

Figure B.8: Pull curves test sequence 4. Duration on x-axis and force on the y-axis

C

Images of ice and concrete after tests

(a) Little portion of ice stuck on concrete after shearing, 682kPa and 5 minute hold time

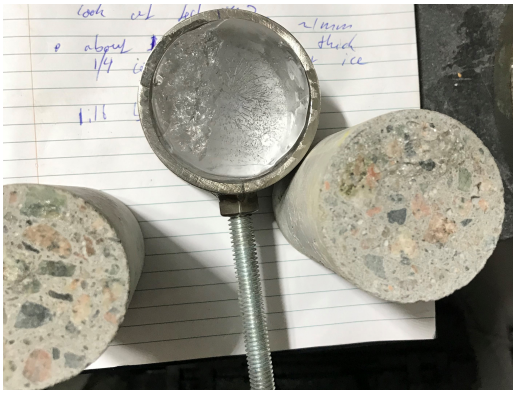

(b) More ice stuck on concrete after 60 minute hold time for 682 kPa pressure

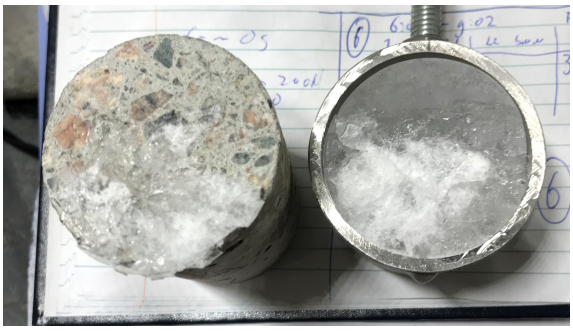

(c) much damage to the ice, going into the ice puck holder after 682 kPa pressure overnight test

Figure C.1: Images showing more ice on concrete surface for longer holding times.

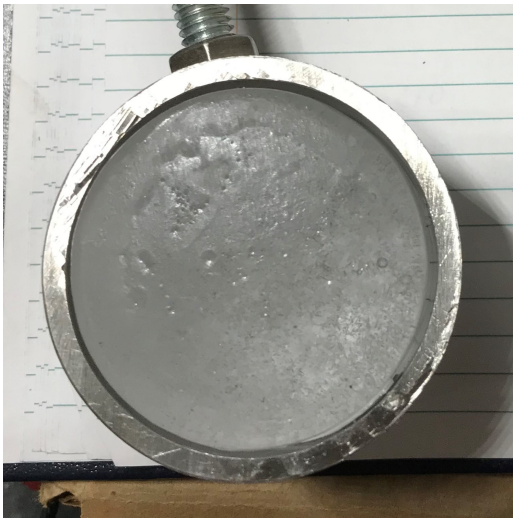

(a) Little damage on the ice

(b) Very thin layer of ice on the concrete indicating some dissipation of ice in concrete

Figure C.2: results after performing sequence 1, 51 kPa pressure 5 minute hold time test

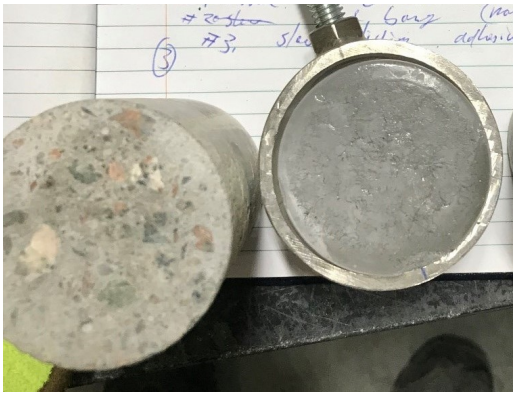

(a)

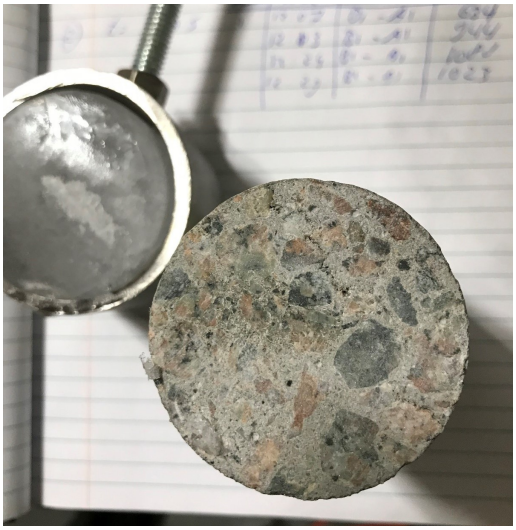

(b)

Figure C.3: Image of ice and concrete after 5 minutes of 316kPa pressure before shearing

Figure C.4: Ice and concrete after shearing from 5 minutes 682 kPa test

Figure C.5: Photograph of an ice puck after test where the ice and concrete were not well aligned and ice is partly molten away.

(a) Photograph of an ice puck and concrete cylinder after 682 kPa, 5 minute hold time test showing substrate failure of the concrete

(b) Photograph of an ice puck after 682 kPa, 5 minute hold time test showing substrate failure of the concrete

(c) Microscope image of concrete (a) after substrate failure of 682 kPa pressure and 5 minute hold time test

(a) Photograph showing paste surface after 682 kPa 20 min hold time test, where substrate failure of the concrete has been observed

(b) Photograph showing ice surface after 682 kPa 20 min hold time test, where a thin layer of concrete paste can be seen stuck on the ice

D

Images of the set-up

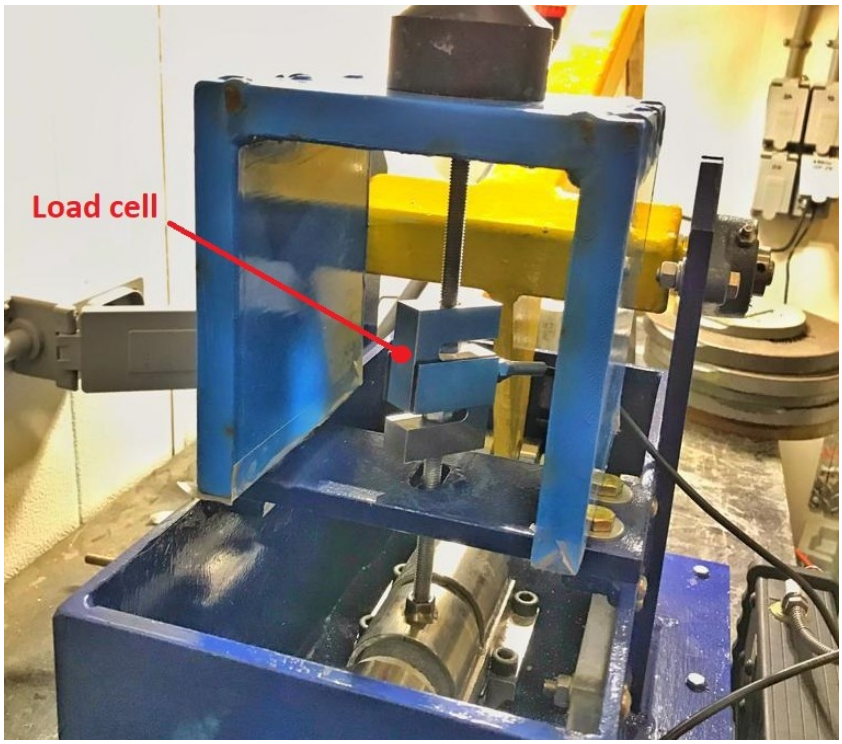

Figure D.1: Final set-up with extra load cell attached

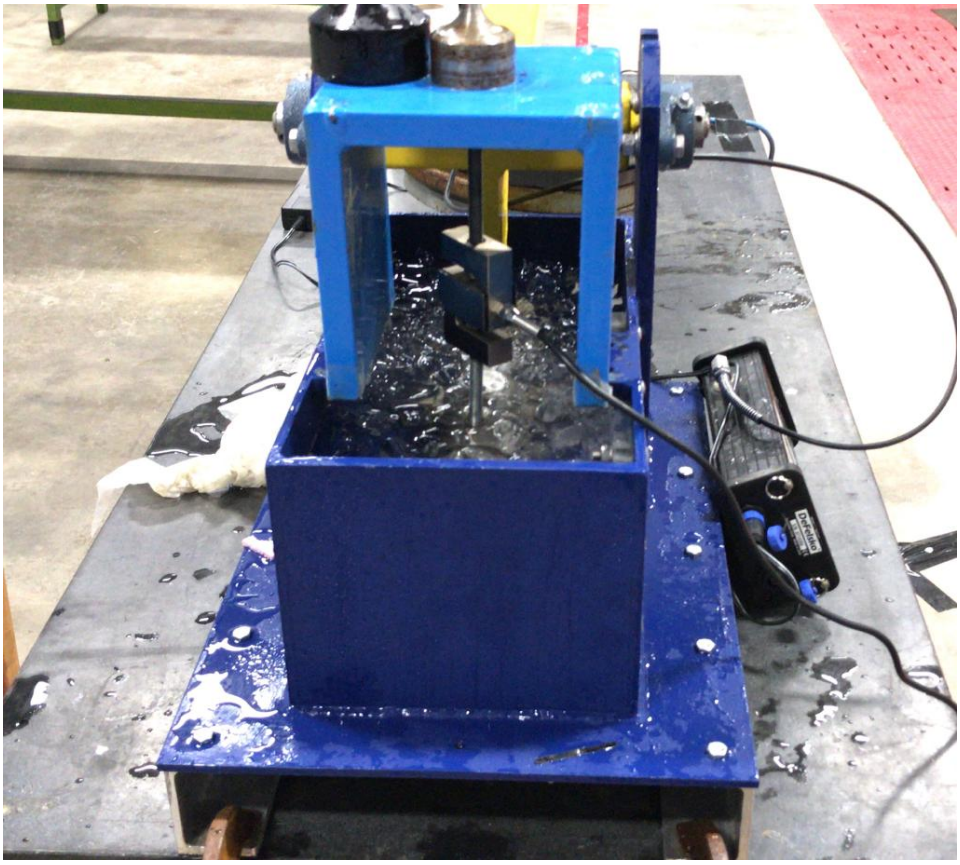

Figure D.2: Photograph of submerged set-up showing full submergence of ice and concrete before applying pressure.

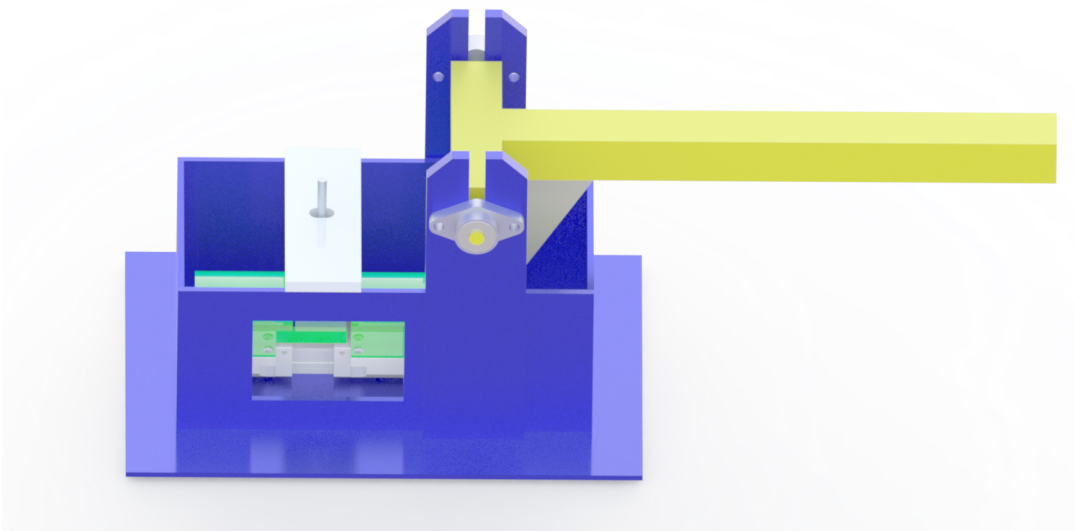

Figure D.3: SolidWorks render

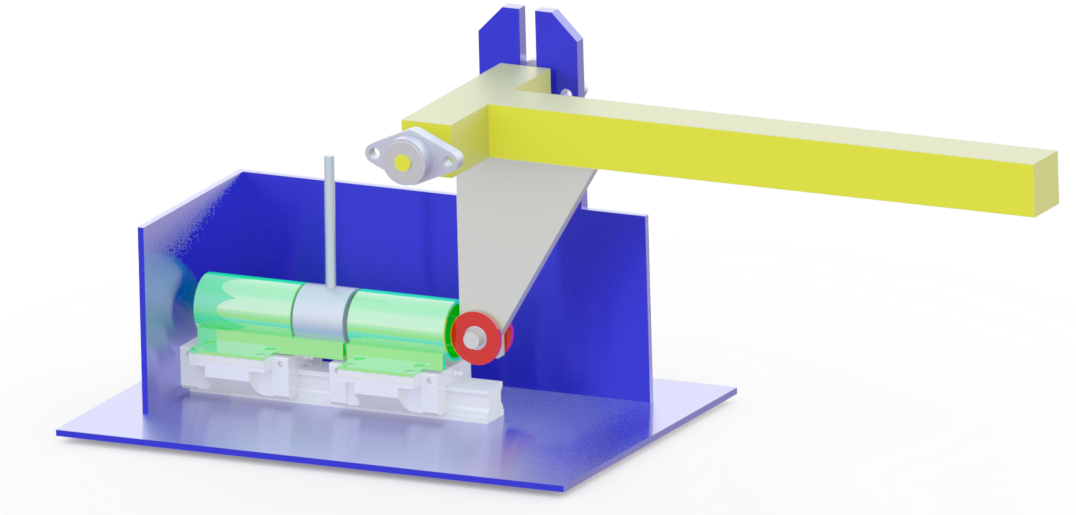

Figure D.4: SolidWorks render with open sides

List of Figures

List of Tables

Bibliography

[1] P. Barnes, D. Tabor, and Walker J. C. F. The Friction and Creep of Polycrystalline Ice. 324(1557):127–155, 1971.

[2] R A Batto and E M Schulson. On the ductile-to-brittle transition in ice under compression. 41(7):2219–2225, 1993.

[3] D G R Bonnel and F C Harper. The thermal expansion of concrete. Engineering research (Summary of a report to be published by the building research station). *Journal of the Institution of Civil Engineers*, 33(4):320–330, 1950. doi: 10.1680/IJOTI.1950.12917. URL https://doi.org/10.1680/IJOTI.1950.12917.

[4] F.P. Bowden and T.P. Hughes. The Mechanism of Sliding on Ice and Snow. 172(949):280–298, 1939.

[5] Y. Brechet and Y. Estrin. The effect of strain rate sensitivity on dynamic friction of metals. *Scripta Metallurgica et Materiala*, 30(11):1449–1454, 1994. ISSN 0956716X. doi: 10.1016/0956-716X(94)90244-5.

[6] S J Calabrese, R Buxton, and G Marsh. Frictional characteristics of materials sliding against ice. *Lubrication engineering*, 36(5), 1980.

[7] Sina Ebnesajjad. *Introduction and adhesion theories*. Elsevier Inc., 2011. ISBN 9781437744613. doi: 10.1016/B978-1-4377-4461-3.10001-X. URL http://dx.doi.org/10.1016/B978-1-4377-4461-3.10001-X.

[8] E Enkvist. On the ice resistance encountered by ships operating in the continuous mode of icebreaking. Technical report, United States Coast Guard, 1972.

[9] Robert Ettema. Review of River-channel Responses to River Ice. 4(December 2002), 2002. doi: 10.1061/(ASCE)0887-381X(2002)16.

[10] D.C.B. Evans, J.F. Nye, and K.J. Cheeseman. The Kinetic Friction of Ice. 347:493–512, 1975.

[11] Bruno Fiorio. Wear characterisation and degradation mechanisms of a concrete surface under ice friction. *Construction and Building Materials*, 19(5):366–375, 2005. ISSN 09500618. doi: 10.1016/j.conbuildmat.2004.07.020.

[12] Bruno Fiorio, Jacques Meyssonnier, and Marc Boulon. Experimental study of the friction of ice over concrete under simplifiedice-structure interaction conditions. *Canadian Journal of Civil Engineering*, 29(3):347–359, 2002. ISSN 0315-1468. doi: 10.1139/l02-012.

[13] Kathryn A Forland and Jean-Claude Tatinclaux. Kinetic friction coefficient of ice. 85-6(March):45, 1985.

[14] Seppo Huovinen. Abrasion of concrete by ice in arctic sea structures. *ACI Materials Journal*, 87(3):266–270, 1990. ISSN 0889325X.

[15] Seppo Huovinen. Abrasion of concrete structures by ice. *Cement and Concrete Research*, 23(1):69–82, 1993. ISSN 00088846. doi: 10.1016/0008-8846(93)90137-X.

[16] S Jacobsen, L V Kim, and E E Pomnikov. Concrete destructure due to ice-indentation pore pressure. *Proceedings of the International Offshore and Polar Engineering Conference*, (January):1258–1263, 2012. URL http://www.scopus.com/inward/record.url?eid=2-s2.0-84866126861{&}partnerID=40{&}md5=546060c76c0d831cf668ff28533788f3.

[17] Stefan Jacobsen, George W. Scherer, and Erland M. Schulson. Concrete-ice abrasion mechanics. *Cement and Concrete Research*, 73:79–95, 2015. ISSN 00088846. doi: 10.1016/j.cemconres.2015.01.001. URL http://dx.doi.org/10.1016/j.cemconres.2015.01.001.

[18] Qing Jia, Wen Tian, Yong Chao Lu, Xu Ming Peng, and Jing Rui Yu. Experimental Study on Adhesion Strength of Freshwater Ice Frozen to Concrete Slab. *Advanced Materials Research*, 243-249:4587–4591, 2011. doi: 10.4028/www.scientific.net/amr.243-249.4587.

[19] D.J. McGuinn J.P. Newhook. Ice abrasion assessment — piers of confederation cridge, Confederation Bridge engineering summit 1997-2007. *Proc Canadian Society for Civil Engineering*, pages 145–157, 2007.

[20] F E Kennedy, E M Schulson, and D E Jones. The friction of ice on ice at low sliding velocities. 8610(2000), 2009. doi: 10.1080/01418610008212103.

[21] Lasse Makkonen. Ice adhesion - Theory, measurements and countermeasures. *Journal of Adhesion Science and Technology*, 26(4-5):413–445, 2012. ISSN 01694243. doi: 10.1163/016942411X574583.

[22] E Møen, S Jacobsen, and H Myhra. Ice Abrasion Data on Concrete Structures–An Overview. *SINTEF Report SBF BK A*, 7036, 2007.

[23] P Oksanen. *Friction and Adhesion of Ice*. Dissertation from Helsinki University of Technology: Teknillinen Korkeakoulu. na, 1983. ISBN 9789513817022. URL `https://books.google.ca/books?id=KwT-PgAACAAJ`.

[24] H E Reinhardt. *Penetration and Permeability of Concrete: Barriers to organic and contaminating liquids*. RILEM proceedings. Taylor & Francis, 1997. ISBN 9780419225607. URL `https://books.google.nl/books?id=tuc3J4QD3LwC`.

[25] A Ya Ryvlin. Experimental study of ice friction. *Proceedings of the Arctic and Antarctic Research Institute*, 309:186–199, 1973.

[26] H Saeki, T Ono, and A Ozaki. Experimental study on ice forces on a cone-shaped and an inclined pile structure. In *Proc. 5th Int. Conf. POAC, Trondheim, Norway*, volume 2, pages 1081–1095, 1979.

[27] Hiroshi Saeki. Mechanical Properties Between Ice and Various Materials Used in Hydraulic Structures : The Jin S . Chung Award Lecture , 2010. 21(2):81–90, 2011.

[28] T. J.O. Sanderson and A. J. Child. Ice loads on offshore structures: The transition from creep to fracture. *Cold Regions Science and Technology*, 12(2):157–161, 1986. ISSN 0165232X. doi: 10.1016/0165-232X(86)90030-3.

[29] M Sayed, S.B. Savage, and R.M.W. Frederking. Two-dimensional extrusion of crushed ice. Part 2: analysis. 21:37–47, 1992.

[30] Mohamed Sayed and Robert M.W. Frederking. Two-dimensional extrusion of crushed ice. Part 1: experimental. *Cold Regions Science and Technology*, 21(1):25–36, 1992. ISSN 0165232X. doi: 10.1016/0165-232X(92)90003-D.

[31] Erland M. Schulson. Friction of sea ice. *Philosophical Transactions of the Royal Society A: Mathematical, Physical and Engineering Sciences*, 376(2129), 2018. ISSN 1364503X. doi: 10.1098/rsta.2017.0336.

[32] Erland M. Schulson and Andrew L. Fortt. Friction of ice on ice. *Journal of Geophysical Research B: Solid Earth*, 117(12):1–18, 2012. ISSN 21699356. doi: 10.1029/2012JB009219.

[33] Erland M. Schulson and Andrew L. Fortt. Friction of ice on ice. *Journal of Geophysical Research B: Solid Earth*, 117(12):1–18, 2012. ISSN 21699356. doi: 10.1029/2012JB009219.

[34] Erland M Schulson and Andrew L Fortt. Static strengthening of frictional surfaces of ice. *Acta Materialia*, 61(5):1616–1623, 2013. ISSN 13596454. doi: 10.1016/j.actamat.2012.11.038. URL `http://dx.doi.org/10.1016/j.actamat.2012.11.038`.

[35] Guzel Shamsutdinova, Max A.N. Hendriks, and Stefan Jacobsen. Concrete-ice abrasion: Wear, coefficient of friction and ice consumption. *Wear*, 416-417(June):27–35, 2018. ISSN 00431648. doi: 10.1016/j.wear.2018.09.007.

[36] S. K. Singh, I. J. Jordaan, J. Xiao, and P. A. Spencer. The Flow Properties of Crushed Ice. *Journal of Offshore Mechanics and Arctic Engineering*, 117(4):276, 1995. ISSN 08927219. doi: 10.1115/1.2827234.

[37] Jean-Claude Tatinclaux and David Murdey. Field tests of the kinetic friction Scoefficient of sea ice. 1985. URL https://apps.dtic.mil/dtic/tr/fulltext/u2/a163170.pdf.

[38] Chenyu Wang, Wei Zhang, Adarsh Siva, Daniel Tiea, and Kenneth J Wynne. Laboratory Test for Ice Adhesion Strength Using Commercial Instrumentation Laboratory Test for Ice Adhesion Strength Using Commercial Instrumentation. (April), 2018. doi: 10.1021/la4044254.

[39] M. Zou, S. Beckford, R. Wei, C. Ellis, G. Hatton, and M. A. Miller. Effects of surface roughness and energy on ice adhesion strength. *Applied Surface Science*, 257(8):3786–3792, 2011. ISSN 01694332. doi: 10.1016/j.apsusc.2010.11.149. URL http://dx.doi.org/10.1016/j.apsusc.2010.11.149.